

**EXPLORING NANOBODIES INTERRUPTING THE INTERACTION  
BETWEEN p53 AND MDM4**

by  
SANEM SARIYAR

Submitted to the Graduate School of Engineering and Natural Sciences  
in partial fulfilment of  
the requirements for the degree of Master of Science

Sabanci University  
July 2019

**EXPLORING NANOBODIES INTERRUPTING THE INTERACTION BETWEEN  
p53 AND MDM4**

Approved by:

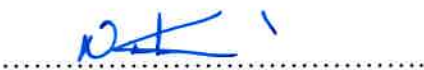
Prof. Dr. Batu Erman

A handwritten signature in blue ink, appearing to read "Batu Erman", written over a horizontal dotted line.

Assist. Prof. Dr. Christopher Mayack

A handwritten signature in blue ink, appearing to read "Chris Mayack", written over a horizontal dotted line.

Assist. Prof. Dr. Nazlı Keskin Toklu

A handwritten signature in blue ink, appearing to read "NKT", written over a horizontal dotted line.

Approval Date: July 17, 2019

SANEM SARIYAR 2019 ©

All Rights Reserved

## ABSTRACT

### EXPLORING NANOBODIES INTERRUPTING THE INTERACTION BETWEEN p53 AND MDM4

SANEM SARIYAR

Molecular Biology, Genetics and Bioengineering, MSc Thesis, July 2019

Thesis Supervisor: Prof. Batu Erman

Keywords: p53/MDM4 interaction, nanobodies, nanobody purification,  
fluorescent two-hybrid assay, surface plasmon resonance

The p53 protein is considered as the guardian of the genome thanks to its important tumor suppressor roles such as cell-cycle arrest, apoptosis and senescence. Because these roles are extremely vital, the p53 pathway is strictly regulated. During unstressed conditions, p53 protein levels are kept in control by both ubiquitination of the p53 protein and inhibition of its transcriptional activity through the MDM2 and MDM4 proteins, respectively. Although MDM2 is the main modulator of p53 activity, there is a collaboration between MDM2 and MDM4 proteins to enable the control of p53. Thus, MDM4 is as important as MDM2 in this mechanism. In most human cancers, there is either a mutation in the Tp53 gene or an overexpression of its negative regulators. Thus, targeting the p53-MDM2-MDM4 interplay is one of the main aims of cancer therapeutics. Also, in some cancers, where there is overexpression of negative regulators, the use of inhibitors for only MDM2 is not enough to activate the p53 protein. For this reason, exploring inhibitors for MDM4 are vital for therapy. In this study, we aimed to optimize the purification of *in silico* designed nanobodies targeting the MDM4-p53 interaction and test their affinity and effectiveness by surface plasmon resonance (SPR) and a fluorescent two-hybrid (F2H) assay.



## ÖZET

### p53 VE MDM4 ETKİLEŞİMİNİ BOZAN NANOBOĐİLERİN KEŞFİ

SANEM SARIYAR

Moleküler Biyoloji, Genetik ve Biyomühendislik, Yüksek Lisans Tezi, Temmuz 2019

Tez Danışmanı: Prof. Batu Erman

Anahtar Kelimeler: p53/MDM4 etkileşimi, nanobodiler, nanobodi saflaştırılması, floresan ikili hibrit tekniği, yüzey plasmon rezonans

p53 proteini hücre bölünmesinin durdurulması, apoptoz ve senesens gibi önemli tümör baskılayıcı rolleri sayesinde genomun gardiyanı olarak bilinir. Bu roller son derece hayati olduğu için, p53 yolağı çok sıkı bir şekilde kontrol edilmelidir. Stres olmayan koşullarda, hücre içindeki p53 protein miktarı, p53 proteininin ubiquitinlenmesi ve transkripsiyon aktivitesinin engellenmesi ile sırasıyla MDM2 ve MDM4 proteinleriyle kontrol altında tutulur. MDM2, p53 proteinin aktivitesinin ana modülatörü olmasına rağmen, p53' ün kontrolünün sağlanması için MDM2 ve MDM4' un işbirliğine ihtiyaç vardır. Bu nedenle, MDM4 proteini bu mekanizmada MDM2 proteini kadar önemlidir. Çoğu kanser tipinde, p53 proteininde mutasyon vardır ya da antagonistlerinin yüksek seviyede üretilmesi gözlenmiştir. Bu nedenle, kanser ilacı geliştirilmesinde p53-MDM2- MDM4 etkileşimi hedeflenmiştir. Buna ek olarak, antagonistlerin yüksek seviyede üretildiği bazı kanserlerde, sadece MDM2 için inhibitör kullanımı p53 proteinini aktive etmeye yeterli olmamıştır. Bu nedenle, MDM4 proteini için inhibitör araştırmaları önem kazanmıştır. Bu çalışmada bilgisayar ortamında tasarlanmış p53/ MDM4 etkileşimini bozan nanobodilerinin saflaştırılmasını optimize etmeyi ve bağlanmalarını yüzey plasmon rezonans (SPR) ve floresan ikili hibrit tekniği ile test etmeyi amaçladık.

## ACKNOWLEDGEMENTS

First of all, I would like to thank my thesis advisor Prof. Dr. Batu Erman for his help and support for my M.Sc study. It was an enlightening experience for me to discover myself more and see what I want. Being part of this nurturing academic environment improved my scientific background. I would also like to thank my thesis jury members, Assist. Prof. Dr. Christopher Mayack and Assist. Prof. Dr. Nazlı Keskin Toklu for their interest and feedbacks about my thesis project.

I thank all my labmates for their help and support: Melike Gezen, Sofia Piepoli, Sarah Barakat, Liyne Noğay and Hakan Taşkiran. Especially I would like to express my gratitude to Melike Gezen, Hakan Taşkiran and Liyne Noğay for helping me through this thesis study. They not only supported and helped me for this project but also with their close friendship, they turned this experience into an unforgettable memory.

Last but not least I would like to thank my family. They were always with me through this journey and they supported me with their love. They were always there to listen and help me anytime. I learnt not to give up no matter what from my parents and my brother who followed his dreams. Thank you very much for encouraging me all the time.

This study was supported by TUBITAK 1003 grant 'Özgün-2 indolinon bileşiklerinin anti-interlökin-1 ve kemoterapötik ilaçlar olarak geliştirilmesi' Grant Number: T.A.CF-16-01568 (215S615)

*To my family...*  
*Canım aileme...*

## TABLE OF CONTENTS

LIST OF TABLES.....	xi
LIST OF FIGURES.....	xii
LIST OF ABBREVIATIONS.....	xiv
1. INTRODUCTION.....	1
1.1. Cancer Development.....	1
1.1.1 p53.....	2
1.1.2. MDM2 and MDM4.....	4
1.2. Structure of p53, MDM2 and MDM4.....	7
1.3. Regulation of MDM2, MDM4 and p53 During Stress Conditions.....	10
1.4. Targeting the MDM4- p53 Interaction for Cancer Treatment.....	12
1.5. Nanobodies.....	14
1.5.1. Discovery, Structure and Advantages.....	14
1.5.2. Production methods for nanobodies.....	17
1.5.3. Uses of Nanobodies.....	18
2. AIM OF THE STUDY.....	22
3. MATERIAL & METHODS.....	24
3.1. Materials.....	24
3.1.1. Chemicals.....	24
3.1.2. Equipment.....	24
3.1.3. Solutions and Buffers.....	24
3.1.4. Growth Media.....	26
3.1.5. Molecular Biology Kits.....	27
3.1.6. Enzymes.....	27
3.1.7. Bacterial Strains.....	27
3.1.8. Mammalian Cell Lines.....	27
3.1.9. Plasmid and Oligonucleotides.....	27
3.1.10. DNA and Protein Molecular Weight Markers.....	30

3.1.11. DNA Sequencing.....	30
3.1.12. Software, Computer-based Programs, and Websites.....	30
3.2. Methods.....	31
3.2.1. Bacterial Cell Culture.....	31
3.2.1.1. The growth of Bacterial Culture.....	31
3.2.1.2. Preparation of competent bacteria.....	31
3.2.1.3. Transformation of competent bacteria.....	32
3.2.1.4. Plasmid DNA Isolation.....	32
3.2.2. Mammalian Cell Culture.....	32
3.2.2.1. Maintenance of Cell Lines.....	32
3.2.2.2. Cryopreservation of cells.....	32
3.2.2.3. Thawing of frozen mammalian cells. ....	33
3.2.2.4. Transient Transfection of Mammalian Cell Lines Using Polyethyleneimine (PEI).....	33
3.2.3. Vector Construction.....	34
3.2.4. Protein Purification.....	35
3.2.4.1. Vector Construction.....	35
3.2.4.2. His-tagged protein expression.....	36
3.2.4.3. Affinity chromatography of His tagged proteins.....	38
3.2.4.4. Purification of His-Tagged proteins by Batch Method.....	41
3.2.4.5. SDS-PAGE gel and Coomassie Blue Staining.....	42
3.2.5. Surface Plasmon Resonance.....	42
3.2.6. Fluorescent two- hybrid (F2H) assay.....	44
3.2.6.1. pcDNA 3.1/ myc- His (-) B- Nanobody BFP Vector Construction.....	44
3.2.6.2. PEI transfection of F2H- assay plasmids.....	45
4. RESULTS.....	46
4.1. Optimization of Nanobody Binding.....	46
4.1.1. Periplasmic Expression.....	47
4.1.2. Cytoplasmic Expression.....	58
4.2. Surface plasmon resonance (SPR) for comparing binding affinities of nanobodies.....	64
4.3. Fluorescent two-hybrid (F2H) assay for interaction between nanobodies and MDM4 protein.....	68
5. DISCUSSION.....	75

BIBLIOGRAPHY.....	79
APPENDIX A- Chemicals.....	93
APPENDIX B- Equipment.....	95
APPENDIX C- Molecular Biology Kits.....	96
APPENDIX D- DNA and Protein Molecular Weight Marker.....	97
APPENDIX F- Plasmid Maps.....	98

## LIST OF TABLES

Table 3.1 List of plasmids.....	28
Table 3.2 List of oligonucleotides.....	29
Table 3.3 List of software and computer-based programs and websites.....	30
Table 3.4 List of ingredients used in PEI transfection in 6 well plate.....	33
Table 3.5 List of ingredients for pET-28a (+) digestion.....	35
Table 3.6 Reaction conditions for PCR by Q5 polymerase.....	45
Table 3.7 Double digest with XhoI and BamHI of both vector and inserts.....	45
Table 4.1 Predicted molecular weights of nanobodies used in this study.....	46
Table 4.2 Groups for temperature, time and IPTG dependent expression.....	62
Table 4.3 Methods used for the expression and purification of nanobodies.....	64

## LIST OF FIGURES

Figure 1.1 p53 downstream pathways.....	4
Figure 1.2 Summary of MDM2, MDM4 and p53 interaction.....	7
Figure 1.3 Gene structures of MDM2, MDM4 and p53.....	10
Figure 1.4 MDM2, MDM4 and p53 pathway.....	12
Figure 1.5 Representation of conventional antibodies, heavy chain only antibodies and nanobodies.....	15
Figure 3.1 Periplasmic protein expression and induction.....	37
Figure 3.2 Cytoplasmic protein expression and induction.....	38
Figure 3.3 First osmotic shock lysis protocol.....	38
Figure 3.4 Second osmotic shock lysis protocol.....	39
Figure 3.5 Nanobody purification with protocol whole cell lysis protocol.....	40
Figure 3.6 His-tag nanobody purification with cobalt resin column.....	41
Figure 3.7 Representation of surface plasmon resonance.....	43
Figure 4.1 Periplasmic nanobody expression using an osmotic shock protocol.....	48
Figure 4.2 Periplasmic nanobody purification .....	49
Figure 4.3 Periplasmic nanobody expression .....	50
Figure 4.4 Periplasmic nanobody purification .....	51
Figure 4.5 Colony screening for GFP CDR3 Nb expression.....	52
Figure 4.6 Colony screening for MDM4 CDR3 Nb and MDM4 CDR1 CDR3 Nb expression.....	53
Figure 4.7 Periplasmic nanobody purification with the whole cell lysis protocol.....	54
Figure 4.8 Colony screening for MDM4 Nb and GFP CDR3 Nb expression.....	55
Figure 4.9 Periplasmic nanobody purification with the whole cell lysis protocol.....	55
Figure 4.10 Colony screening for MDM4 CDR1 CDR3 Nb expression.....	56
Figure 4.11 Periplasmic nanobody purification with the whole cell lysis protocol.....	57
Figure 4.12 Time dependent periplasmic nanobody expression with whole cell lysis protocol.....	57
Figure 4.13 Colony screening for cytoplasmic expression.....	59
Figure 4.14 Cytoplasmic nanobody purification with the whole cell lysis protocol.....	59
Figure 4.15 Cytoplasmic nanobody purification with the Bugbuster® protocol.....	60



Figure 4.16 Cytoplasmic nanobody purification with the whole cell lysis protocol.....	61
Figure 4.17 IPTG, temperature and time dependent cytoplasmic nanobody expression with the whole cell lysis protocol.....	62
Figure 4.18 Colony screening for cytoplasmic expression.....	64
Figure 4.19 pH scouting experiment.....	65
Figure 4.20 Immobilization of MDM4 on CM5 chip.....	66
Figure 4.21 Binding at different concentration of the MDM4 Nb, MDM4 CDR3 Nb And GFP Nb.....	67
Figure 4. 22 Plasmids used in fluorescent two hybrid assay.....	69
Figure 4. 23 Mechanism of fluorescent two hybrid assay.....	69
Figure 4.24 Verification of protein- protein interaction and the disruption of interaction by nanobodies using the F2H assay .....	71
Figure 4.25 A bar graph showing the amount of the GFP foci containing cells and the percentages of co-localization in these cells.....	72
Figure 4.26 F2H assay with nanobodies.....	74
Figure D.1 GeneRuler DNA Ladder Mix.....	97
Figure D.2 Color Prestained Protein Standard, Broad Range (11-25 kDa) .....	97
Figure F.1 The plasmid map of pET22b.....	98
Figure F.2 The plasmid map of pET28a.....	98
Figure F.3 The plasmid map of pcDNA3.1 Myc His B (-).....	99
Figure F.4 The plasmid map of pRRL Tag BFP Plasmid.....	99

## LIST OF ABBREVIATIONS

$\alpha$	Alpha
$\beta$	Beta
$\mu$	Micro
A	Ampere
Apaf1	Apoptotic protease activating factor 1
ARF	Alternative reading frame protein
ATM	Ataxia telangiectasia mutated
ATR	Ataxia telangiectasia and Rad3 related
Bad	Bcl-2-associated death promoter
Bak	Bcl-2 homologous antagonist/killer
Bax	Bcl-2-associated X protein
Bcl-2	B-cell lymphoma 2
bGH	Bovine growth hormone
BHK	Baby Hamster kidney
Bid	BH3 interacting-domain death agonist
bp	Base pair
CBP	CREB-binding protein
ARF	ADP ribosylation factor
Cdk	Cyclin-dependent kinase
CIP/CIAP	Calf intestinal alkaline phosphatase
DBD	DNA binding domain
DMEM	Dulbecco's Modified Eagle Medium
DMSO	Dimethyl sulfoxide
DNA	Deoxyribonucleic acid
dNTPs	Deoxynucleotide triphosphates
Dr5	Death receptor 5
<i>E. coli</i>	<i>Escherichia coli</i>
EDTA	Ethylenediaminetetraacetic acid
F2H	Fluorescent 2 hybrid
FBS	Fetal bovine serum
GFP	Green Fluorescent Protein
GBP	GFP-binding protein
IMAC	Immobilized Metal Affinity Chromatography
kDa	Kilo Dalton
LB	Luria broth
MDM4	Murine double minute 4
mRNA	Messenger ribonucleic acid
NCBI	National Center for Biotechnology

NES	Nuclear export signal
NLS	Nuclear localization signal
PBS	Phosphate-buffered saline
PCR	Polymerase chain reaction
PEI	Polyethyleneimine
PI3K	Phosphoinositide 3-kinase
Puma	p53 upregulated modulator of apoptosis
RB	Retinoblastoma tumor suppressor
RING	Really Interesting New Gene
Rpm	Revolution per minute
SDS-PAGE	Sodium Dodecyl Sulfate-Polyacrylamide Gel Electrophoresis
TAD	Trans-activation domain
TBE	Tris-Borate-EDTA
TCEP	Tris (2-carboxyethyl) phosphine hydrochloride
TF	Transcription factor
V	Volt
WT	Wild-type

# 1. INTRODUCTION

## 1.1. Cancer Development

Cancer cells divide in an uncontrolled manner compared to normal cells. Normal cells go through several control mechanisms that they regulate their growth- promoting signals which leads to cell division. However, in cancer cells these signals are not regulated and are hijacked produce their own growth factor ligands and through receptors they respond to these signals to divide without control (Hanahan and Weinberg 2011). This imbalance is due to genetic abnormalities like deletions, duplications, inversions and translocations which cause genetic instability (Thompson and Compton 2011) and point mutations (Hart et al. 2015). If these genetic changes occur in genes like oncogenes, tumor-suppressor genes and stability genes, it is inevitable to observe tumorigenesis (Vogelstein and Kinzler 2004).

Oncogene and tumor suppressor gene mutations work in a similar fashion. They increase by inducing cell division and preventing cell death or cell- cycle arrest (Hanahan and Weinberg 2000). On the other hand, stability genes control recombination during cell division and chromosomal segregation. These gene products prevent large scale genetic changes and when there is a mutation in these genes several other mutations occur with higher incidence. Cancer cells in general show evading apoptosis, self- production of growth signals, insensitivity to anti-growth signals, sustained angiogenesis, limitless replication and metastasis which are hallmarks of cancer development (Hanahan and Weinberg 2000). These mutations can occur in somatic cells which are in single cells and they do not show hereditary transmission. On the other hand, they can also occur in germline cells which will lead to hereditary predisposition to cancer development (Milholland et al. 2017).

Proto- oncogenes are genes which when mutated, turn into oncogenes and affect cellular proliferation and cancer formation. Oncogenes are genes which can lead to cancer development and their mutation or change in expression causes gain-of-function effects (Osborne, Wilson, and Tripathy 2004). On the other hand, tumor suppressor genes negatively regulate the growth of cells or metastasis. When there is loss of function mutation, they can contribute to cancer development (Osborne, Wilson, and Tripathy 2004). Discoveries or identification of these genes are very important because they can pave a way for the development of novel therapeutic applications which target these genes (Chen, Liu, and Qing 2018). ErbB2, PI3KCA and MYC are well studied example oncogenes and BRCA 1/2, PTEN and TP53 are also examples of tumor suppressors (Lee and Muller 2010).

### **1.1.1. p53**

The p53 protein is one of the most important tumor suppressors. It has very crucial role in inhibiting cancer development, this function can be understood from the observation of mutations in the TP53 gene in approximately 50% of human cancers (Brown et al. 2009). The Wild type p53 gene induces G2/M and G1 cell-cycle arrest, senescence and apoptosis. p53 is a transcription factor and it was first discovered in 1979. This protein functions to sense cellular stresses like DNA damage, oncogene activation, viral infection and telomere shortening (Bourdon, Laurenzi, et al. 2003). Thus, p53 inhibits the increase in the number of damaged or stressed cells. For all of these reasons, it is called guardian of the genome (Bourdon, Laurenzi, et al. 2003). Because p53 is a transcription factor, it binds to specific sequences on DNA in the regulatory regions of various genes and it does so as a tetramer. From various studies, in total 346 p53 target genes were found (Fischer 2017). These genes have crucial functions in senescence, angiogenesis and autophagy (Joerger and Fersht 2016). During stress conditions, tetrameric p53 is activated by multiple phosphorylation events. According to the type of stress, activation of p53 leads to the upregulation or downregulation of target genes. In vertebrates p53 protein levels are regulated by the MDM2 and MDM4 proteins which are negative regulators. Under homeostasis condition, p53 gets ubiquitinated by MDM2 and MDM4 and gets degraded which keeps p53 protein levels very low (Joerger and Fersht 2016).

p53, as mentioned earlier, can lead to cell cycle arrest due to DNA damage and this is carried out with the activation of the transcription of the p21/ WAF1 gene, which encodes a small protein with 165 amino acids belonging to CIP/Kip family, a cyclin- dependent kinase inhibitor which results in cell cycle arrest (Gartel 2006). It is the first p53 target gene which is found (El-deiry et al. 1993). After p53 is activated, it binds to the 5' end of the p21 promoter and leads to the production of p21 mRNA. The p21 protein binds to CyclinE/ Cdk2 and Cyclin D/ Cdk4 and inhibits their activity (Georgakilas, Martin, and Bonner 2017). Retinoblastoma protein (pRb) phosphorylation, a substrate of these cdk's is prevented in this way and pRb can bind to E2F1. With this binding, E2F1 is transcriptionally inactivated, so there is no transcription of E2F1 target genes related to DNA replication and cell-cycle which will lead to G<sub>1</sub> arrest (Luo, Hurwitz, and Massagué 1995). p53 activation also leads to G<sub>2</sub>/ M arrest through other p53 target genes like 14-3-3 $\sigma$  and cdc25c (Martín-Caballero et al. 2001). After DNA repair and decrease in p53 amounts, cells can through division again.

Senescence, on the other hand, is due to the chronic activation of p53 which is triggered by telomere erosion, DNA damage signaling, disruption in chromatin organization and the activation of certain oncogenes (Beauséjour et al. 2003). Senescent cells have specific characteristics like, large cell size, active autophagy and increase secretion of proinflammatory cytokines (Campisi 2005). Cell cycle arrest via p53 is very crucial for senescence because without p21 there is no induction of senescence by p53. Although the common perception about senescence is that it is not reversible but cells can go through the cell cycle when there is inactivation of p53 (Beauséjour et al. 2003). The decision between cell cycle arrest and senescence is decided with the several pathways and their interaction with p53. Not only p53, but activities of pRb, NF-Kb and m-TOR are crucial for senescence. pRb causes formation of heterochromatin on E2F1 target genes and NF-Kb is needed for proinflammatory cytokine expression (Chen 2016).

Apart from cell cycle arrest and senescence induction, p53 activation can cause apoptosis in certain cell types. They can go through apoptosis instead of cell cycle arrest. After p53 is activated transcriptionally with several stimuli, it induces several genes related to apoptosis signaling in addition to the genes mention above. These p53 targets are the BH3 domain- only pro-apoptotic proteins such as Puma, Noxa, Bad, Bax and Bak, death

receptors like Fas and factors for apoptosis execution such as Apaf1 and caspase 6 (Chen 2016). There are two apoptosis pathways; intrinsic and extrinsic (Figure 1.1). In the extrinsic apoptotic pathway, activation of death receptors like Fas causes dimerization of these receptors which is activates downstream signaling pathways such as the activation of procaspase 8 and the activation of caspase 3 and 7. On the other hand, the intrinsic pathway is the p53 dependent one in which p53 activation causes induction of BH3- only proteins. This induction causes mitochondrial membrane permeabilization (MOMP) which leads to cytochrome c, Smac and Omi release from the inter membrane space of mitochondria. The released cytochrome c binds to adenosine triphosphate (ATP) and Apoptotic Peptidase activating factor 1 (Apaf1) which forms apoptosome complex which in turn activates procaspase 9 and the executioner caspases 3 and 7 (Chen 2016).

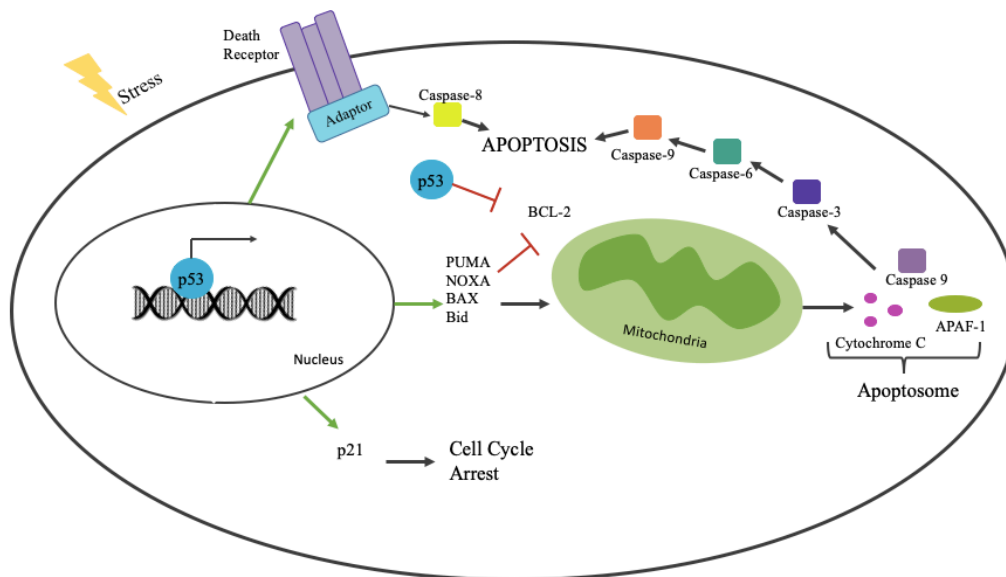


**Figure 1.1 p53 downstream pathways** When p53 is activated, depending on the severity of the damage, the cell can choose between apoptosis or cell cycle arrest. The p53 protein can activate genes related to both the intrinsic or extrinsic apoptosis pathways and also by activating p21, it can activate cell cycle arrest.

### 1.1.2. MDM2 and MDM4

*MDM2*

In the late 1980s, the murine double minute 2 (MDM2) gene was identified. This is one of three unknown genes MDM1-3 which was observed in spontaneously transformed the 3T3-DM mouse cell line (Cahilly-Snyder et al. 1987). After several studies, it was found that MDM2 protein can bind and inhibit p53 (Momand et al. 1992) and also the oncogenic character of MDM2 was also revealed because the human gene homolog, HDM2 was found in human wild-type p53 sarcomas at high levels. In 10% of human cancers, the MDM2 gene was found to be amplified (Toledo and Wahl 2006). The oncogenic property of MDM2 is related with its ability to interact with and inhibit of p53. Because p53 is an important tumor suppressor, MDM2 itself should be controlled strictly; when needed such as under stress conditions, MDM2 should set p53 free so that it can reach and activate its target genes.

The release of p53 is carried out by post-translational modifications of MDM2 which temporarily release p53 from inhibition. However, under conditions without stress, p53 is kept under control so that it does not cause any unwanted cell cycle arrest, senescence or apoptosis (Shadfan, Lopez-Pajares, and Yuan 2013). This inhibition is done in two ways, by binding to the p53 transactivation domain which prevents the transcriptional activity of p53 (Figure 1.2) (Momand et al. 1992) or by acting as E3 ubiquitin ligase which leads to the delocalization of p53 from the nucleus and finally its proteosomal degradation (Shadfan, Lopez-Pajares, and Yuan 2013). The regulation of p53 is very important especially during embryonic development. The crucial function of the MDM2 protein is shown with experiments including *mdm2*- null embryos which die in uteri. This lethality is rescued when the *p53* gene is deleted. This finding demonstrates that the MDM2 protein carries out a paramount mission because without MDM2, cells go through apoptosis which is initiated as early as the blastocyst stage (3.5 days fertilization) in an uncontrolled manner due to uncontrolled activation of p53 (Chavez-Reyes et al. 2003). As a result, MDM2 deficient embryos are smaller than wild-type MDM2 containing ones and shows disorganized structure (Gannon and Jones 2012).

#### *MDM4*

Murine double minute 4 (MDM4) also in humans HDM4 or MDMX is a homolog of the MDM2 protein and was discovered from a cDNA library screen for attempting to identify binding partners of p53 (Shvarts et al. 1996). MDM4, similar to MDM2, is negative



regulator of p53. They share 34% protein homology. MDM4 is also overexpressed in 10-20% of lung, stomach, breast and colon cancers and, 65% of retinoblastomas (Toledo and Wahl 2006). However, MDM4 has no E3 ubiquitin ligase activity like MDM2, it inhibits the activity of p53 by just binding to the p53 transactivation domain and also by forming a heterodimer with MDM2. This heterodimer is an effective degradation complex compared to a MDM2 homodimer (Gu et al. 2002). MDM4, on the other hand, cannot homo-oligomerize. MDM4 not only affects p53, but also MDM2 by increasing its stability during non-stress conditions. Binding of MDM4 prevents the auto-ubiquitination degradation of MDM2 (Gu et al. 2002). It can be said that MDM4 has a longer half-life compared to MDM2 because of this. For the effective regulation of p53, collaboration from both proteins is very important.

Another difference between the two proteins is, the absence of nuclear localization and export signals in MDM4, which means that it needs MDM2 for nuclear localization (Wade, Li, and Wahl 2013). While MDM2 is thought to be the main regulator of p53 several mice experiments conducted in mice show that the loss of either MDM2 and MDM4 cannot be compensated. Thus, *mdm4*- null mice shows embryonic lethality at E8.5-9.5. Similar to *mdm2*- null mice models, this phenotype can be rescued by the deletion of p53 (Migliorini, Denchi, et al. 2002). Thus, MDM4 is another paramount negative regulator of p53 during development. Compared to *mdm2*- null mice, *mdm4*-null mice died later so there is a time difference. Another difference is, *mdm4*-null mice lethality is observed due to absence of cellular proliferation which is completely different in the *mdm2*- null mouse model in which lethality is due to apoptosis (Gannon and Jones 2012). In the *mdm2*- null mice embryo, lethality due to increased apoptosis can be rescued through the loss of BAX which is a pro-apoptotic and p53 target gene (Chavez-Reyes et al. 2003). On the other hand, in the *mdm4*- null mice embryo, lethality due to cell proliferation arrest is rescued by the loss of cyclin-dependent kinase inhibitor 1A (Cdkn1a) which encodes the p21 protein and a p53 target gene (Steinman et al. 2004). These differences show that, two similar negative regulators of p53 have non overlapping functions.

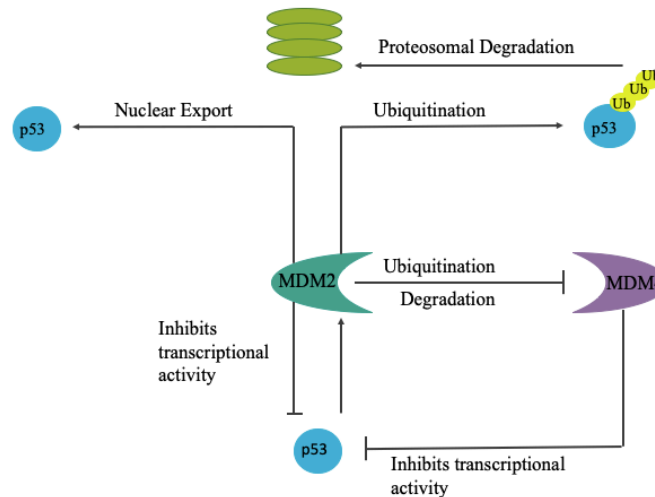


**Figure 1.2 Summary of MDM2, MDM4 and p53 interaction** MDM2 protein ubiquitinates both the MDM2s and MDM4 protein which inhibit the transcriptional activity of p53. Also p53 when it is activated can induce the expression of the MDM2 protein which is important this negative feedback loop.

## 1.2. Structure of p53, MDM2 and MDM4

### *p53*

Human p53 forms a homotetramer of 4x 393 amino acids in an active form. p53 is composed of an N-terminal transactivation domain (TAD) which is an intrinsically disordered and proline (Pro)- rich region (Figure 1.3). This is followed by a central structured DNA-binding domain (DBD). This DBD domain is connected to a tetramerization domain with a linker. At the C terminus, an intrinsically disordered regulatory domain is present. This regulatory domain is mostly composed of basic amino acids and they bind DNA nonspecifically (Joerger and Fersht 2008). The N-terminal region contains two transactivation domains which are TAD1 (1-40) and TAD2 (40-61). These are intrinsically disordered and they are rich in acidic residues (Chang et al. 1995). The proline- rich region (amino acids 64-92) is crucial for binding to the transcription machinery (Thoden et al. 2008), the transcriptional coactivators p300/ CBP and the negative regulators MDM2 and MDM4 (Schon et al. 2002). Generally important

signaling proteins which are leading or cooperating in many pathways have disordered binding sites like in the case of the p53 TAD domain, this enables binding of several different target proteins (Itoh et al. 2018). After binding to its target, the TAD changes its conformation from a disordered to ordered state. TAD1 forms an  $\alpha$ -helix when N-terminal domain of both MDM2/MDM4 and the Taz2 domain of p300 binds.

Tetramerization is important for p53, in *in vitro* tetramerization is not required for DNA binding but *in vivo* p53 without tetramerization ability, cannot efficiently act as a transcription factor (Jeffrey, Gorina, and Pavletich 2016). Without any stress, p53 levels are low in cells and the main form of p53 in these cells are as monomers. During stress conditions, however, tetramerization of p53 is induced via post-translational modification like phosphorylation at serine-392 (Sakaguchi et al. 1997). Also when p53 is activated, there is multiple phosphorylation at N terminal serine and threonine residues due to the activity of several protein kinases (Toledo and Wahl 2006). These post translational modifications cause a decline in the binding affinities of negative regulators like MDM2/MDM4, and strengthens the binding of the coactivators p300/ CBP (Lambert et al. 1998). The proline-rich region links the TAD and DNA-binding domain in human p53. The function of the proline-rich region is not known clearly (Joerger and Fersht 2008). On the other hand, the DNA binding domain contains an immunoglobulin-like  $\beta$ -sandwich region. This enables binding to DNA. One half of the DNA binding domain docks to the DNA major groove and the other half is composed of large loops and stabilized by zinc ions (Joerger and Fersht 2008).

### *MDM2 and MDM4*

MDM2 and MDM4 are structurally similar to each other (Figure 1.3). They have common domains like a N terminal p53 binding domain and a RING domain. Different from MDM4, MDM2 contains a nuclear localization signals and acidic domain. MDM2 and MDM4 interacts with p53 using a binding domain which is located at the N terminus (J Chen, Marechal, and Levine 1993). MDM2 and MDM4 have very similar p53 binding domains in which the amino acids needed for interaction between p53 are conserved (Freedman et al. 1997). With the binding of these proteins to p53, its transcriptional activity is prevented. p53 binding to this domain of MDM2 is targeted through several drugs like Nutlins (Carvajal et al. 2004). Although there is around 80% similarity between

the MDM2 and MDM4 p53 binding domains, Nutlin-3a does not bind to the MDM4 p53 binding domain due to the different topologies and electrostatic potentials of these domains of the two proteins (Karim 2017). This difference can also be understood from binding affinity of MDM2 and MDM4 towards p53. The MDM2 p53 binding domain has a higher affinity for p53 compared to that of MDM4 which can be explained by the ability of MDM2 with this enhanced affinity to shuttle p53 protein out of the nucleus for degradation (Joseph et al. 2010).

Another common domain between MDM2 and MDM4 is the RING (Really Interesting New Gene) domain. Through their RING domains, MDM2 and MDM4 can form heterodimers. In addition to this ability to form heterodimers, the MDM2 RING domain has a special function. With the help of this domain MDM2 has E3 ubiquitin ligase activity (Honda, Tanaka, and Yasuda 1997). E3 ubiquitin ligases generally have RING domains which enables interactions between proteins. By this activity MDM2 can target p53, MDM4 and itself for proteasomal degradation which is important for the negative feedback loop of MDM2-MDM4 and p53. Hetero dimerized MDM2 and MDM4 proteins were shown to be more efficient negative regulators of p53 than homodimers. This result is related with the ubiquitination catalyzed by MDM2. MDM2 homodimer by itself can only carry out the multiple monoubiquitination of p53 (Lai et al. 2001) but several studies shows that the MDM2/ MDM4 heterodimer is more effective provider of polyubiquitination (X. Wang, Wang, and Jiang 2011). For degradation mainly polyubiquitination is needed because this is a recognition signal for the 26S proteasome. On the hand, monoubiquitination has different roles independent from degradation such as endocytosis and transcriptional regulation (Hicke and Dunn 2003).

The acidic domain and nuclear localization/ export sequences are only present in MDM2. The function of the acidic domain is controversial. There are some studies showing that the acidic domain is also needed for the E3 ligase activity of MDM2 (Kawai, Wiederschain, and Yuan 2003). On the other hand, nuclear localization sequences are very crucial for MDM2 to carry out its vital role. When there is no stress, MDM2 is localized in the nucleus but with the help of both its nuclear localization and nuclear export sequences, it can shuttle between the cytoplasm and nucleus (Roth et al. 1998). Because MDM4 lacks a nuclear localization and export signal, it is generally located in

the cytoplasm when there is no MDM2 to shuttle it into the nucleus (Migliorini, Danovi, et al. 2002).

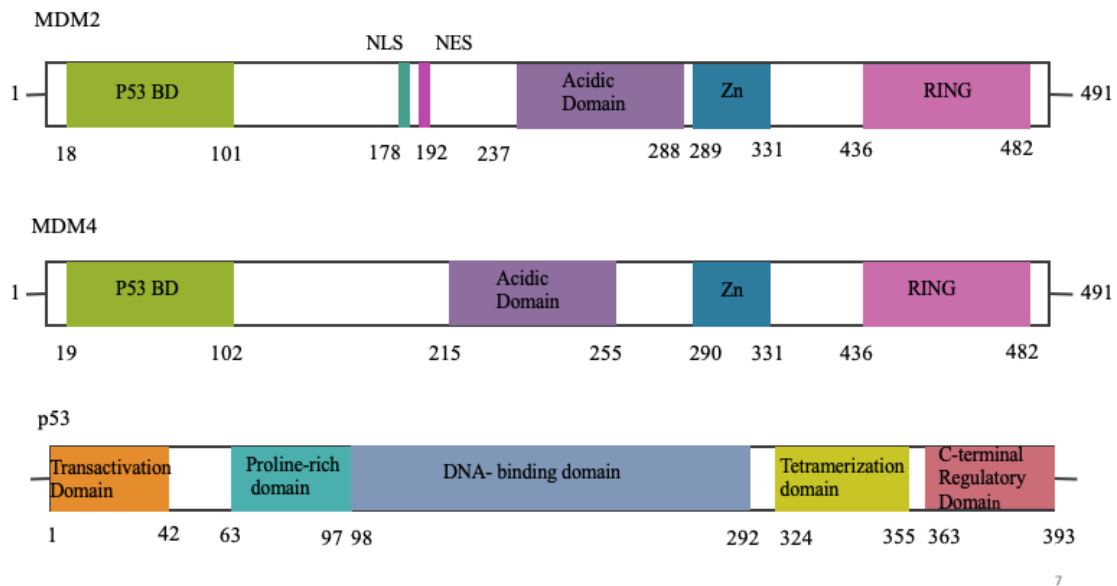


**Figure 1.3 Gene structures of MDM2, MDM4 and p53** Full length MDM2 and MDM4 each have a p53 binding domain, an acidic domain, a zinc finger domain and a RING finger domain in common. MDM2, different from MDM4, has a nuclear localization signal (NLS) and nuclear export signal (NES). p53 has a transactivation domain, proline rich domain, DNA binding domain, tetramerization domain and C-terminal regulatory domain.

### 1.3. Regulation of MDM2, MDM4 and p53 During Stress Conditions

When there is no stress, p53 is kept under control through both MDM2 and MDM4 (Figure 1.4). With the ubiquitination activity of MDM2, p53 is shuttled from the nucleus to the cytoplasm and undergoes P26 proteasome dependent degradation which keeps p53 levels a low steady state level. However, during stress conditions, p53 is released to carry out its function as the guardian of the cell. This equilibrium is enabled with several different proteins which are induced in different stress conditions. When there is no stress in the cell, an important ubiquitin- specific protease, HAUSP (Herpes virus- associated ubiquitin- specific protease) increases the stability of MDM2, MDM4 and p53 by decreasing the self ubiquitinating activity of MDM2 (Sheng et al. 2006). Also, Death-

domain associated protein (Daxx) is cooperates with both MDM2 and HAUSP and this complex increases the stability of MDM2 in the cell (Toledo and Wahl 2007).

After DNA damage occurs in the cell, a cascade of kinase reactions is initiated and several different proteins are recruited to the damage site (Figure 1.4). These activated kinases phosphorylate p53 to induce cell cycle arrest, apoptosis or senescence (Shadfan, Lopez-Pajares, and Yuan 2013). The main kinase in this cascade is, ATM (Ataxia Telangiectasia Mutated) which is activating p53. The general regulation of p53 level is controlled by the post-translational modifications on negative regulators or on the p53 protein itself. When ATM kinase is activated, it phosphorylates MDM2 at S395 which is located in the RING domain (Maya et al. 2001). In addition to this phosphorylation, ATM also phosphorylates p53 at S15 which allows p53 to escape MDM2 inhibition. This increases the transcriptional activity of p53 (Shieh et al. 1997)(Lambert et al. 1998). MDM2 stops p53 degradation and cytoplasmic export. A second DNA damage induced kinase is DNA-PK (DNA- activated Protein Kinase) which phosphorylates MDM2 again but in a different domain, on S17 in the p53- binding domain (Mayo, Turchi, and Berberich 1997). This modification in the p53 binding domain decreases the binding strength between p53 and MDM2. p53 released from MDM2 inhibition can activate downstream signaling pathways. On the other hand, ATM phosphorylates MDM4 at S403, this modification causes MDM4 to be targeted by MDM2 for proteasomal degradation (Pereg et al. 2005). Overall, these post translational modifications remove p53 from MDM2 and result in MDM2 changing its ubiquitination target from p53 to MDM4. Because MDM4 is degraded, MDM2 is not stable anymore and it degrades itself too. On the other hand, activated p53 transcriptional activity causes an increase in MDM2 levels which prevents an uncontrolled increase in p53 activity.

The mitogenic signals causes activation of several proteins. E2F1 controls the transcription of many genes related to G<sub>1</sub> and S phase in the cell cycle. Also it causes accumulation of ARF (Alternate open Reading Fame of locus p16INK4a) which will eventually leads to p53 activation (Zhu et al. 1999) by preventing the ubiquitination of MDM2 bound to p53. ARF does this by sequestering MDM2 in the nucleolus which will causes the separation of p53 from MDM2 which ubiquitinates MDM4 and itself as mentioned above. Also it was shown that ARF can interact with MDM4 and like in the case of MDM2, it can sequester MDM4 within the nucleolus (Jackson, Lindström, and

Berberich 2001). Also K-Ras and insulin-like growth factor-1 (IGF-1) can have an effect on MDM4 levels (Gilkes et al. 2008). p53 is activated when there is a problem with the regulation of ribosomal biogenesis. This activation is done by ribosomal proteins like L5, L12, L23 and S7. Also the binding of these ribosomal proteins to MDM2 initiate the degradation of MDM4, further releasing p53 from inhibition (Gilkes, Chen, and Chen 2006).

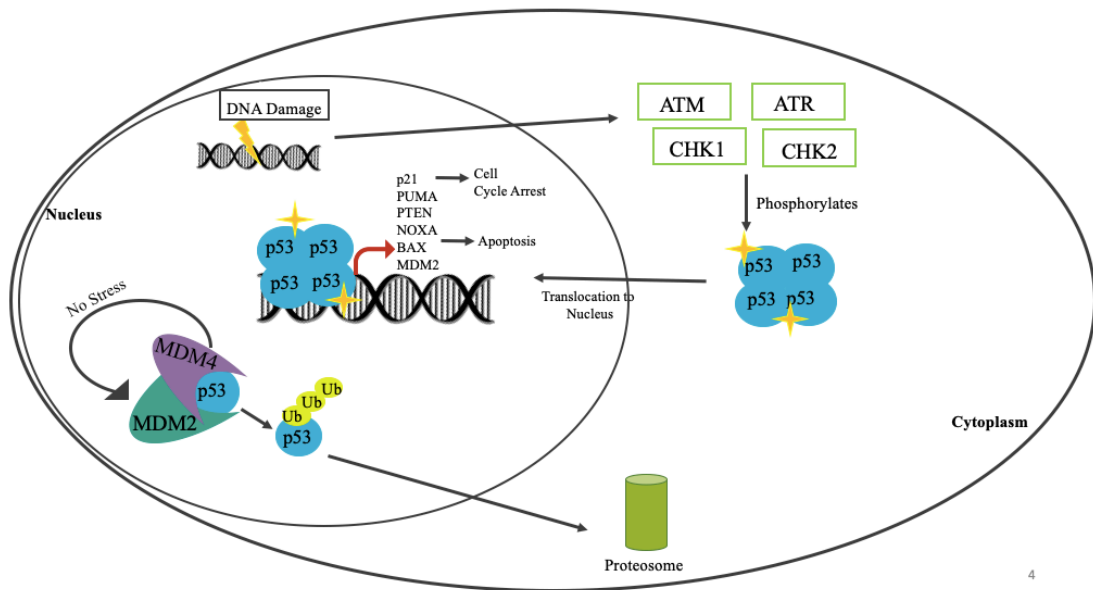


**Figure 1.4 MDM2, MDM4 and p53 pathway** When there is no stress, MDM4 and MDM2 heterodimerize using their RING domains, inhibits transcriptional activity of p53 protein and ubiquitinates the p53 protein and target it for proteosomal degradation. When there is stress or DNA damage, p53 tetramers gets phosphorylated by several kinases and this causes the translocation of p53 into the nucleus. Inside the nucleus p53 activated the transcription of genes related to cell cycle arrest or apoptosis, according to the levels of damage.

#### 1.4. Targeting the MDM4- p53 Interaction for Cancer Treatment

MDM2 is overexpressed in several cancer types like sarcomas, gliomas, melanomas and carcinomas (Onel and Cordon-Cardo 2004). In these cancer types, generally p53 is in wild type form. That's why MDM2 antagonist research is very crucial. Structural analysis

of MDM2 and p53 binding interface is essential. In this interface, three amino acids, F19, W23, L26 on p53 interact with MDM2, the small area of interaction is suitable for inhibition by small peptides or molecules (Chène 2004). One of the first compounds targeting the MDM2-p53 interaction is Nutlin-3a. This compound is a cis- imidazolidine derivative and it binds MDM2 with  $IC_{50}= 90$  nM (Vassilev 2004). In *in vitro* experiments, it is shown that Nutlin-3a separates p53 from MDM2. Tumor shrinkage and no induction in toxicity is observed in experiments with nude mice containing human xenografts tumors treated with Nutlin-3a (Toledo and Wahl 2007).

The second type of inhibitors are spiro- oxindoles (Shangary and Wang 2009) and third group is the benzodiazepinedione family (Grasberger et al. 2005). AM-7209 is another known and effective MDM2 inhibitor with  $K_D$  (dissociation constant) 38 pM. N- terminal part of MDM2 (6-24) when binds to AM-7209 becomes ordered and it folds on to the ligand which will end up in interfering with p53 binding (Rew et al. 2014). Although these compounds show high affinity towards MDM2, they have low affinity towards MDM4. Some studies show that MDM4 inhibition is more suitable and less hazardous compared to MDM2 inhibition. When MDM2 inhibitors are given, it is very possible that normal adult tissues can enter apoptosis, induced by p53 (Marine and Lozano 2009). However, MDM4 inhibitors shows no hazardous effect on normal adult tissues (Garcia et al. 2011). In addition to this, it is found that Nutlin-3a is ineffective in cells where there is MDM4 overexpression (Hu et al. 2006). These results show that, MDM4 is also a crucial target for cancer therapy. MDM4 is overexpressed in solid tumors like cutaneous melanoma, retinoblastoma and hematological malignances and it is also overexpressed in 65% of human melanomas (Gembaraska et al. 2012). For these cancer types, MDM4 is a target for therapeutics. Although, clinical trials for small molecule inhibitors of MDM4 is limited, there is still a research going on to find more potent inhibitors for MDM4.

There are several small molecules targeting MDM4 such as WK298, the binding of WK298 is similar to binding of p53 peptide, it has  $EC_{50}= 20\mu M$  (Popowicz et al. 2010). On the other hand, SJ-172550 is the first small molecule inhibitor of MDM4 binding to the N- terminal p53 interaction pocket (Reed et al. 2010). It binds to MDM4 with a  $EC_{50}= 5\mu M$  and it successfully disrupts its interaction with p53 (Reed et al. 2010). There is another study which shows a high throughput screening result for MDM4 inhibitors; three candidates are NSC207895, NSC146109 and NSC25485 (Wang et al. 2012). NSC207895



has less toxicity and shows dose dependent increase in binding to MDM4 and also they showed that it enhances p53 transcriptional activity and inhibits p53 degradation.

Another class of inhibitors are single domain antibodies. These single domain antibodies bind the p53 binding domain of MDM4. In order to find the best binding single domain antibody, a selection was performed using a synthetic single- domain VH library with random complementarity- determining regions. After multiple rounds of selection, binders were screened by ELISA and their efficiency of separation of a p53 peptide from the MDM4 N terminal cleft was evaluated. After selection, a single domain antibody (VH9) was found to be the best binder with an affinity of 44 nM against MDM4 (Yu et al. 2009). This study demonstrated that, single domain antibodies can also be used for targeting the interaction between MDM4 and p53.

## **1.5. Nanobodies**

### **1.5.1. Discovery, Structure and Advantages**

Other than small molecule or peptide inhibitors as drugs, antibody- based drugs are highly advantageous as therapeutics for several diseases like cancer, inflammatory diseases, infectious disease and allergies (Mullard 2015). Monoclonal antibodies (MAbs) are the mostly used antibody type for several purposes. They are antibodies produced by a single B lymphocyte clone. Although they have some advantages, they are not easy to produce and their cost of production is very high. Also they have a large size which is 150 kDa (Figure 1.5) (10- 15 nm long and 7-9 nm wide) and this is a limitation for tissue penetration especially very important in case of tumor therapy. In addition to this, they can initiate unwanted immune responses and because of the half- life which is several days, they are not useful for molecular imaging (Lipman et al. 2005). A new type of antibody was discovered in the 1990s by the Hamers- Casterman group, called heavy chain only antibodies (HcAbs) which are found in members of the Camelidae family (camels, llamas, alpacas and dromedaries) and sharks. These animals contain both conventional immunoglobulin G antibodies (IgG) and these heavy chain only antibodies in their sera. Heavy chain only antibodies do not have light chain and first constant

domain. In overall, they contain two constant domains CH2 and CH3, a hinge and antigen binding domain in other words variable heavy chain domain (VHH) (Hamers-Casterman et al. 1993). The VHH domain was recently expressed as a single domain and trademarked as Nanobody® by the Ablynx company.

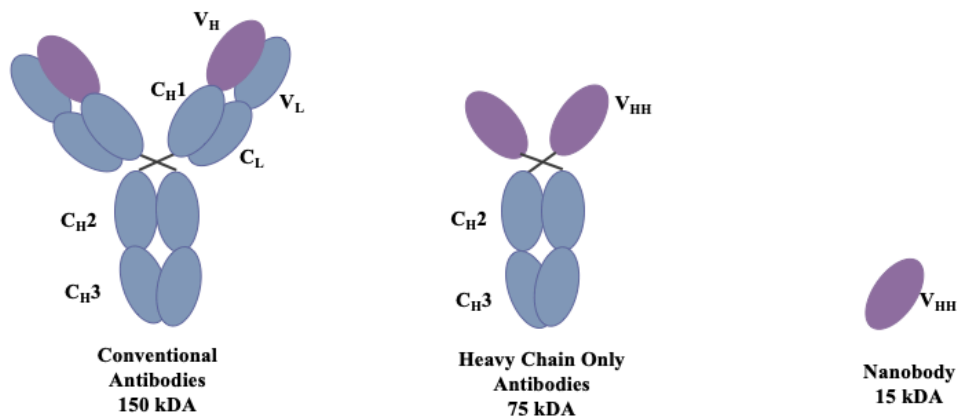


**Figure 1.5 Representation of conventional antibodies, heavy chain only antibodies and nanobodies.** The antigen binding domain is labelled in purple. For conventional antibodies, this domain is made up of both the heavy and light chains. Nanobodies are biotechnologically developed antibodies composed of only the antigen binding domain.

The VHH part of the HcAbs contains just the antigen binding portion and it still has antigen binding capability. The size of the nanobodies are around 15 kDa (4nm long and 2.5 nm wide) (Van Audenhove and Gettemans 2016). VHHs contain four framework regions and between them there are three complementarity- determining regions (CDR) (Muyldermans et al. 2009). The VHH domain has an Ig fold of two beta-sheets, those beta strands are connected via loops which are responsible for antigen recognition. The loops are connected via disulfide bonds generally so that they are not flexible and this provides antigen binding (Beghein and Gettemans 2017). In conventional antibodies, the framework region 2 (FR2) of VHs has lots of hydrophobic amino acids which enable their interaction with VLs but in nanobodies this region is exposed and does not participate in molecular interactions so it is replaced with hydrophilic amino acids (V37F, G44E, L45R and W47G). This change explains the high solubility of nanobodies and their decreased propensity for aggregation (Muyldermans 2013). The CDR3 loop is the main antigen binding domain of nanobodies and it provides 60- 80% of the contacts with the antigen

compared to CDR1 and CDR2 (De Genst et al. 2006). Also the CDR3 loop has a convex structure which provides binding to cavities or hidden epitopes on antigen surface like active site of enzymes and they mostly bind to conformational epitopes (De Genst et al. 2006). In addition to this, CDR1 and CDR3 loops in nanobodies are longer compared to conventional antibodies.

Nanobodies have advantages in size, stability and solubility. Also they have special physical and chemical robustness. During the nanobody selection process to select the best binding nanobody, harsh selection procedures can be applied like extreme temperatures, selection with presence of proteases, high pressure and low pH (Renisio et al. 2001). Nanobodies have good shelf- life, they are very stable and do not lose their binding activities when they are incubated in 37°C for 1 week (Ghahroudi et al. 1997). They can resist high temperatures like 90 °C (Linden et al. 1999). Their stability is not destroyed with the use of chaotropic agents (Dumoulin et al. 2002). In addition to this, nanobodies do not cause unwanted immune response when administrated in the human body. This is likely due to their lack of Fc regions, a property that prevents them from undergoing Fc receptor dependent internalization. In contrast to normal IgG molecules undergo rapid clearance from the blood (Muyldermans 2013).

Another advantage of nanobodies is their ability to generate multidomain constructs (Saerens, Ghassabeh, and Muyldermans 2008). Nanobodies due their size and stability shows a monomeric behavior, this enables ease in generation of multidomain nanobodies like bivalent monospecific nanobodies with high avidity towards antigen or biparatopic, monospecific nanobodies binding to different epitopes on the same antigen which again increases the avidity (Emmerson et al. 2011). Also bivalent nanobodies which are binding to two different antigens can be generated (Conrath et al. 2001). Nanobodies are encoded by a single gene which is approximately 360 base pairs can be easily linked to different molecules like fluorescent proteins, this structure is called a Chromobody®. They are very useful for real-time visualization of intracellular proteins (Rothbauer et al. 2006). Moreover, for *in vivo* imaging purposes, they can be linked to radionucleotides or near-infrared fluorophores (Chakravarty, Goel, and Cai 2014). In addition to these advantages, nanobodies can be expressed in very high amounts economically in microorganisms like bacteria (*Escherichia coli*) and yeast (*Saccharomyces cerevisiae*), also in mammalian cell lines and plants (Frenken et al. 2000)(Ismaili et al. 2007).

### 1.5.2. Production methods for nanobodies

In order to generate nanobodies for a specific antigen, several selection steps should be carried out to find the best binding nanobody. Generally, the method for this selection contains, generation of a nanobody library, panning from that library and after selection, production of that nanobody in *E. coli* or *S. cerevisiae* followed by His-Tag or GST-tag affinity purification. Initially, to form a nanobody library llamas were subcutaneously injected with the desired antigen together with Freund's complete adjuvant. Before and after each immunization the sera of the immunized llama were collected and the antibody titers were checked with ELISA. After the last immunization, blood samples from the llama were taken and peripheral blood mononuclear lymphocytes (PBMCs) were isolated. Total RNA was isolated and a cDNA library was produced with reverse transcription (Kazemi-lomedasht, Behdani, and Pooshang 2015). Because all nanobodies are encoded by a single exon and each exon has similar sequences at the beginning and at the end, the same single set of primers can be used to amplify the nanobody genes (Reverts, De Baetselier, and Muyldermans 2005).

In the second step, nested PCR is used to amplify more and to add specific restriction sites for cloning. After digestion with the desired restriction enzymes the nanobody sequences were ligated into a plasmid/phagemid, generating a library of nanobody genes (Ghahroudi et al. 1997). The VHH library in this phagemid were transferred to bacteriophages for *in vitro* phage display. Each phage (approximately  $10^{12}$ ) displays a unique nanobody on its surface from the library (which can have a complexity of  $10^6$ - $10^{11}$ ) (Bazan, Calkosiński, and Gamian 2012). The screening procedure is a multi-step procedure, each step selecting nanobodies with highest binding affinity. The selected nanobody displaying bacteriophage particles are further selected with increasing the washing solution's stringency in each step for several rounds. Phages displaying strong antigen binding nanobodies are not eliminated but others are eliminated due to this harsh selection procedure. After the last step of panning, bacteriophages are used to infect bacteria and individual colonies are used to purify nanobody proteins and identify their binding affinities (Ebrahimizadeh and Rajabibazl 2014).

Because nanobodies contain disulfide bonds and the bacterial cytoplasm is a reducing environment, is not a suitable for the formation of disulfide bonds (Stewart, Åslund, and Beckwith 1998). On the other hand, the bacterial periplasm, with disulfide bond (Dsb)

catalysts, peptidyl-prolyl cis/ trans isomerases and chaperones (Salema and Fernández 2013), is a favorable environment for the folding of nanobodies. With the help of vectors containing an N- terminal pelB leader and C- terminal protein tag like the hexa- histidine tag, selected nanobodies can be expressed and purified using periplasmic purification methods and further purified by immobilized metal- affinity chromatography (IMAC) (Salema and Fernández 2013). Following this purification, the binding affinities of individual nanobodies can be determined by surface plasmon resonance or ELISA techniques. Recently the *in vivo* steps of nanobody library generation were bypassed by the generation of naïve libraries that were selected by phage display. In this way, animal immunization were eliminated and high affinity nanobodies were selected by panning nanobodies (Reverts, De Baetselier, and Muyldermans 2005). In addition to phage display, ribosomal or yeast display methods can also be used for the selection of nanobodies.

In addition to nanobody selection from library using display methods, there are also some studies showing that nanobody binding can be optimized by *in silico* modelling. Models contain *in silico* site-directed mutagenesis and molecular dynamics simulations to visualize and measure the binding affinities of mutated nanobodies (Farasat et al. 2016). This study generated higher affinity variants of a wild type EGFR binding nanobody which is used for treatment or diagnosis of cancer. This nanobody is selected from a library by phage display. This wild type nanobody was taken as a reference and mutated at critical amino acids interacting with EGFR, their free energies were calculated by *in silico* steered molecular dynamics, where the nanobody was pulled away from the ligand and the force applied was calculated. For modelling the nanobody- ligand interaction dynamic properties, root mean square deviation was calculated for each mutated candidate. After all tests, the best binding nanobody was selected tested by *in vitro* binding assays (Farasat et al. 2016).

### **1.5.3. Uses of Nanobodies**

Nanobodies are advantageous due to their size, stability and ease of production. Primarily nanobodies are used as a research tools. For real-time and live-cell imaging in order to visualize intracellular molecules, nanobodies can be expressed, fused to green or red fluorescent proteins. These intracellular fluorescently tagged reagents were trademarked

as Chromobodies® which were generated by the Chromotek® company (Rothbauer et al. 2006). They can be expressed in cells by transfection of encoding plasmids or in stable cell lines and interact with the target without interfering with their cellular function. Due to their high specificity, they can provide superresolution images showing single-molecule localization. Also, they do not form aggregations inside the cell and they can track important components of the cell cycle with no effect on the process and viability (Rothbauer et al. 2006). In addition to intracellular protein targeting, nanobodies can also target GFP (Kubala et al. 2010) which is a fluorescent molecule that has been used to tag numerous endogenous proteins.

One application of nanobodies are in the mammalian two hybrid system that is used to detect protein- protein interactions. In this system there is a GFP tagged bait protein and mCherry tagged prey protein, when GFP nanobody is also expressed in cells, it binds to the GFP tagged bait protein, localizing it to specific foci. With this system both localization of bait and prey proteins can be observed. Moreover the activity of inhibitors of this molecular interaction can be monitored (Beghein and Gettemans 2017). For molecular imaging, nanobodies should not interfere with the function of the target protein. However, in order to explore a protein function, nanobodies interfering with its function can be used. In other words, it can be used as inhibitors (Newnham et al. 2015). Also, nanobodies can be used in protein purification and immunoprecipitation experiments. Because they are stable and monomeric, they can be easily immobilized to solid surfaces (Meyer, Muyldermans, and Depicker 2014). They can also be used for chromatin immunoprecipitation together with DNA microarrays (Nguyen-Duc et al. 2013) or for structural biology purposes like crystallization. They can stabilize dynamic proteins in a preferred confirmation or they can help the crystallization of detergent-solubilized membrane proteins (Koide 2009).

Secondly, nanobodies can be used as diagnostic tools. In order to use nanobodies in detection systems, there are several important points. When nanobodies are coated on plates for ELISA experiments, due to their small size they may not be exposed for antigen binding so C-terminal peptide extensions must be used (Harmsen and Fijten 2012). Because they are highly stable and can withstand to harsh regeneration conditions, they can be used in surface plasmon resonance based detection systems (Saerens et al. 2008). Some studies show that nanobodies can be used for pathogen diagnosis. There are

nanobodies which can distinguish *Brucella* from a similar pathogen called *Yersinia*. Nanobodies can pave the way for solving important health problems; used as diagnostic tools they can help identify the best antigens for vaccine development (Abbady et al. 2012). Also, for HIV diagnosis p24-VHH fusions were generated which can be used to detect the HIV antigen in the serum by its ability to cause agglutination (Habib et al. 2013).

Nanobodies can also be used for diagnostic imaging. Diagnostic imaging tracers used should have low background signals, high stability and solubility and low immunogenicity (Meyer, Muyldermans, and Depicker 2014). Full length of antibodies labelled with radionuclides are used as tracers but they have high serum half- life and low ratio of tumor to background signal which is not suitable for imaging purposes. Nanobodies, on the other hand, can penetrate tumor easily due to their small size and unbound nanobodies can be rapidly cleared from the body which enables high tumor to background signaling. Also, they can reach to target tissue in a few hours so this enables the use of short-lived radio nucleotides which are better to reduce side effects suffered by patients (Vaneycken et al. 2011). In addition to their use as diagnostic imaging tracers, nanobodies can be used for diagnostic cancer tests. For example, for prostate cancer, nanobodies detecting different isoforms of prostate- specific antigen (PSA) in the blood circulation were generated (Mikolajczyk et al. 2004). Nanobodies designed in a way that, they can easily discriminate between different isoforms and change conformation according to it. This is important for giving information about stages of the prostate cancer (Saerens et al. 2004).

Thirdly, nanobodies can be used as therapeutic agents. There are lots of studies about generating nanobodies against scorpion toxins, bacterial toxins and snake venom. Nanobodies are very suitable for these purposes since they can recognize special epitopes (Hmila et al. 2010). They can reach hidden epitopes which cannot be reached via conventional antibodies so this is an important advantage when considering nanobodies as therapeutic agents. Another advantage is, nanobodies are stable and they have high tumor penetration, they can be used for targeting tumor antigens (Conrath et al. 2001). For cancer therapy, there are lots of different nanobodies targeting growth factor receptors, death receptors and chemokine receptors. For example, targeting epidermal growth factor receptor (EGFR) is a commonly used target (Bruin et al. 2014), also

nanobodies can target human epidermal growth factor (HER2) (Rahimi et al. 2012). Another target for cancer therapy can be DR5 which is a death receptor (Huet et al. 2014). In addition to these, nanobodies can be used for the delivery of nanoparticles. There are several ways for the delivery of these nanoparticles like liposomes, micelles and polymer-based polymersomes (Bannas, Hambach, and Koch-Nolte 2017). For drug delivery there are some problems like poor solubility, stability, immunogenicity and rapid clearance from the body (Audenhove and Gettemans 2016). Addition of nanobodies on these nanoparticles can increase the stability, specificity and decrease the immunogenicity (Sapra and Allen 2003). Another example for the use of nanobody as therapeutic agent are CAR (Chimeric antigen receptor) expressed in T lymphocytes and natural killer (NK) cells. This system includes a single- chain fragment variable domain of an antibody specific to a target and a T cell receptor signaling domain (Maus et al. 2019). However single chain variable antibodies are not that stable, so the use of nanobodies as the antigen recognition component may be a good option for generating CAR expressing T/NK cells (Bannas, Hambach, and Koch-Nolte 2017).



## 2. AIM OF THE STUDY

p53 is an important tumor suppressor protein which has vital roles such as cell cycle arrest, senescence and apoptosis. The regulation of the p53 protein is provided by MDM2 and MDM4 proteins which are negative regulators of p53. In most cancers, either there is a mutation in p53 or an overexpression of its negative regulators. In this context, identification of inhibitors of the p53 inhibitory MDM2/ MDM4 proteins to activate p53 for targeting tumor cell death is an attractive alternative to other chemotherapeutics. For some cancers the use of MDM2 inhibitors are not enough to activate p53 so MDM4 inhibitors are needed. In this project, we used *in silico* designed nanobodies, which are single chain variable domain antibodies, as inhibitors of the interaction between p53 and the MDM4 protein. We optimized the purification of these nanobody proteins and tested their binding affinities against the MDM4 protein by surface plasmon resonance and the fluorescent two hybrid (F2H) assay.

In the first part of the project, we aimed to optimize nanobody purification. For periplasmic expression, we used the pET22b plasmid and the Rosetta 2 DE3 pLYSs bacterial expression strain. We tried osmotic pressure and whole cell lysis protocols to purify these proteins. On the other hand, for cytoplasmic expression, we generated sulfhydryl oxidase expressing BL21 DE3 cells and used the pET28a plasmid to express nanobodies in the cytoplasm.

In the second part of the project, we tested the affinity of purified anti-MDM4 nanobodies by surface plasmon resonance and compared their binding affinities of different nanobodies to p53 binding domain of MDM4 protein. In the third part of the project, we optimized fluorescent two hybrid (F2H) assay to show the interaction of selected nanobodies with the MDM4 protein. We used Baby Hamster Kidney cells (BHK) cells for this system. Both p53 and the p53 binding domain of the MDM4 proteins were tagged

with fluorescent proteins which co-localized to overlapping foci in the nuclei of these cells. The presence of an MDM4 binding nanobody resulted in the inhibition of the co-localization and was used to estimate the affinity of these nanobodies against the MDM4 protein. In summary, we aimed to optimize nanobody purification and test their binding using two different methods in order to explore novel nanobodies which can be used as therapeutics for cancers with over expressed MDM4 protein.

### **3. MATERIAL & METHODS**

#### **3.1. Materials**

##### **3.1.1. Chemicals**

All the chemicals used in this thesis is shown in Appendix A.

##### **3.1.2. Equipment**

All the equipment used in this thesis is shown in Appendix B.

##### **3.1.3. Solutions and Buffers**

Calcium Chloride (CaCl<sub>2</sub>) solution: 60 mM CaCl<sub>2</sub>, 15% glycerol and 10mM PIPES (pH 7.0) were mixed. Mixture is completed to 500 ml with ddH<sub>2</sub>O. The solution was sterilized with filter (0.22 μM) and stored at 4°C.

Agarose Gel: For 100 ml 1% w/v agarose gel, 1g of agarose powder is dissolved in 100 ml 0.5XTBE buffer with the help of heating in a microwave.

Tris-Borate-EDTA (TBE) Buffer: To prepare 1L 5X stock solution, 54g Tris-Base, 27.5g boric acid, and 20 ml 0.5M EDTA pH 8.0 were dissolved in ddH<sub>2</sub>O and stored at room temperature.

Phosphate-Buffered Saline (PBS): For 1 L 1X solution, 100 ml 10X PBS was mixed with

900 ml ddH<sub>2</sub>O. The solution was sterilized with filter (0.22 μM).

Polyethyleneimine (PEI) Solution: To prepare working solution of 1 mg/ml (w/v), 100 mg polyethyleneimine powder was dissolved in 100 ml of ddH<sub>2</sub>O. The pH was adjusted to 7.0 with 33% HCl. Then, filter-sterilized solution was kept at -20°C.

SDS Separating Gel: To prepare 10 ml 10% separation gel, 2.5ml 1.5M Tris pH 8.3, 3.34ml Acrylamide: Bisacrylamide (37.5:1), 100 μl 10% (w/v) SDS, 100 μl 10% (w/v) APS and 10 μl TEMED was mixed and completed to 10 ml with ddH<sub>2</sub>O.

SDS Stacking Gel: For 5 ml 4% stacking gel, 1.25 ml 0.5 M Tris pH 6.8, 50 μl 10% SDS (w/v), 1 ml Acrylamide: Bisacrylamide (37.5:1), 15 μl 10% APS (w/v), and 7.5 μl TEMED were mixed and completed to 5 ml with ddH<sub>2</sub>O.

Tris-Glycine Solution: To prepare 1 L 10X stock solution, 40 g Tris base and 144 g Glycine were dissolved in ddH<sub>2</sub>O and pH was adjusted to 8.3.

SDS Running Buffer: 100 ml of 10X Tris-Glycine was mixed with 895 ml dH<sub>2</sub>O and 5 ml of 20%(w/v) SDS.

Protein Loading Buffer: To prepare 4X protein loading buffer, 2.4 mL Tris from 1 M pH 6.8 stock, 0.8 g SDS, 4 ml glycerol (100%), 0.01% bromophenol blue, and 2 ml β-mercaptoethanol were mixed and was completed to 10 ml.

Lysis Buffer: In order to prepare 50 ml 1X lysis buffer, 50 mM HEPES, 250 mM NaCl, 0.5 mM TCEP, 10 mM imidazole, EDTA-free protease inhibitor cocktail (Roche) and 10 μl DNase I (100U/ μl) were mixed and completed to 50 ml with ddH<sub>2</sub>O.

Cell resuspension buffer for Osmotic Shock: 0.5 M sucrose, 0.2 M Tris pH 8 and 0.5 mM EDTA was mixed and kept in 4°C.

Tris- Sucrose- EDTA (TSE) buffer: This buffer was used for osmotic shock. 200 mM Tris-HCl at pH 8, 500 Mm sucrose and 1 mM EDTA were mixed with EDTA-free protease inhibitor cocktail (Roche). For 10 ml of TSE buffer, 1 tablet of EDTA-free protease inhibitor cocktail was used. Protease inhibitor should be added freshly to TSE buffer.

Buffer IMAC-A: To prepare 1L of IMAC-A solution, 50 mM HEPES, 250 mM NaCl, and 10 mM imidazole were mixed and completed to 1 L with ddH<sub>2</sub>O. The solution was filter-sterilized kept at 4°C. 0.5 mM TCEP was added before using the solution freshly.

Buffer IMAC-B: 50 mM HEPES, 250 mM NaCl, and imidazole were mixed and filter-sterilized. Imidazole amount is added according to the need. 0.5 mM TCEP was added before using the solution freshly. This solution was used as the elution buffer of His-tagged affinity chromatography. Elution buffer with 50 mM, 100 mM, 300 mM, and 600 mM imidazole concentrations were used.

#### **3.1.4. Growth Media**

Luria Broth (LB): For 1 L 1X LB medium, 20 g LB powder was completed to 1 L with ddH<sub>2</sub>O and autoclaved at 121°C for 15 minutes. For antibiotic selection, final concentrations of antibiotics were; kanamycin 50 µg/ml, ampicillin 100 µg/ml and chloramphenicol 34 µg/ml.

LB Agar: For 1 L 1X LB-agar medium, 35 g LB-Agar powder was completed to 1L with ddH<sub>2</sub>O and autoclaved at 121°C for 15 minutes. The antibiotic was added after cooling down. For antibiotic selection, final concentrations of antibiotics were; kanamycin 50 µg/ml, ampicillin 100 µg/ml and chloramphenicol 34 µg/ml. 15 ml of LB-Agar solution was poured into a sterile petri dish under bacteria hood and plates were kept at 4°C.

DMEM: BHK cells were maintained in culture in DMEM growth medium containing 10% heat-inactivated fetal bovine serum (FBS) and 1% PenStrep containing 100 U/mL Penicillin and 100 µg/mL Streptomycin.

Freezing Medium: Heat-inactivated fetal bovine serum containing 10% DMSO (v/v) was used for freezing cells.

Terrific Broth (TB): For 1 L 1X TB medium, 47.6 g TB powder and 8 ml glycerol was mixed, and completed to 1 L with ddH<sub>2</sub>O. The mixture was autoclaved at 121°C for 15 minutes. For antibiotic selection, final concentrations of antibiotics were; kanamycin 50 µg/ml, ampicillin 100 µg/ml and chloramphenicol 34 µg/ml.

### **3.1.5. Molecular Biology Kits**

All the molecular biology kits used are shown in Appendix C.

### **3.1.6. Enzymes**

All the enzymes; restriction and modifying enzymes, polymerases and their buffers and PCR reaction ingredients were obtained from New England Biolabs (NEB).

### **3.1.7. Bacterial Strains**

*Escherichia coli* (*E. coli*) DH-5 $\alpha$  is used for general cloning applications and *E. coli* Rosetta 2 DE3, Rosetta 2 DE3 pLysS and BL21 DE3 expression strains were used for nanobody production and purification.

### **3.1.8. Mammalian Cell Lines**

BHK: BHK21 cell line was derived from the kidneys of Syrian hamsters and the cell line we used has Lac operator repeats in their genome.

### **3.1.9. Plasmid and Oligonucleotides**

All the plasmids and oligonucleotides used are shown in Table 3.1 and 3.2 respectively.

**Table 3.1 List of plasmids**

<b>PLASMID NAME</b>	<b>PURPOSE OF USE</b>	<b>SOURCE</b>
pET22b	Bacterial expression plasmid for nanobody expression in periplasm	
pET28a	Bacterial expression plasmid for cytoplasmic expression	Lab Construct
SOX plasmid	Sulphydryl oxidase	Kindly gifted from Ario de Marco
pCDNA3.1/ myc- His (-) B	Mammalian expression plasmid with CMV promoter	Thermo Fischer Scientific, (V85520)
pCDNA3- GFP	Positive control for F2H assay, GFP expressing plasmid	Lab Construct
Pet47 b	Bacterial expression plasmid for MDM4 plasmid	Lab Construct

**Table 3.2 List of oligonucleotides**

<b>OLIGONUCLEOTIDES</b>	<b>SEQUENCE</b>	<b>PURPOSE OF USE</b>
MDM4 Nb and MDM4 CDR3 Nb XhoI Forward	ATTCCTCGAGAATGGAAGTGCAGCT  GCTGGAAAGC	Cloning for F2H assay
MDM4 Nb and MDM4 CDR3 Nb Reverse	ACCACTTCCACCGCCTCCAGAACCTC  CTCCACCTAAGCTTCTCGCGCTGCTCA  CGGTCAA	Cloning for F2H assay
Linker Forward	GGCGGTGGAAGTGGTGGCGGAGGTA  GCGGTGGAGGAGGTTCTATGAGCGAG  CTGATTAAGGAGAAC	Cloning for F2H assay
BFP BamHI Reverse	TGCTTAGGATCCTCAATTAAGCTTGTG  CCCCAGTTTG	Cloning for F2H assay
GFP CDR3 Nb Forward	ATTCCTCGAGAATGTTTGTGCAGCTGG  TGGAAAGC	Cloning for F2H assay
GFP CDR3 Nb Reverse	ACCACTTCCACCGCCTCCAGAACCTCC  TCCACCTAAGCTTCTTTTGCTGCTCACG  GTCACCT	Cloning for F2H assay



### 3.1.10. DNA and Protein Molecular Weight Markers

DNA ladder and protein ladder which were used is shown in Appendix E.

### 3.1.11. DNA Sequencing

DNA sequencing analysis was provided by McLAB, CA, USA. (<https://www.mclab.com/home.php>)

### 3.1.12. Software, Computer-based Programs, and Websites

Software, computer-based programs and websites used are shown in Table 3.3.

**Table 3.3 List of software and computer-based programs and websites**

<b>SOFTWARE, PROGRAM, WEBSITE NAME</b>	<b>COMPANY/WEBSITE</b>	<b>PURPOSE OF USE</b>
CLC Main Workbench v7.9.4	QIAGEN Bioinformatics	Cloning, primer design, sequence analysis and alignment
NCBI BLAST	<a href="https://blast.ncbi.nlm.nih.gov">https://blast.ncbi.nlm.nih.gov</a>	Alignment tool
Addgene	<a href="https://www.addgene.org">https://www.addgene.org</a>	Plasmid map information
ExpASy	<a href="https://www.expasy.org">https://www.expasy.org</a>	Protein translation and parameter tool
BIACORE T200 software v3.0	GE Healthcare Life Sciences	Controlling and evaluating SPR experiments

## **3.2. Methods**

### **3.2.1. Bacterial Cell Culture**

#### **3.2.1.1. The growth of Bacterial Culture**

*E.coli* DH5 $\alpha$ , Rosetta DE3, Rosetta DE3 pLYSs strains were cultured in LB with antibiotics for selection, overnight around 12-16 hours at 37 °C with vigorous shaking (221 rpm). In order to get single bacterial colony, the culture was spread via autoclaved glass beads onto LB-Agar plate including the antibiotics for selection and plates incubated overnight at 37 °C. For glycerol stock preparation, 10% (v/v) glycerol is added to the bacterial culture for 1 ml final volume under hood. Cryovials were used for glycerol stocks and they are stored at -80 °C.

#### **3.2.1.2. Preparation of competent bacteria**

Competent *E. coli* DH5 $\alpha$  was added into 40 ml LB in a 250 flask without any antibiotics because it has no resistance and incubated overnight at 37 °C with shaking at 221 RPM. Next day, 4 ml of overnight- grown culture was taken from 40 ml culture and put into 400 ml LB in 2L flask. In this step optical density (OD) was checked and when OD<sub>590nm</sub> reached to 0.375 incubation was stopped. 400 ml culture was separated into 8 50 ml tubes and they are incubated on ice for 10 min. Then, they were centrifuged at 1600xg for 10 min at 4°C. Supernatant were removed and pellets were resuspended in 10 ml ice-cold CaCl<sub>2</sub> solution. Cells were incubated on ice for 30 min. After incubation, cells were centrifuged at 1100 xg for 5 min at 4°C. Supernatant was removed and pellet was resuspended in 2 ml ice- cold CaCl<sub>2</sub> solution. All the suspensions were put together in 50 ml tube and separated into 200  $\mu$ l aliquots. Aliquots were put into pre-chilled microcentrifuge tubes and flash- frozen in liquid nitrogen at -80 °C. Their transformation efficiency was checked by transforming pUC19 plasmid. The same protocol was applied for preparation of Rosetta 2 DE3, Rosetta 2 DE3 pLYSs, BL21 competent bacteria.

### **3.2.1.3. Transformation of competent bacteria**

Flash frozen aliquots of bacteria were thawed on ice until it became viscous. Then plasmid with the desired concentration was added on the bacteria and incubated on ice for 30 min. After ice incubation, cells were heat shocked at 42 °C for 90 sec and put into ice for 2 min. 800 µl of LB was added and bacteria incubated in 37 °C for 45 min. After 45 min, cells were centrifuged at 13,200 rpm for 30 sec and after supernatant was removed, pellet was resuspended in 100 µl of LB and spread onto agar plate containing antibiotics and plates were incubated at 37 °C overnight.

### **3.2.1.4. Plasmid DNA Isolation**

For isolation of plasmid DNA from *E.coli* DH5 $\alpha$ , alkaline lysis protocol from Molecular Cloning: A Laboratory Manual (Sambrook et al.) was used. For midiprep, Macherey Nagel Midiprep kit was used. The acquired plasmid DNA concentration and purity analyzed by a Nanodrop spectrophotometer.

## **3.2.2. Mammalian Cell Culture**

### **3.2.2.1. Maintenance of Cell Lines**

BHK cells were maintained in complete DMEM medium in sterile 10 cm tissue culture plates and incubated in incubator which is set to 37 °C and 5% CO<sub>2</sub>. Cells were split after they reached 70-80% confluency. In order to split cells, first cells were washed with serum-free DMEM and trypsin was added afterwards. Cells waited in trypsin 5 min inside incubator which is set to 37 °C and 5% CO<sub>2</sub>. Then, cells were suspended in complete DMEM and split to a new sterile 10 cm tissue plate at 1:10 ratio. Splitting should be done every 2-3 days.

### **3.2.2.2. Cryopreservation of cells**

Cells were split to become 30-40% confluent one day before freezing. Next day, cells were counted and 1-5x 10<sup>6</sup> cells were centrifuged at 300x g for 5 min. Pellet was resuspended in 1ml freezing medium and put into a cryovial tubes. Cryovials put into a

freezing container containing isopropanol and placed into -80 °C fridge. Cryovials were transferred to the liquid nitrogen for long term storage.

### 3.2.2.3. Thawing of frozen mammalian cells

Cryovials inside nitrogen tank were taken out and quickly thawed by adding 9 ml DMEM. Cells were centrifuged at 300x g for 5 min to get rid of DMSO. Supernatant was removed and pellet was resuspended with 10 ml complete DMEM inside 10 cm tissue culture plate and incubated at 37 °C and 5% CO<sub>2</sub>. Next day, medium was changed to fresh one.

### 3.2.2.4. Transient Transfection of Mammalian Cell Lines Using Polyethyleneimine (PEI)

One day before transfection, desired number of cells were seeded according to plate type. Next day, for transfection, the required amount of DNA was mixed with 200 µl serum-free phenol red- free DMEM in a sterile microcentrifuge tube. PEI (1µg/µl) was vortexed well and added to DNA- DMEM mix (the ratio of PEI to DNA should be 3:1). The mixture was vortexed immediately after addition of PEI and incubated at room temperature 15 min. The mixture was added drop wise on top of cells. The summary of ingredients of PEI transfection in 6 well plate and their amounts shown in Table 3.4.

**Table 3.4 List of ingredients used in PEI transfection in 6 well plate.**

Cell number seeded	2.5x 10 <sup>5</sup>
DMEM amount in which cells were seeded	2 ml
Total DNA amount	3 µg

The DMEM Amount in which transfection was performed	200 $\mu$ l
PEI: DNA ratio	1:3

### 3.2.3. Vector Construction

#### Restriction enzyme digestion

Template DNA, enzymes, and its buffer was incubated for 30 min to 2 h at optimum temperature depending on the enzyme. After digestion, DNA was run on an agarose gel for cloning.

#### Dephosphorylation of 5' phosphate groups

In order to remove 5' phosphate groups, which will prevent circulation of vector after digestion, alkaline phosphatase enzyme (calf intestinal alkaline phosphatase, CIP) was used.

#### Agarose gel electrophoresis and DNA purification from the gel

CIP added vector or digested vector was run on gel. Based on the DNA fragment size, 0.7-2 % agarose gels were prepared with 100 ml of 0.5X TBE solution and then heated with microwave. After gel was heated, it was cooled and 0.0002% ethidium bromide was added and mixed well. 10 minutes later when gel was solidified, DNA samples were loaded and run at a constant voltage 100 V. In order to get the digested vector, gel extraction was carried out by cutting the DNA band from the gel.

#### Ligation

100 ng vector was used for ligation reactions with required amount of insert. Control gel with same volumes of both vector and insert can be prepared to see the ratio difference between them. After determining the ratio, ligation reaction with 1:3 vector to insert ratio

was prepared. The ligation reaction incubated at 16 °C overnight. Next day, ligation product was transformed to competent *E.coli* DH5 $\alpha$ .

### 3.2.4. Protein Purification

#### 3.2.4.1. Vector Construction

For cytoplasmic expression of nanobodies pET-28a (+) bacterial expression vector was used. The vector has C- terminal His-tag. Nanobody DNA sequences were obtained from pET-22 b (+) vector via digestion with NcoI and NotI. Also pET-28a (+) was digested with the same enzymes. Both enzymes worked at 37 °C and digested for 1 h. After digestion gel extraction was carried out and digested inserts which are Fersht original, Fersht CDR3 optimized, Fersht CDR1 CDR3 optimized, GFP original and GFP CDR3 nanobody DNA sequences, and digested pET-28a (+) was obtained. Before ligation via control gel, concentrations of each insert and vector were decided. Vector and inserts ligated with 1:3 ratio and ligation reaction incubated at 16 °C overnight. Ligation products were transformed to DH5 $\alpha$ . Next day, single bacterial colonies were picked and their pDNAs were isolated. In order to confirm whether ligations worked or not, diagnostic digestion with known cut sites were carried out.

**Table 3.5 List of ingredients for pET-28a (+) digestion**

	Insert	pET-28a (+)
DNA	2 $\mu$ g	2 $\mu$ g
CutSmart Buffer (NEB)	5 $\mu$ l	3 $\mu$ l
NcoI	1 $\mu$ l	1 $\mu$ l
NotI	1 $\mu$ l	1 $\mu$ l
ddH <sub>2</sub> O	To 50 $\mu$ l	To 30 $\mu$ l

### 3.2.4.2. His-tagged protein expression

For periplasmic expression, pET-22b (+) plasmid was used and plasmid contains all the features for protein expression and purification; T7 promoter, lac operator, LacI gene, N-terminal pelB sequence, C-terminal His-tag and finally ampicillin resistance gene for selection. LacI normally binds to lac operator and blocks the transcription of protein from T7 promoter; after IPTG was added to the medium, it competes with LacI. With the help of removing the blockage, protein can be expressed. N-terminal His-tag was needed for affinity chromatography and N-terminal pelB sequence was needed to send the protein to periplasmic space where disulfide bonds can be formed. pET-22b (+) plasmid with nanobody sequences were transformed to both Rosetta 2 DE3 and Rosetta 2 DE3 pLYSs. Rosetta 2 DE3 strains are derivative of BL21 strain and designed to express eukaryotic proteins which contains rarely used codons in bacteria. These strains have extra tRNAs for rare codons and backbone of this rare tRNA coding vector has chloramphenicol resistance gene. DE3, on the other hand, shows that the strain is a lysogen of  $\lambda$ DE3 which means a prophage presents as DNA expressing T7 RNA polymerase gene under the control of the lacUV5 promoter and protein production is controlled via IPTG. pLYSs strains produces T7 lysozyme and this system provides controlled protein production by preventing basal expression of T7 RNA polymerase and reduces the leakage in protein production.

For both expression and purification of the proteins, many methods were tried with variations. In the first trials, different osmotic pressure protocols were tried for periplasmic protein expression and purification. It generally includes, addition of Tris-Sucrose- EDTA buffer to pellet and addition of water to provide osmotic pressure which will cause shrinkage of cytoplasm and periplasmic contents were released to environment. After several trial, it was decided to check more than one colonies to see whether they are all producing the same nanobody in the same concentration. After transformation of, pET-22b (+) vectors to both Rosetta 2 DE3 and Rosetta 2 DE3 pLYSs for periplasmic protein purification several colonies were picked and inoculated into 3 ml LB containing both ampicillin and chloramphenicol. After incubation of 3 ml pre-cultures at 37 °C for 16 h 221 rpm then they were transferred to 100 ml cultures containing 40% of general ampicillin and chloramphenicol concentrations. 100 ml culture was incubated at 37 °C 221 rpm until optical density at 600 nm reaches to 0.6. After cultures reached to the desired optical density, cultures were incubated on ice and 0.5 mM final

concentration of IPTG added. Protein induction was performed by incubating the culture at 18 °C overnight in shaker incubator with 180 rpm (Figure 3.1). For negative control one culture may not be induced with IPTG.

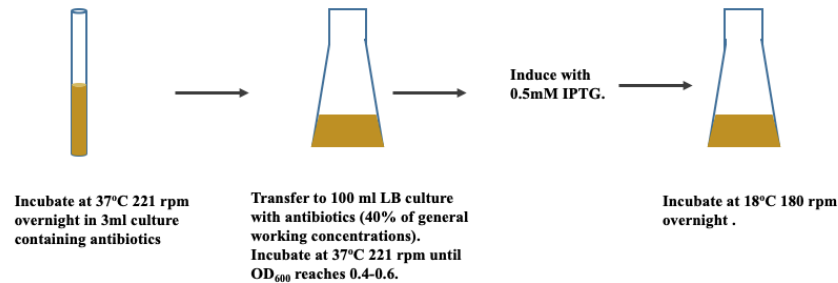


**Figure 3.1 Periplasmic protein expression and induction.**

On the other hand, for cytoplasmic expression pET-28a plasmid construct was used and it is transformed into competent BL21 DE3 strain containing SOX plasmid (Nguyen et al. 2011) Different from other methods, arabinose is added prior to induction with IPTG because disulfide bond forming enzymes is under the control of the arabinose promoter. A colony was picked from the plate and put into 5ml LB containing chloramphenicol and kanamycin and incubated overnight at 30 °C 200 rpm. Next day, 5 ml culture was transferred to 50 ml LB containing chloramphenicol and kanamycin and incubated overnight at 30 °C 200 rpm. After incubation, 50 ml culture was put in 1 L LB culture with the same antibiotics. The culture was left in incubator at 30 °C 200 rpm for a while and optical density was checked to reach 0.4. 0.5% w/v arabinose was added after the culture reached to 0.4 optical density and incubated at 30°C 200 rpm for 30 min. 0.5 mM IPTG was added and culture was induced for 4 h at 30°C 200 rpm (Figure 3.2).



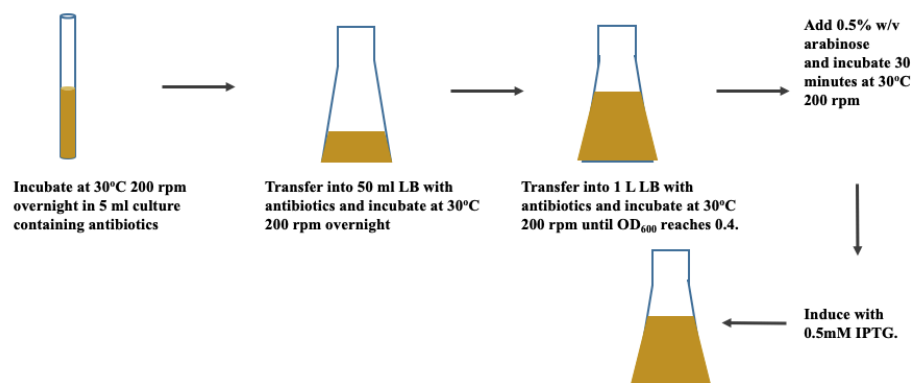


**Figure 3.2 Cytoplasmic protein expression and induction.**

### 3.2.4.3. Affinity chromatography of His tagged proteins

For periplasmic protein purification, there are three main protocols applied. First protocol which is based on osmotic pressure application to induced cultures was used (McMahon et al. 2018). Next day after induction, cells were pelleted at 3500 g 15 min at 4 °C and cells were resuspended in 100 ml cold 0.5 M sucrose, 0.2 M Tris pH8 and 0.5 mM EDTA. Cells incubated on ice 5 min and cold 200 ml water was added. 300 ml culture was put into 500 ml flask and with a magnetic stirrer, it was mixed 45 min. This step is important because it will release the periplasmic content. On top of the lysate, NaCl, MgCl<sub>2</sub> and imidazole was added as the final concentrations were 150 Mm NaCl, 2 Mm MgCl<sub>2</sub> and 20 Mm imidazole. The mixture was centrifuged at 20.000 g for 20 min at 4 °C (Figure 3.3). In order to see the protein presence in the soluble part, SDS-PAGE was carried out and afterwards according to situation, His Tag protein purification protocol was applied.

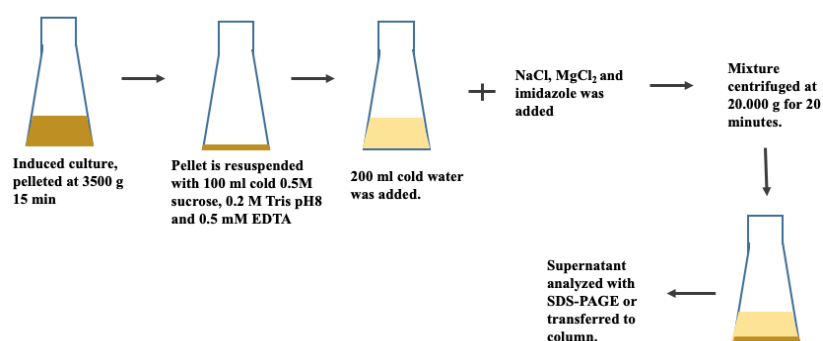


**Figure 3.3 First osmotic shock lysis protocol.**

Second protocol was also based on osmotic shock application (Quan et al. 2013). After induction, next day, 100 ml bacterial cultures were harvested by centrifugation at 3,000xg for 20 min at 4°C. Supernatants were removed and pellets were resuspended with 1 ml TSE buffer and they were incubated on ice for 15 min. 2 ml cold water was added on top of TSE buffer and pellet mixture. Suspensions were transferred to microcentrifuge tubes and centrifuged at 16,000 xg for 30 min at 4 °C. Supernatants which were containing periplasmic protein contents was transferred into new microcentrifuge tubes. In order to screen the contents of periplasms of different colonies, SDS- PAGE was carried out (Figure 3.4). After SDS- PAGE, positive colonies which are producing nanobodies were selected and the same protocol was applied with higher culture amounts. After 3 ml pre culture, the culture was transferred to 50 ml culture instead of 100 ml and afterwards it was transferred to 1 L culture and whole procedure was repeated.

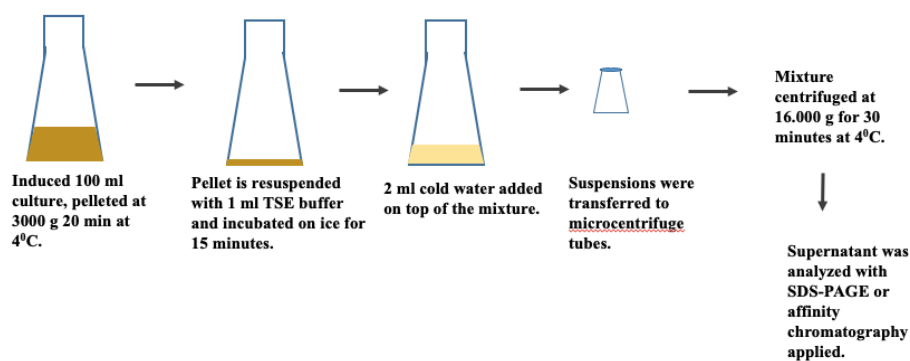


**Figure 3.4 Second osmotic shock lysis protocol.**

Third protocol tried for periplasmic expression was general whole cell lysis His tag protein purification protocol used our laboratory. Before preparing large cultures, for this one again colony screening was carried out with 3 ml precultures and induced 25 ml cultures. After that, using positive colonies large scale protein expression and purification was carried out. For large scale 1L culture and whole cell lysis, cells were harvested at 4000 rpm 10 min. Supernatant was removed and pellet was dissolved in 25 ml of lysis buffer for 1 L culture pellet. The cells were lysed at 4°C in a box full of ice by sonication using Qsonica Q500. Sonication was carried out at 5 seconds on and 10 seconds off with total elapsed time 6 min and 30 sec was used (Figure 3.5). The cell lysate was then

centrifuged at 15,000 rpm 45 min at 4°C. Samples for SDS-PAGE was taken from both pellet and supernatant.

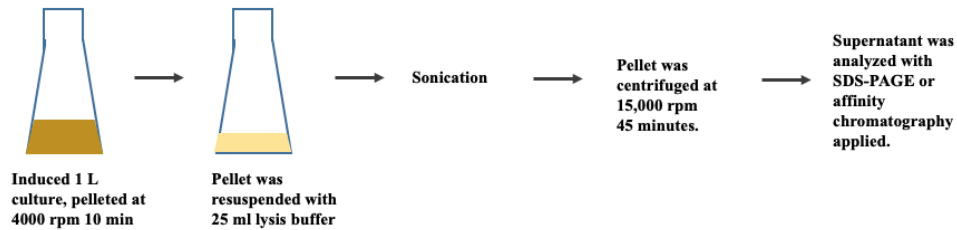


**Figure 3.5 Nanobody purification with protocol whole cell lysis protocol.**

The steps after applying supernatants to column are the same for both osmotic pressure protocols and whole cell lysis protocol. After supernatant which will be loaded to column was prepared, the column was washed with ddH<sub>2</sub>O. For 1L culture lysate, 3 ml HisPur Cobalt Superflow Agarose was added on to column. Since the resin solution was diluted 1:1 in EtOH, 1.5 ml actual resin was added. After column is loaded with resin, it was equilibrated and washed with ddH<sub>2</sub>O. After water was removed, 10 ml IMAC-A buffer was used 2 times washing. Supernatant which was coming from osmotic pressure protocol or whole cell lysis protocol was poured into column and resin-protein mixture was incubated with end- to-end rotation for 30 min at 4 °C. Flow through was collected after incubation in 50 ml tube. This fraction contains proteins which did not have His-tag. Then, resin and protein mixture in the column was washed with 10 ml IMAC A 3 times. For elution of the nanobodies, IMAC-B solutions with different imidazole concentrations were used. Starting from lowest concentration of imidazole, IMAC-B solutions were applied to column and fractions were collected in 15 ml tubes 4 °C (Figure 3.6).

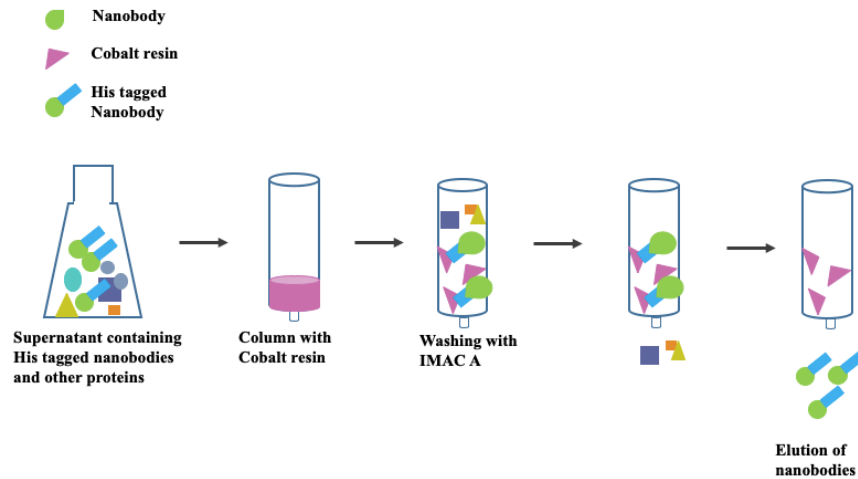


**Figure 3.6 His-tag nanobody purification with cobalt resin column.**

#### **3.2.4.4. Purification of His-Tagged proteins by Batch Method**

After His Tag protein expression and osmotic pressure application, Batch method were also used for some nanobodies. Whole procedure was carried out in 4 °C. Required amount of Cobalt Superflow Resin inside 15 ml falcon were put and centrifuged for 2 minutes at 700 xg to get rid of ethanol. 2 resin bed volumes of equilibration buffer which is IMAC A was added and mixed until the resin is fully resuspended. By centrifuge for 2 min at 700 xg buffer was removed. The supernatant containing His tag proteins, was mixed with IMAC A buffer to a volume greater than or equal to the resin bed volume. The mixture of supernatant and IMAC A was added on the tube with resin and mixed slowly for 30 min. After centrifuge for 2 min at 700x g, supernatant was removed. Resin was washed with two resin bed volumes of IMAC A. Again after centrifuge with the same conditions, supernatant was removed. This washing step was repeated 3 times. Elution step was carried out by addition of IMAC D buffer on the resin and mixture was rotated 10 min. After that by centrifuge for 2 min at 700 g, supernatant was removed and elution steps were repeated 2-4 times and each fraction was separated into different tubes. The content of fractions was checked via SDS-PAGE.

#### **3.2.4.5. SDS-PAGE gel and Coomassie Blue Staining**

14% separating gel and 4% stacking gel were prepared and the samples from each step of protein purification, cell lysate after sonication, pellet, non-retained fraction and elutes were mixed with 4X protein loading buffer and denatured at 95 °C for 10 min. After the samples were loaded, it was run with 1X running buffer for 2- 2.5 h. The gel was separated from the glasses after the run. The stacking part of the gel was discarded and separating part of the gel was stained with Coomassie blue with the help of heating via microwave with the staining solution prior to incubation overnight.

#### **3.2.5. Surface Plasmon Resonance**

BIACORE T200 was used for surface plasmon resonance (SPR) experiments. SPR is a method for investigating quantitative protein- protein interactions and kinetic parameters of these protein interactions. This method is basically uses the change in refractive indices when polarized light hits a gold film. There is light source and via prism light is focused on the gold film and reflected light is collected with a detector (Figure 3.7). The system relies on change in refractive index of medium at the interface and it depends on the mass attached to gold surface. According to mass change on the surface, refractive index is changing proportionally and some part the light is absorbed. This gives information about the quantification of the binding occurs on the surface as resonance unit (RU).

In this method, ligand is the attached molecule on the gold surface and analyte is the molecule in mobile phase which is flowing on the surface of the chip with running buffer. There are several steps to follow such as, pH scouting and immobilization of the ligand on the surface, injection of ligand and regeneration of the surface. In this study, p53 binding domain of MDM4 was immobilized covalently on Sensor Chip CM5. CM- series sensor chips carry a matrix of carboxymethylated dextran attached to gold surface. The ligand, which is p53 binding domain of MDM4, was covalently attached to sensor surface via amine coupling. For immobilization, initially, surface of the gold chip should be activated. For activation, mixture of 1-ethyl-3-(3- dimethylaminopropyl) carbodiimide (EDC) and N- hydroxysuccinimide (NHS) was used. When EDC and NHS was passed on the surface, it reacted with carboxyl groups of the dextran and formed succinimide esters. This reactive ester groups interact with amino groups of ligand and formed

covalent bonds between dextran surface and ligand. For this reaction to be successful, electrostatic interaction between ligand and dextran should be strong. The dextran matrix has negative charge at pH values above 3.5. The matrix should have negative charge and ligand should have positive charge so isoelectric point of the ligand should also be considered. To provide this, the pH of immobilization buffer which is acetate buffer should be above 3.5 and below the isoelectric point of the ligand. In order to decide the pH of acetate buffer for coupling, pH scouting was carried out. Different acetate buffers were used such as pH 4, 4.5, 5 and 5.5 and the interaction with the surface and ligand was compared by examining the RU differences.

After pH scouting, immobilization with the decided acetate buffer was performed and deactivation of unbound surface was done with ethanolamine with pH 8.5. In the second step, different concentrations of analyte, which was MDM4 Nb, MDM4 CDR3 Nb and GFP Nb, passed on the surface separately. Dilutions for nanobodies was prepared with HBS-EP + buffer which also used as running buffer in SPR system. After this step, regeneration of the surface was performed to remove the bound analyte from the ligand on the surface. This step is very important because it affects the binding activity of the surface for further experiments and life time of the chip. For regeneration step, NaOH was used and chip was prepared for further experiments.

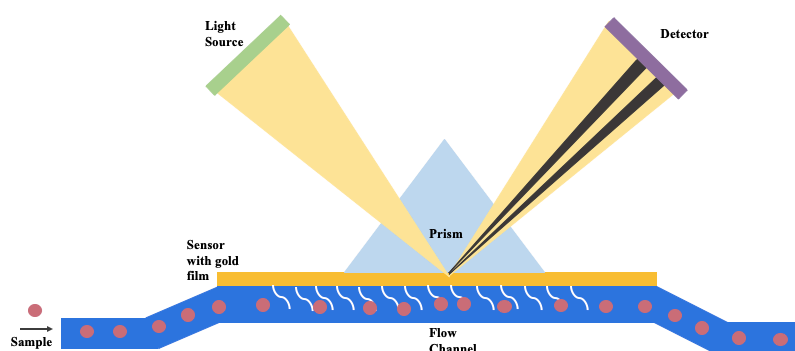


**Figure 3.7 Representation of surface plasmon resonance.**

### **3.2.6. Fluorescent two- hybrid (F2H) assay**

#### **3.2.6.1. pcDNA 3.1/ myc- His (-) B- Nanobody BFP Vector Construction**

pcDNA 3.1/ myc- His (-) B vector which is a mammalian expression vector was selected since it had XhoI and BamHI cut sites in multiple cloning site in the correct order. Nanobody sequences such as Fersht original, Fersht CDR3 optimized and GFP CDR3 optimized were obtained from pET22b plasmids via PCR with Fersht Original and Fersht CDR3 XhoI forward and reverse primers (Table 3.5). BFP protein sequence, on the other hand, obtained from PRLI BFP plasmid via PCR with linker forward and BFP reverse primer. 5' end of nanobody reverse primers and 5' end of linker primer is complementary to each other. PCR products were run on gel and gel extraction were carried out for each of them. Nanobody sequences with part of linker sequence and BFP sequence with part of linker sequence denatured at 95°C and annealed when temperature was gradually decreased. Before this reaction, control gel was run to see the concentrations of each DNA band. According to concentrations, 1:1 ratio was used for annealing the two DNA fragments. Gel extraction was carried out afterwards. In order to ligate nanobody sequences linked to BFP sequence to pcDNA 3.1/ myc- His (-) B vector, both insert and vector were cut via BamHI and XhoI enzymes (Table 3.6). After digestion, gel extraction was carried out and control gel were prepared to ligate both vector and inserts in 1:3 ratios. Ligation product was transformed to DH5 $\alpha$ . Single bacterial colonies were picked and their pDNAs were isolated. In order to confirm whether ligations worked or not, diagnostic digestion with known cut sites were carried out.

**Table 3.6 Reaction conditions for PCR by Q5 polymerase**

5X Q5 reaction buffer	5 $\mu$ l
10 mM dNTP	0.5 $\mu$ l
10 $\mu$ M forward primer	1.25 $\mu$ l
10 $\mu$ M reverse primer	1.25 $\mu$ l
Template DNA (1 ng)	1 $\mu$ l
Q5 Polymerase	0.25 $\mu$ l
ddH <sub>2</sub> O	To 25 $\mu$ l

**Table 3.7 Double digest with XhoI and BamHI of both vector and inserts**

	Insert	pcDNA 3.1/ myc- His (-) B
DNA	2 $\mu$ g	2 $\mu$ g
CutSmart Buffer (NEB)	5 $\mu$ l	3 $\mu$ l
XhoI	1 $\mu$ l	1 $\mu$ l
BamHI	1 $\mu$ l	1 $\mu$ l
ddH <sub>2</sub> O	To 50 $\mu$ l	To 30 $\mu$ l

### 3.2.6.2. PEI transfection of F2H- assay plasmids

After 200.000 cell / well BHK cells were seeded in 6 well plate, 1  $\mu$ g from each plasmid, TagGFP-p53, TagRFP- MDM4, pcDNA3.1/ myc- His (-) B- GBP-LacI and pcDNA3.1/ myc- His (-) B- Nanobody BFP were transfected with 12  $\mu$ l PEI.



## 4. RESULTS

### 4.1. Optimization of Nanobody Binding

In this study we aimed to identify high affinity nanobodies binding to the human MDM4 protein and test their ability to block the interaction between MDM4 and p53. We tested five nanobodies for this function (Table 4.1). Two of these nanobodies were used as a reference and optimized by *in silico* design. Reference nanobodies are from Yu *et al.*, 2009 which was previously developed against the p53 binding domain of MDM4 and from Kubala *et al.*, 2010, which is against the green fluorescent protein (GFP). These will be referred as MDM4 Nb and GFP Nb respectively. These reference nanobodies were used to generate new nanobody candidates, which were optimized for binding to the p53 binding domain of the MDM4 protein better than the references, by *in silico* mutagenesis of their complementarity determining regions (CDRs). The best candidate nanobodies were selected by molecular docking and steered molecular dynamics (Manuscript in preparation, Hacısüleymanoglu *et al.*). The Derived nanobodies are, MDM4 CDR3 Nb, MDM4 CDR1 CDR3 Nb and GFP CDR3 Nb.

**Table 4.1 Predicted molecular weights of nanobodies used in the study**

Nanobodies	Molecular Weight (kDA)
MDM4 Nb	15 kDA
MDM4 CDR3 Nb	15 kDA
MDM4 CDR1 CDR3 Nb	15 kDA
GFP Nb	13.9 kDA
GFP CDR3 Nb	13.9 kDA

#### 4.1.1. Periplasmic Expression

To test the success of *in silico* affinity optimization on nanobody affinity, we expressed and purified the nanobodies shown in Table 4.1 in *E.coli*. Both the reference and the derived nanobodies have disulfide bonds. The cytoplasm of the bacterial systems is not suitable for disulfide bond formation because it is a reducing environment and for the formation and stability of disulfide bonds, an oxidizing environment is necessary (Stewart, Åslund, and Beckwith 1998). On the other hand, the bacterial periplasm has an oxidizing environment and expresses enzymes for disulfide bond formation. We aimed to direct our nanobodies to the periplasmic space for proper folding. For this purpose, we cloned these nanobody encoding cDNA's into different bacterial expression plasmids, used these to transform bacteria and attempted to extract these nanobody proteins by different lysis and purification methods.

First, we used the pET22 b (+) plasmid for the periplasmic production of nanobodies. The plasmid encodes an N terminal pelB leader sequence for directing nanobodies to the bacterial periplasm and a C- terminal His tag for affinity purification. Starting from the protein sequences of the five different nanobodies, we reverse translated protein sequences using the EMBOSS Backtranseq online tool (Rice, Longden, and Bleasby 2000)([https://www.ebi.ac.uk/Tools/st/emboss\\_backtranseq/](https://www.ebi.ac.uk/Tools/st/emboss_backtranseq/)). Then sequences were commercially synthesized in the pET22 b (+) plasmid (<https://www.biocat.com>). We transformed the synthetic plasmids into the chemically competent Rosetta 2 DE3 pLYSs bacterial strain. This is a strain designed to express eukaryotic proteins at the high levels because it contains the pLYSs plasmid which expresses tRNAs for rare codons. This strain is designed to have low levels of basal expression before induction because the T7 promoter which initiates insert transcription is blocked by the LacI protein which can be released by induction with IPTG, a lactose analog, that results in high levels of expression.

We first attempted to express and purify nanobody proteins using a previously published protocol (McMahon et al. 2018). For our initial attempt to express the MDM4 Nb (Yu et al. 2009), we prepared 3ml and 50 ml pre cultures, transferred these to an 1L culture and amplified the transformed bacteria overnight at 37 °C with vigorous shaking. We induced

protein expression with IPTG and harvested induced cells by centrifugation. We resuspended these cells in ice cold lysis solution containing sucrose and added ice cold water to induce osmotic shock. We separated soluble proteins from non-soluble cell debris and analyzed lysate, pellet and supernatant fractions by SDS gel electrophoresis. To capture any protein in the supernatant fraction, we loaded the supernatant onto a previously equilibrated His tag affinity column. The bound proteins were washed with a high salt buffer with low concentrations of imidazole in order to remove non-specific binding. Bound proteins were eluted using 400 mM and 600 mM imidazole. The protein contents of these different fractions were analyzed on an SDS-PAGE gel. (Fig. 4.1).

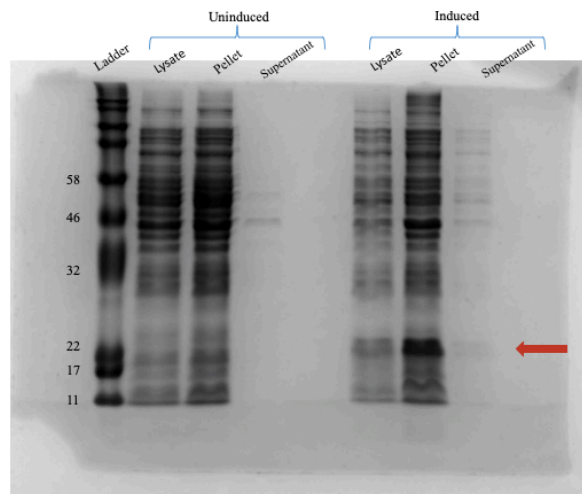


**Figure 4.1 Periplasmic nanobody expression using an osmotic shock protocol.** Before His tag affinity column, the expressed MDM4 Nb protein was analyzed on a 14% SDS-PAGE gel. The expected protein size is around 15 kDA. Compared to uninduced controls, IPTG induced samples contained a band at the expected size but this protein was predominantly localized in the pellet fraction and only a minor fraction was in the soluble supernatant.

The appearance of a specific band at the expected size indicated that the constructed expression plasmid and the induction of expression was successful. But in the supernatant fraction, the amount of MDM4 Nb was not detectable. This may be due to the low concentration of protein because of the dilution of the nanobody protein during the osmotic shock procedure. To purify and concentrate this protein, we performed affinity

purification by binding the His tagged protein with a nickel affinity matrix and we performed elutions with increasing concentrations of imidazole, 400 mM and 600 mM (Figure 4.2).

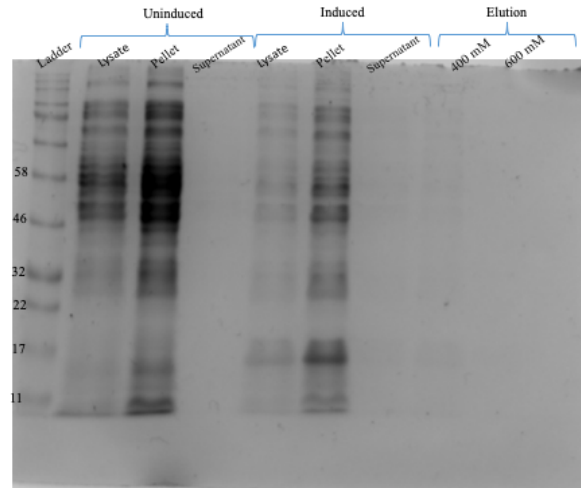


**Figure 4.2 Periplasmic nanobody purification.** MDM4 Nb expressed in 14% SDS-PAGE gel was used and expected protein size is around 15 kDA.

We could not purify MDM4 Nb with this protocol. Although there is no problem in induction, the nanobody proteins was insoluble and remained in the pellet fraction. This could be due to incorrect folding of these proteins in the periplasmic space or possibly due to problems in secretion into the periplasm even though they contained a pelB leader sequence. To increase the amount of soluble nanobodies, we tried to optimize the culture size and altered the composition of buffers used in the lysis. Lysis of bacterial cells in TSE buffer containing Tris, Sucrose and EDTA followed by ice- cold water for osmotic shock was successful (Quan et al. 2013). After lysis and centrifugation, we were able to detect nanobodies in the supernatant fractions. Unfortunately, the MDM4 Nb expressing Rosetta 2 DE3 pLYSs cells lysed during osmotic shock treatment, possibly due to the overexpression of this protein. However, GFP Nb expressing Rosetta 2 DE3 pLYSs cells were intact and could be lysed and proteins from these lysates were identified in the soluble fractions (Fig. 4.3). We tried expressing and extraction all five nanobodies using this protocol, but, similar to MDM4 Nb expressing bacteria, GFP CDR3 Nb expressing bacteria could not yield soluble protein in the supernatant after centrifugation (Figure 4.3).

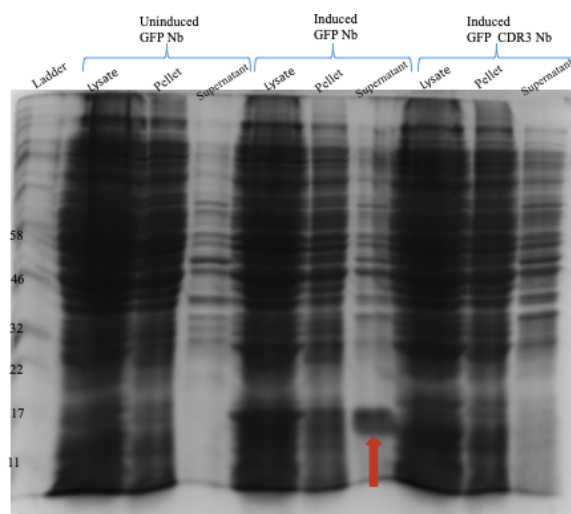


**Figure 4.3 Periplasmic nanobody expression.** GFP Nb and GFP CDR3 Nb was induced and their expression identified using 14% SDS-PAGE gels and we observed a band in the soluble fraction of the GFP Nb and not the GFP CDR3 Nb expressing lysates at the expected protein size, around 13.9 kDa.

GFP Nb was induced clearly when compared to uninduced controls and also it was in the supernatant. On the other hand, we could not detect a clear induction of GFP CDR3 Nb likely due to the low resolution of this gel. We continued to purify the GFP Nb using a batch method for His- tagged proteins. After this observation, the next step which is, purification was applied for GFP Nb (Figure 4.4). We examined the fractions for the presence of His- tagged proteins by SDS-PAGE. The non- retained fraction was the fraction which contains proteins not binding to the cobalt resin. The fractions from the washing step were also collected and as before with affinity chromatography, we performed the elutions with increasing concentrations of imidazole (Figure 4.4).

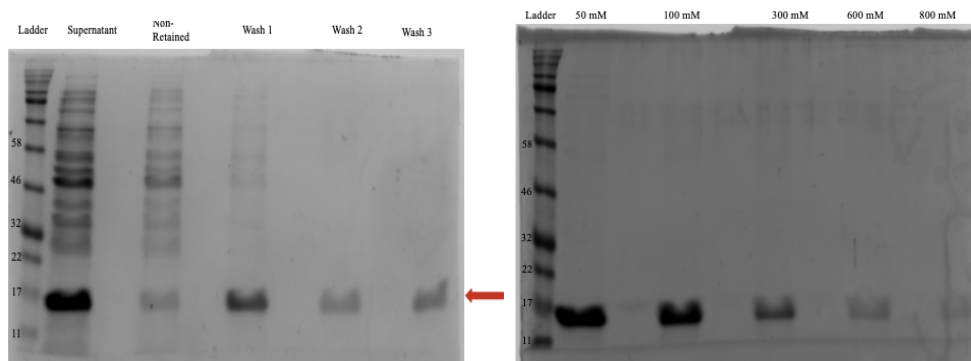


**Figure 4.4 Periplasmic nanobody purification.** Non-retained, washing supernatants and the elutions of GFP Nb were examined by SDS-PAGE. GFP Nb was purified with His tag batch method. Concentrations of purified proteins in the eluted fractions were, 50 mM Imidazole elution: 0.42 mg/ml, 100mM Imidazole elution: 0.26 mg/ml, 300Mm Imidazole elution: 0.02 mg/ml. For long term storage, the 50 mM and 100mM Imidazole elutions were pooled with the addition of 20% glycerol and snap frozen in liquid nitrogen. 14% SDS-PAGE gel was used and the expected protein size is around 13.9 kDA.

For GFP CDR3 Nb, we performed colony screening (Figure 4.5). After transformation of the GFP CDR3 Nb encoding plasmid into the Rosetta2 pLysS bacterial expression strain, we observed that colonies formed were not uniform in size and shape and this finding raised the possibility that basal level of leaky expression of this protein may be toxic to bacterial cells and we questioned whether all colonies were capable of producing the nanobody or not. By using the protocol of Quan *et al.* 2013, we induced protein expression in small scale and tested the protein expression in several colonies selected from the transformation plate. After application of the osmotic shock lysis and the centrifugation, we observed that for most samples the pellet and supernatant were not clearly separated.

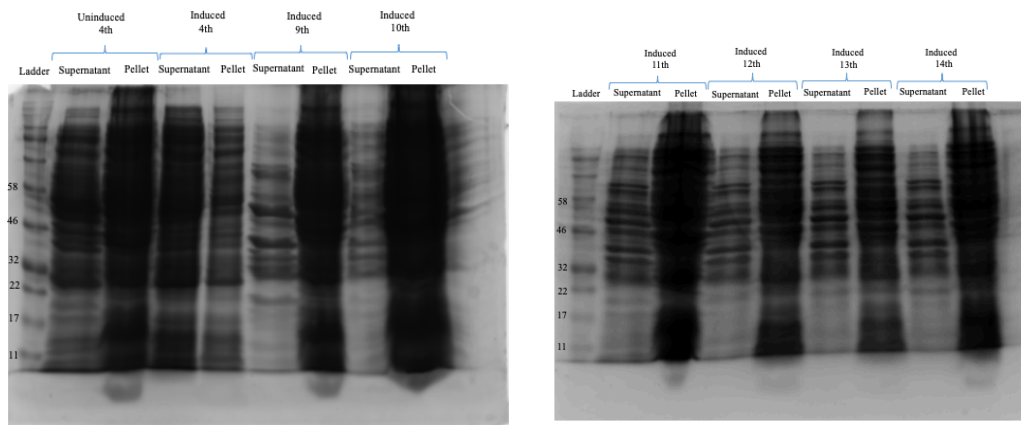


**Figure 4.5 Colony screening for GFP CDR3 Nb expression.** 7 colonies were screened. There were no positive colonies for GFP CDR3 Nb expression. 14% SDS-PAGE gel was used and expected protein size is around 13.9 kDa.

Next, we performed colony screening to transformed bacteria expressing MDM4 CDR3 Nb and MDM4 CDR1 CDR3 Nb. We selected 3 colonies from each transformation plate and applied the same protocol that was performed on the GFP CDR3 Nb. Different from the previous protocol, after we applied osmotic shock and centrifugation, we applied sonication after the lysis buffer application because the pellet was sticky and difficult to load to the SDS-PAGE gel due to cell lysis. We used a whole cell lysis protocol which contains HEPES, NaCl, imidazole, TCEP, protease inhibitors and benzonase. The high viscosity of the pellet was decreased by DNA shearing and digestion by sonication and benzonase treatment. For sonication, we used Diagenode Bioruptor with a cycle consisting of 20 seconds on and 20 seconds off for 5 min. As before, the supernatant and pellet fractions were separated and analyzed by SDS-PAGE (Figure 4.6).

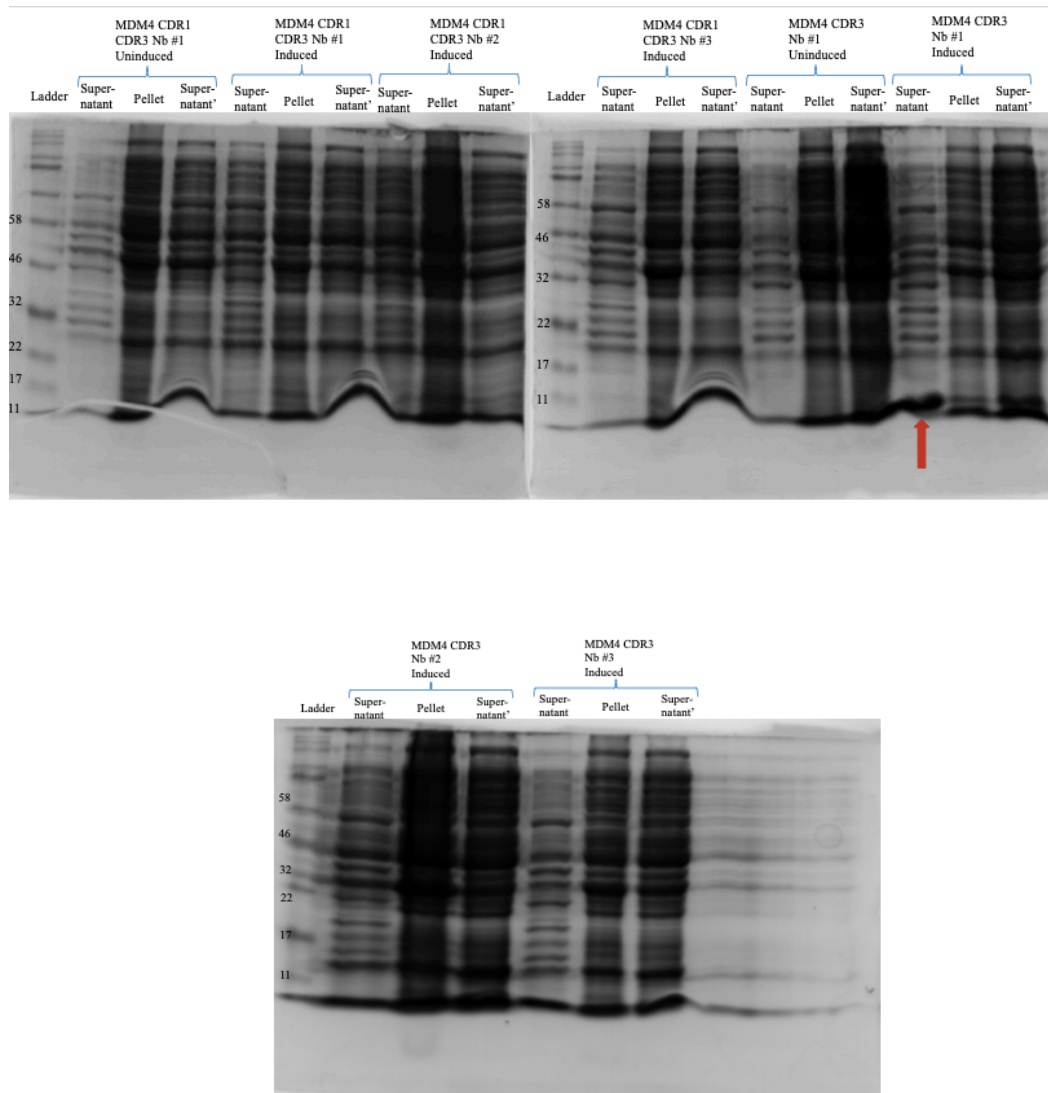


**Figure 4.6 Colony screening for MDM4 CDR3 Nb and MDM4 CDR1 CDR3 Nb expression.** There was no positive colonies for MDM4 CDR1 CDR3 Nb but for MDM4 CDR3 Nb, there was induction but it was not clear due to the low resolution of the gel. 14% SDS-PAGE gel was used and expected protein size is around 15 kDa.

Because we were not able to obtain soluble nanobody proteins in the periplasmic expression systems, we decided to apply the whole cell lysis protocol instead of the osmotic shock protocol. We induced a 1L culture with 0.5mM IPTG, resuspended the pellet in lysis buffer and sonicated in a Qsonica Q500 sonicator with 5 seconds on and 10 seconds off with amplitude 40%. We centrifuged the cell lysate again and loaded the supernatant to a column with 3 ml cobalt affinity resin. After several washes with IMAC



A buffer, we eluted bound proteins with 50mM, 100mM, 300mM and 600mM Imidazole containing elution buffer (Figure 4.7).

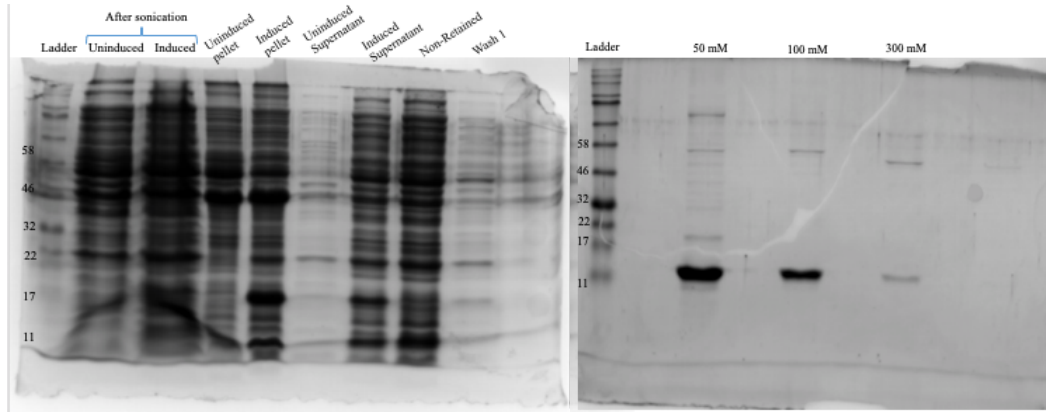


**Figure 4.7 Periplasmic nanobody purification with the whole cell lysis protocol.** MDM4 CDR3 Nb was purified. Concentrations of nanobody proteins obtained in the various elution fractions were, 50 mM Imidazole elution: 0.8 mg/ml, 100mM Imidazole elution: 0.3 mg/ml. For long term storage, the 50 mM and 100 Mm Imidazole elutions were pooled with the addition of 20 % glycerol and snap frozen in liquid nitrogen. 14% SDS-PAGE gel was used and expected protein size is around 15 kDA.

To optimize the expression of the MDM4 Nb and GFP CDR3 Nb we performed colony screening and found positive colonies for bacteria transformed with MDM4 Nb expressing plasmids. For colony screening, we induced 25 ml cultures and boiled the pellets with 4x Laemmli Buffer at 95 °C and analyzed by SDS-PAGE. On the other hand, unfortunately we could not find any colonies expressing the GFP CDR3 Nb. This may be because of a problem with the expression vector which is being re-analyzed.

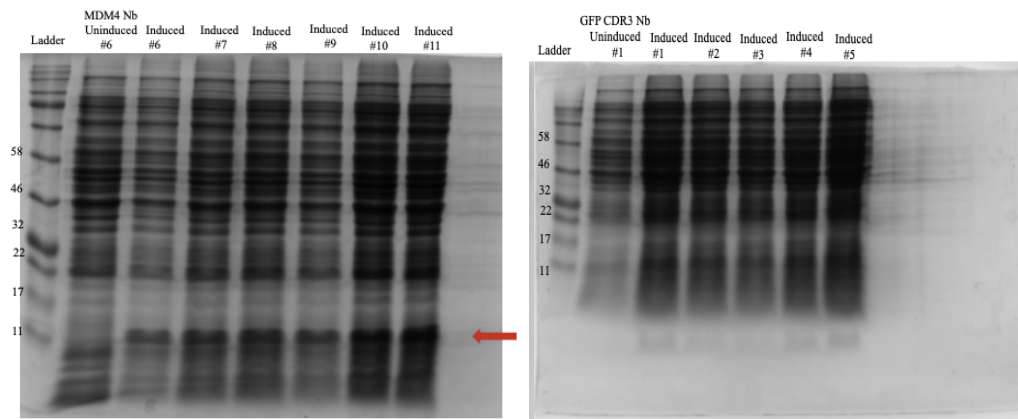


**Figure 4.8 Colony screening for MDM4 Nb and GFP CDR3 Nb expression.** There were positive colonies for MDM4 Nb but there was no positive colony for GFP CDR3 Nb. 14% SDS-PAGE gel was used and expected protein size was around 15 kDa for MDM4 Nb and 13 kDa for GFP CDR3 Nb.

We choose the 6<sup>th</sup> colony from MDM4 Nb colony screening to continue with the protein purification and we applied the protocol for whole cell lysis His tag protein purification (Figure 4.9). For the GFP CDR3 Nb, colony screening was performed again but colonies were not positive. We induced a 1 L culture with 0.5mM IPTG and after cell lysis, supernatant fractions were separated by affinity chromatography using cobalt affinity columns.

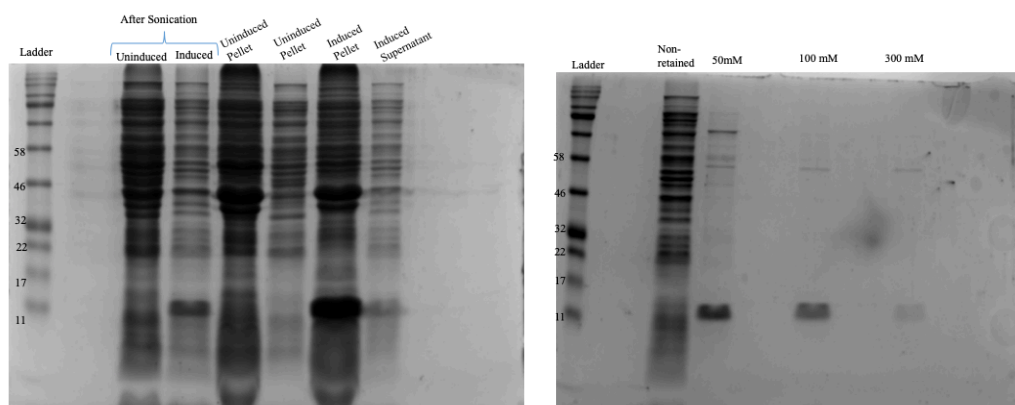


**Figure 4.9 Periplasmic nanobody purification with the whole cell lysis protocol.** MDM4 Nb was also purified with this method. Concentrations of nanobody proteins obtained in the various elution fractions were, 50 mM Imidazole elution: 0.34 mg/ml, 100mM Imidazole elution: 0.15 mg/ml. For long term storage, the 50 mM and 100 Mm Imidazole elutions were pooled with the addition of 20 % glycerol and snap frozen in

liquid nitrogen. 14% SDS-PAGE gel was used and expected protein size is around 15 kDA.

We re-attempted the identification of MDM4 CDR1 CDR3 Nb expressing bacteria by repeated colony screening. For new colony screenings, new transformations were carried out (Figure 4.10). We induced 25 ml cultures with 0.5mM IPTG and whole cell lysis was carried out with 4x Laemmli buffer at 95 °C. From colony 3, we prepared a preculture for His tag affinity purification (Figure 4.11). We applied the same protocol for whole cell lysis to a 1 L culture. However, although there was the induction of nanobody, nearly all of the nanobody protein was stuck in the pellet. This failure may be due to the hydrophobicity of the protein itself or inappropriate induction conditions such as high IPTG concentrations that result in rapid induction which precludes the expression in the periplasm.

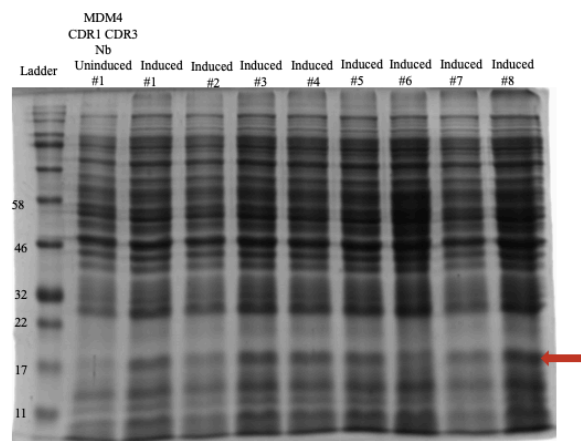


**Figure 4.10 Colony screening for MDM4 CDR1 CDR3 Nb expression.** There are positive colonies for MDM4 CDR1 CDR3 Nb. 14% SDS-PAGE gel was used and expected protein size is around 15 kDA for MDM4 CDR1 CDR3 Nb.

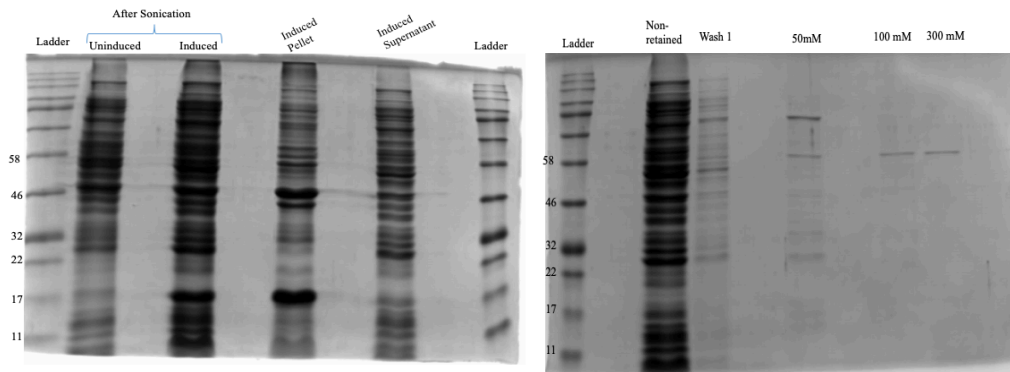


**Figure 4.11 Periplasmic nanobody purification with the whole cell lysis protocol.** MDM4 CDR1 CDR3 Nb could not be purified because it was insoluble in the pellet fractions.

Unfortunately, after repeated attempts, the MDM4 CDR1 CDR3 Nb protein was stuck in the pellet fractions. In order to optimize the induction time, we performed a time course induction of expression experiment from 5, 10 and 15 hours. We prepared 3 ml pre cultures and we performed induction inside 40 ml with 0.5 mM IPTG. Then we incubated cultures at 18 °C 180 rpm according to the time periods mentioned. After induction, we applied the whole cell lysis protocol with sonication. Unfortunately, 5 hours induction was not sufficient to express nanobody proteins in these bacteria, and while 10 and 15 hours inductions revealed the presence of expressed proteins, these were again insoluble in the pellet fractions. We suspect this insolubility problem is due to the insoluble character of the specific protein (Figure 4.12).

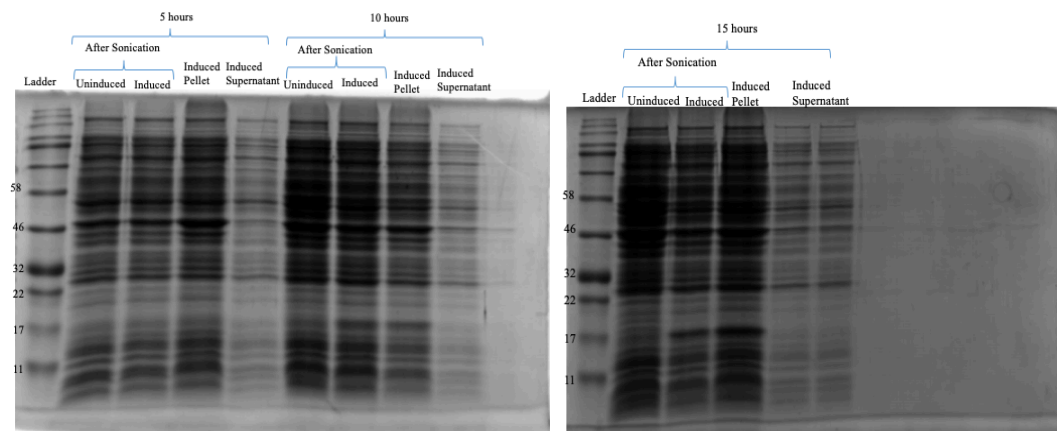


**Figure 4.12 Time dependent periplasmic nanobody expression with whole cell lysis protocol.** MDM4 CD1 CDR3 nanobody was expressed for 5 hours, 10 hours and 15 hours but failed to be expressed in the soluble fraction.

#### 4.1.2. Cytoplasmic Expression

For cytoplasmic expression, we used the BL21 DE3 strain. However, the bacterial cytoplasm has a reducing environment which is not suitable for the formation of disulfide bonds. We transformed the SOX plasmid into these bacteria which expresses recombinant sulfhydryl oxidase enzyme into BL21 DE3 competent strain and after selection with chloramphenicol, we prepared a preculture and we made BL21 DE3 strain containing SOX plasmid competent again for transformation with nanobody expression plasmids. The sulfhydryl oxidase enzyme can form disulfide bonds in reducing environments (Nguyen et al. 2011). Nanobody plasmids used in cytoplasmic expression were different from those used for periplasmic expression. We cloned nanobody sequences from the pET22b plasmid into the pET28a plasmid which has no periplasmic leader peptide and has a C- terminal His tag for purification purposes. The induction was also different from periplasmic induction, initially, because sulfhydryl oxidase enzyme was under control of an arabinose promoter, arabinose was added to the culture for 30 minutes at 30 °C. After this step, 0.5mM IPTG was added to induce nanobody protein for 4 hours at 30 °C. For colony screening to identify cytoplasmic expression, we chose to express the MDM4 Nb which was previously purified with periplasmic expression and two nanobodies which we could not purify with periplasmic production; MDM4 CDR1 CDR3 Nb and GFP CDR3 Nb. Colony screening results were positive for all three nanobodies (Figure 4.13). Surprisingly, GFP CDR3 which we could not express in periplasmic production, was expressed in this cytoplasmic expression system. Following this, we attempted solubilization and His tag affinity column chromatography for MDM4 CDR1 CDR3 in a 1 L culture. After whole cell lysis unfortunately the nanobody was insoluble in the pellet fraction (Figure 4.14).

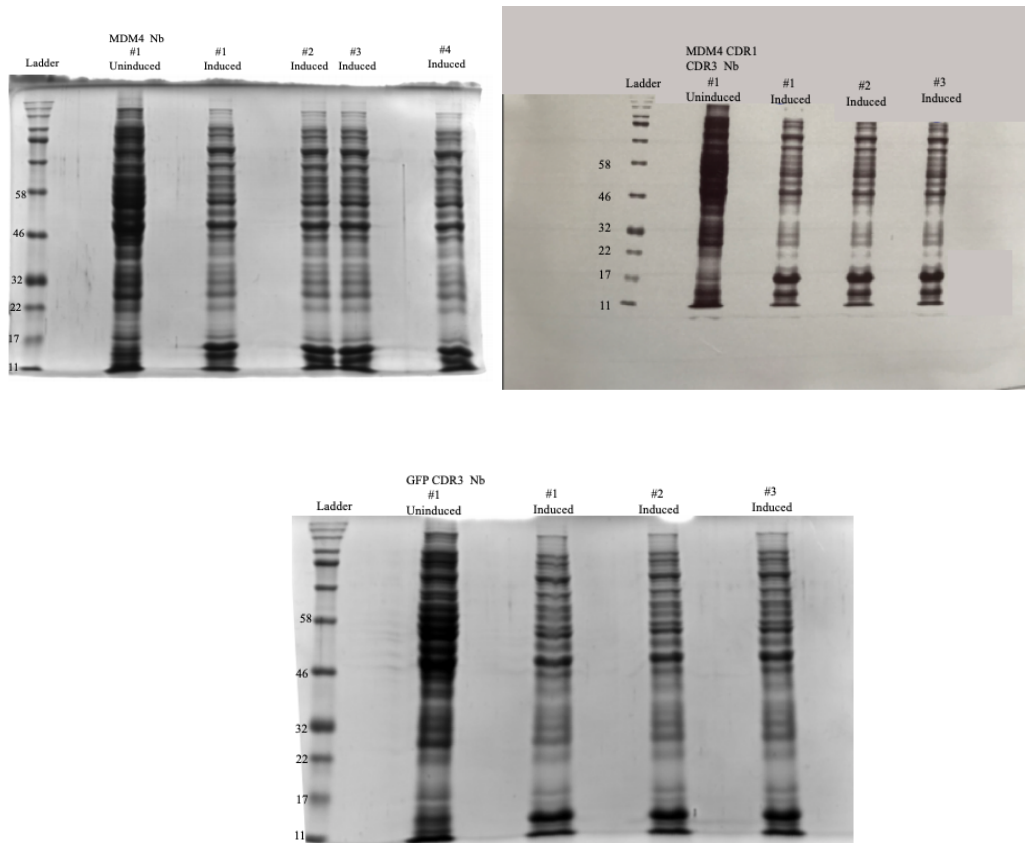


**Figure 4.13 Colony screening for cytoplasmic expression.** MDM4 Nb, MDM4 CDR1 CDR3 Nb and GFP CDR3 Nb were expressed in BL21 DE3 bacteria containing the SOX plasmid. 14% SDS-PAGE gel was used and expected protein size is around 15 kDA for MDM4 Nb and MDM4 CDR1 CDR3 Nb, and 13.9 kDA for GFP CDR3 Nb.

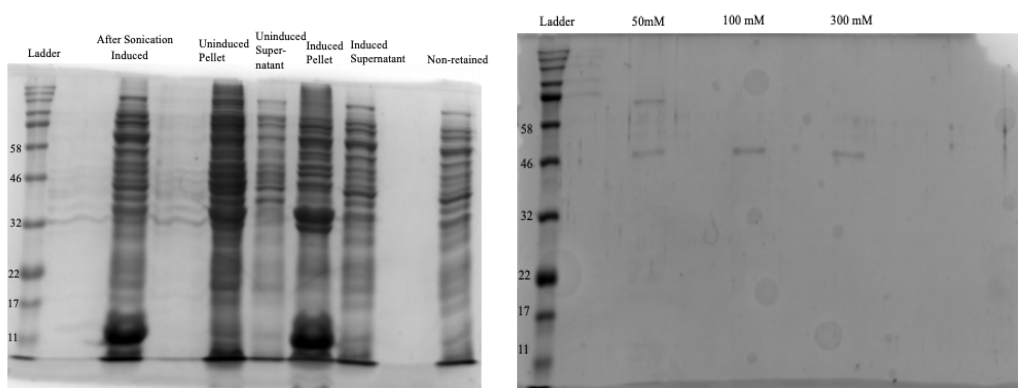


**Figure 4.14 Cytoplasmic nanobody purification with the whole cell lysis protocol.** MDM4 CDR1 CDR3 Nb was expressed in BL21 DE3 bacteria containing the SOX

plasmid. Nanobody stuck at pellet. 14% SDS-PAGE gel was used and expected protein size is around 15 kDA.

After the observation of the MDM4 CDR1 CDR3 Nb in the insoluble fractions, we attempted the use the Bugbuster® protein extraction reagent. This is a reagent that disrupts the *E.coli* cell wall. It contains Tris-buffer based mixture of several non-ionic and zwitterionic detergents which enables degradation of the cell wall without causing denaturation of proteins. After arabinose and IPTG induction, as mentioned before, we harvested the cells via centrifugation and weighed the dry pellet. We resuspended the pellet with Bugbuster reagent using 5 ml Bugbuster reagent per gram of wet cell paste. Benzonase and protease inhibitors were also added in this step. We mixed the cell suspension for 20 minutes and centrifuged again to separate the soluble supernatant and pellet fractions which were analyzed by SDS-PAGE. Unfortunately, the Bugbuster reagent did not work for the MDM4 CD1 CDR3 Nb which was again stuck in the insoluble pellet (Figure 4.15).

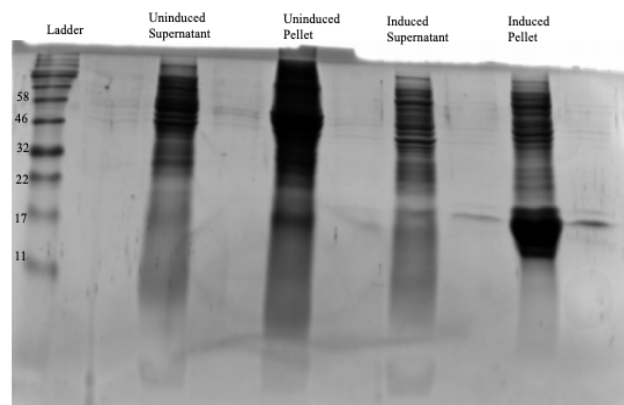


**Figure 4.15 Cytoplasmic nanobody purification with the Bugbuster® protocol.** MDM4 CDR1 CDR3 Nb was expressed in BL21 DE3 bacteria containing SOX plasmid and Bugbuster reagent was used for lysis of the cell. Nanobody stuck at pellet. 14% SDS-PAGE gel was used and expected protein size is around 15 kDA.

We also attempted to express the MDM4 Nb as a soluble protein using the whole cell lysis protocol but could not obtain soluble protein for this protein as well (Figure 4.16). This may be due to the temperature which is 30°C for induction or IPTG concentration. To understand the reason, we carried out temperature, IPTG and time dependent protein expression with 25 ml cultures. We induced all cultures with arabinose initially to express the sulfhydryl oxidase enzyme and induced with IPTG. There were two groups for temperature which were 30°C for 4 hours of induction and 18°C overnight induction. Each group was induced with different IPTG concentrations 0.1mM, 0.3mM and 0.5mM. We also tested the expression time-dependence of solubility induced at 30°C with 0.5mM IPTG for 1 hour, 2 hours, 3 hours and 4 hours (Table 4.2). For all groups, we harvested the cells and lysed with the whole cell lysis buffer and sonicated using the Bioruptor Sonicator and analyzed by SDS-PAGE (Figure 4.17).

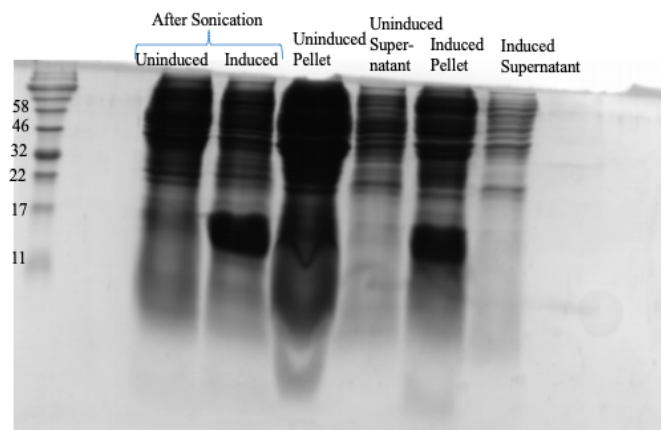


**Figure 4.16 Cytoplasmic nanobody purification with the whole cell lysis protocol.** Positive colony from MDM4 Nb colony screening was chosen and large culture of MDM4 Nb was prepared and expressed in BL21 DE3 bacteria containing SOX plasmid and whole cell lysis buffer used for lysis of the cell. Nanobody stuck at pellet. 14% SDS-PAGE gel was used and expected protein size is around 15 kDA.



**Table 4.2 Groups for temperature, time and IPTG dependent expression**

30 °C 4 Hours		30 °C 0.5mM IPTG	
Induction	Group Name	Time of Induction	Group Name
Uninduced	1	Uninduced	5
0.1mM IPTG	2	1 Hour	6
0.3mM IPTG	3	2 Hours	7
0.5mM IPTG	4	3 Hours	8
		4 Hours	9

18 °C Overnight	
Induction	Group Name
Uninduced	10
0.1mM IPTG	11
0.3mM IPTG	12
0.5mM IPTG	13

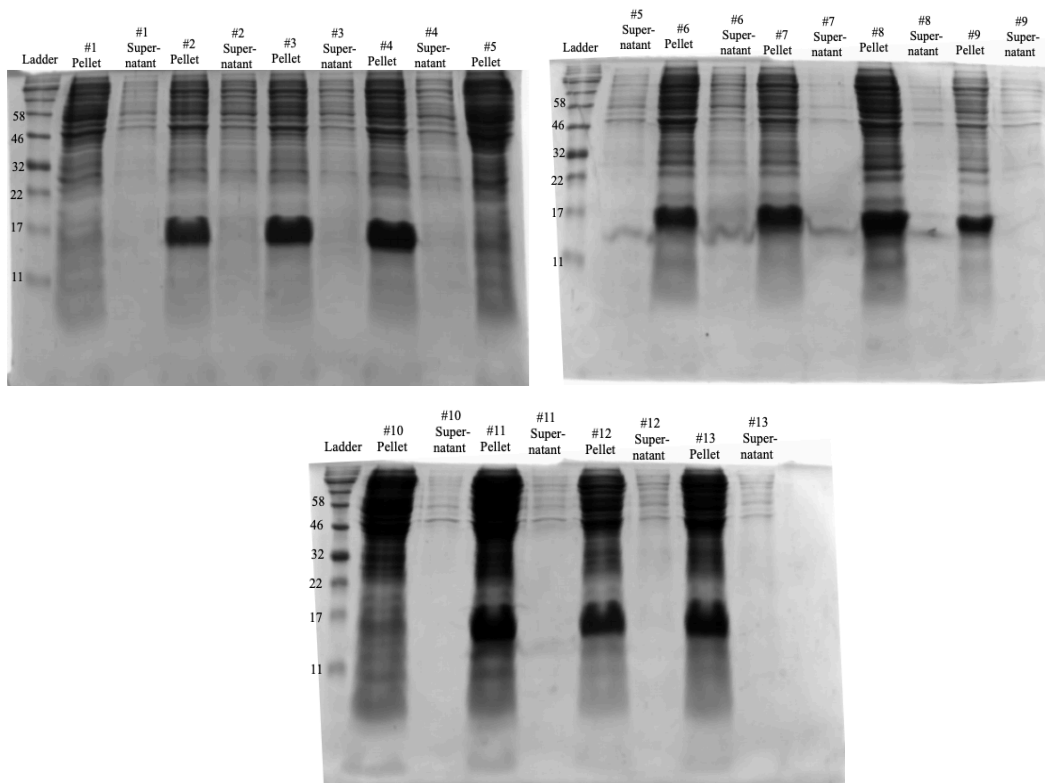


**Figure 4.17 IPTG, temperature and time dependent cytoplasmic nanobody expression with the whole cell lysis protocol.** There was no difference between groups and in all of them MDM4 Nb proteins were stuck in the insoluble pellet fractions.

In these dose- response and time course experiments, we observed that in general cytoplasmic expression of nanobodies in the BL21DE3 SOX strain did not change much with the changing parameters. The SOX plasmid used in this study was a gift from Prof. Ario DeMarco. Unfortunately, because we did not have an appropriate plasmid map for this vector. We could not be certain that the protein expression and induction were sufficiently upregulated before nanobody expression. Colony screening was not successful in identifying soluble proteins in the cytoplasm (Figure 4.18).

In summary, we purified GFP Nb, MDM4 Nb and MDM4 CDR3 Nb. MDM4 CDR1 CDR3 and GFP CDR3 Nb could not be purified. GFP Nb was expressed in the periplasm and purified with the osmotic shock application. Also, we expressed MDM4 Nb and MDM4 CDR3 Nb in the periplasm and purified these with the whole cell lysis (Table 4.3).

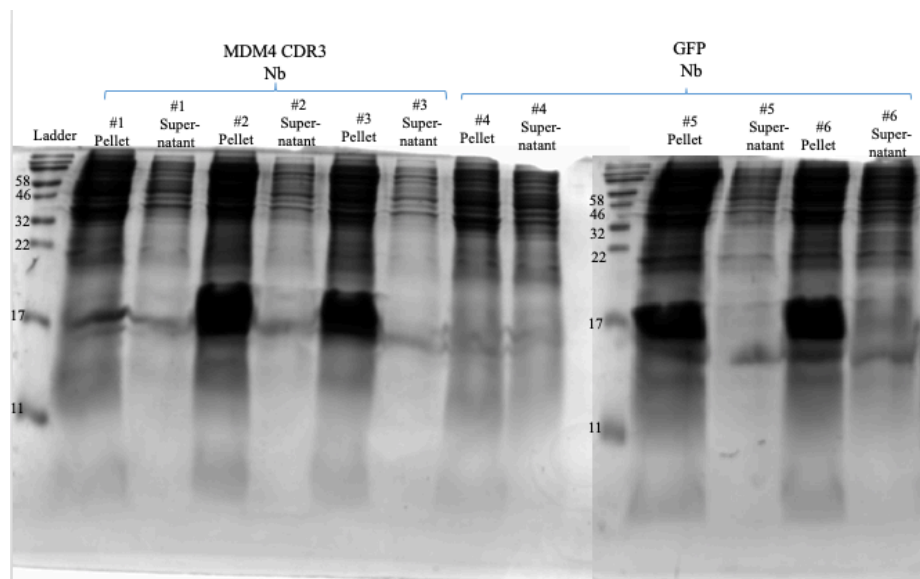


**Figure 4.18 Colony screening for cytoplasmic expression.** MDM4 CDR3 Nb and GFP Nb were not detected in the soluble fraction.

**Table 4.3 Methods used for the expression and purification of nanobodies**

Nanobodies	Colony Screening	Cytoplasmic Expression/Purification	Periplasmic Expression/Purification	Osmotic Shock Lysis	Whole Cell Lysis	His Tag Purification	Concentration
MDM4 Nb	✓	✗	✓	✗	✓	✓	0.45 mg/ml
MDM4 CDR3 Nb	✓	✗	✓	✗	✓	✓	1.1 mg/ml
GFP Nb	✓	✗	✓	✓	✗	✓	0.68 mg/ml
MDM4 CDR1 CDR3 Nb	✓	✗	✓	✗	✗	✗	-
GFP CDR3 Nb	✓	✗	✗	✗	✗	✗	-

#### 4.2. Surface plasmon resonance (SPR) for comparing binding affinities of nanobodies

We used surface plasmon resonance to find binding affinities of the purified nanobodies. We used the Biacore T200 SPR machine for this purpose. The first step was pH scouting to decide the pH of the acetate buffer which is used for the immobilization of the p53 binding domain of the MDM4 protein. In our first trial, we used 10  $\mu\text{g}/\text{ml}$  MDM 4 protein and contact time was 180 seconds and the flow rate was 5  $\mu\text{l}/\text{min}$ . Arbitrary response units (RU) reflecting the change in refractive index and the binding to the surface were plotted as a function of time. However, we observed a very sharp increase when ligand was injected so we decided to decrease the concentration of the MDM4 protein and the flow rate, and decrease the contact time of the protein with the chip surface. In our second trial, we used 2,5  $\mu\text{g}/\text{ml}$  MDM4 protein and contact time was 120 seconds and the flow rate was 10  $\mu\text{l}/\text{min}$  (Figure 4.19). We chose the pH of the acetate buffer as 4.5 and performed immobilization of the MDM4 protein. The chosen pH of 4.5 was higher

compared to the pH of the surface which is 3.5 and lower than the isoelectric point of the p53 binding domain of MDM4 protein. We used the same values and buffer for immobilization. NHS/ EDC was used to activate the surface and further ligand with 2,5  $\mu\text{g}/\text{ml}$  concentration was injected over the surface. After this step, NaOH was used to block the surface of the chip to deactivate unreacted esters. At the end of the immobilization, 500 RU of material was deposited onto chip surface (Figure 4.20).

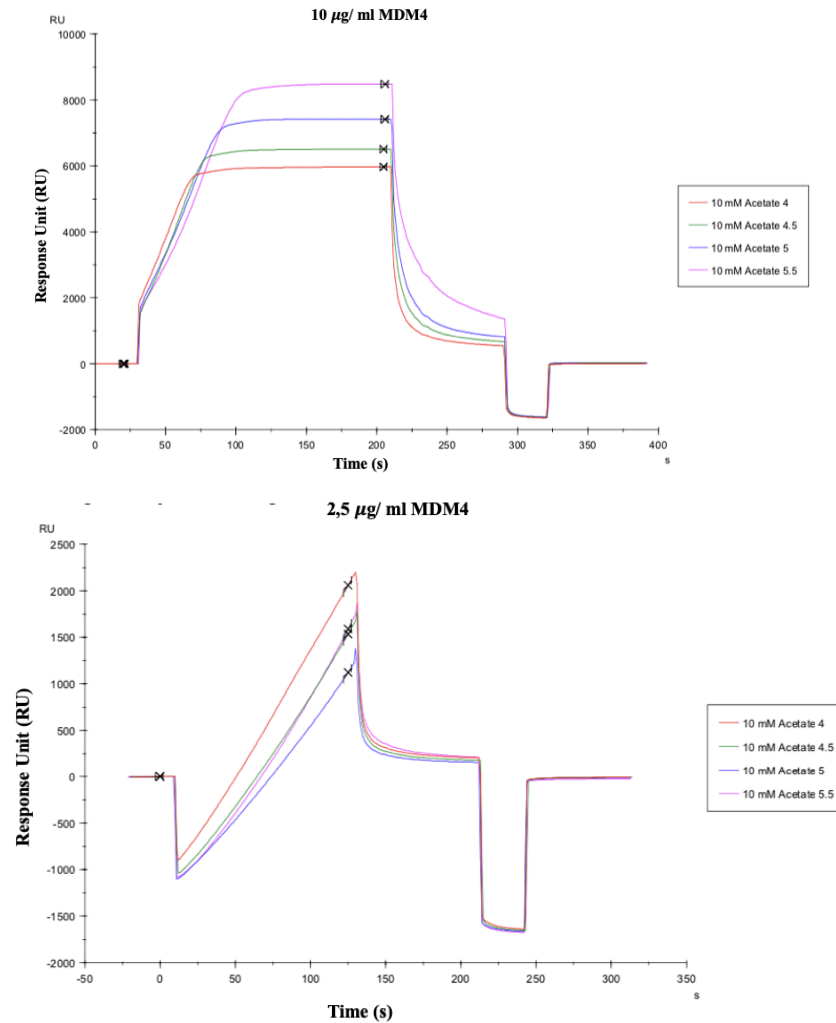


**Figure 4.19 pH scouting experiment** 10  $\mu\text{g}/\text{ml}$  and 2,5  $\mu\text{g}/\text{ml}$  MDM4 was used. When 10  $\mu\text{g}/\text{ml}$  was used RU increased immediately after injection so concentration was decreased to 2,5  $\mu\text{g}/\text{ml}$ . pH 4.5 was chosen for acetate buffer.

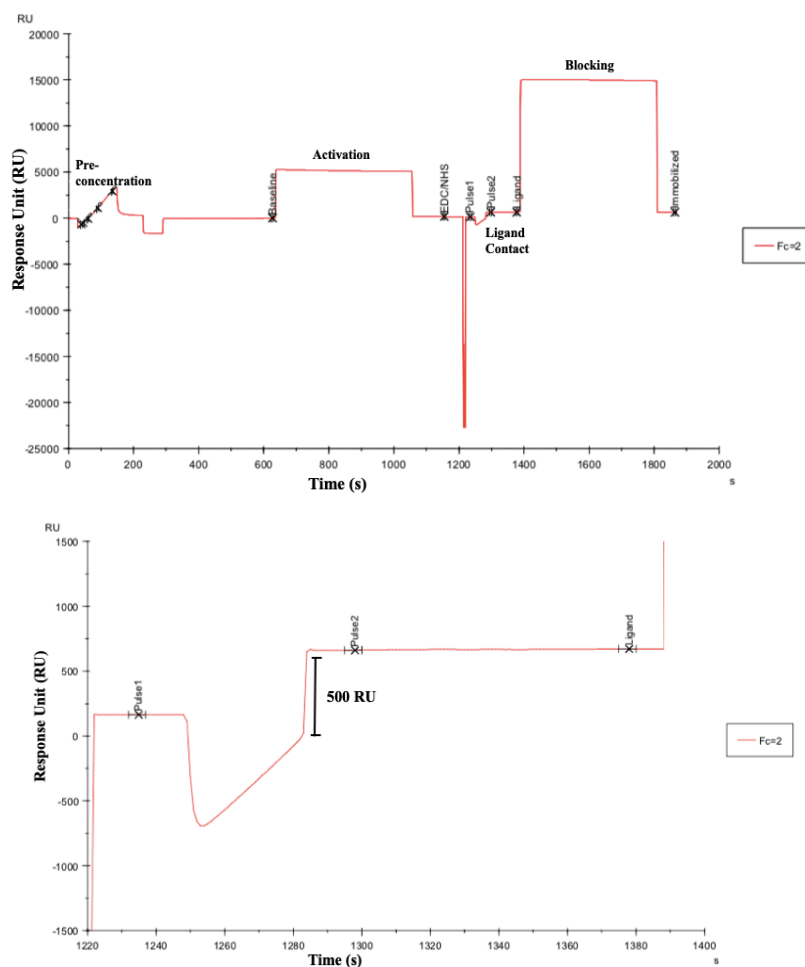


**Figure 4.20 Immobilization of MDM4 on CM5 chip** 2,5  $\mu\text{g}/\text{ml}$  of p53 binding domain of MDM4 was immobilized with contact time 120 seconds and rate 10  $\mu\text{l}/\text{min}$ . 500 Net RU was observed.

After immobilization of the MDM4 on the CM5 chip we performed nanobody binding kinetics experiments. As an analyte, we used three different nanobodies, MDM4 Nb, MDM4 CDR3 Nb and GFP Nb. MDM4 Nb was our positive control because it is our reference nanobody and GFP Nb was a negative control because it is specific to GFP and not to MDM4. We could not test the remaining proteins, MDM4 CDR1 CDR3 Nb and GFP CDR3 Nb, with SPR because we could not obtain purified protein. Three nanobodies were injected separately on the CM5 chip containing MDM4 protein and we used five different concentrations, 1000 nM, 2000 nM, 3000 nM, 4000 nM and 5000 nM. For all dilutions, we used HBS- EP + buffer which was also running buffer.

We compared the resonance units (RU) for all of the nanobodies at the same concentration. In all concentrations, the MDM4 CDR3 Nb exhibited higher response units compared to our reference nanobody which was the MDM4 Nb protein. Thus, MDM4 CDR3 Nb binds better compared to the reference nanobody. However, there were fluctuations when the concentrations were increased. For example, at 1000 nM, MDM4 CDR3 and MDM4 Nb exhibited 29,2 RU and 17,3 RU respectively. But when we increased the concentration to 2000 nM, the responses were 20,7 and 6.3 RU for MDM4 CDR3 Nb and MDM4 Nb respectively. This unproportional increase in apparent binding precludes the performance of binding kinetics analysis (Figure 4.20). However, these preliminary experiments indicate that the *in silico* optimized anti- MDM4 nanobodies can in fact have a better binding affinity to MDM4 than the reference nanobody.

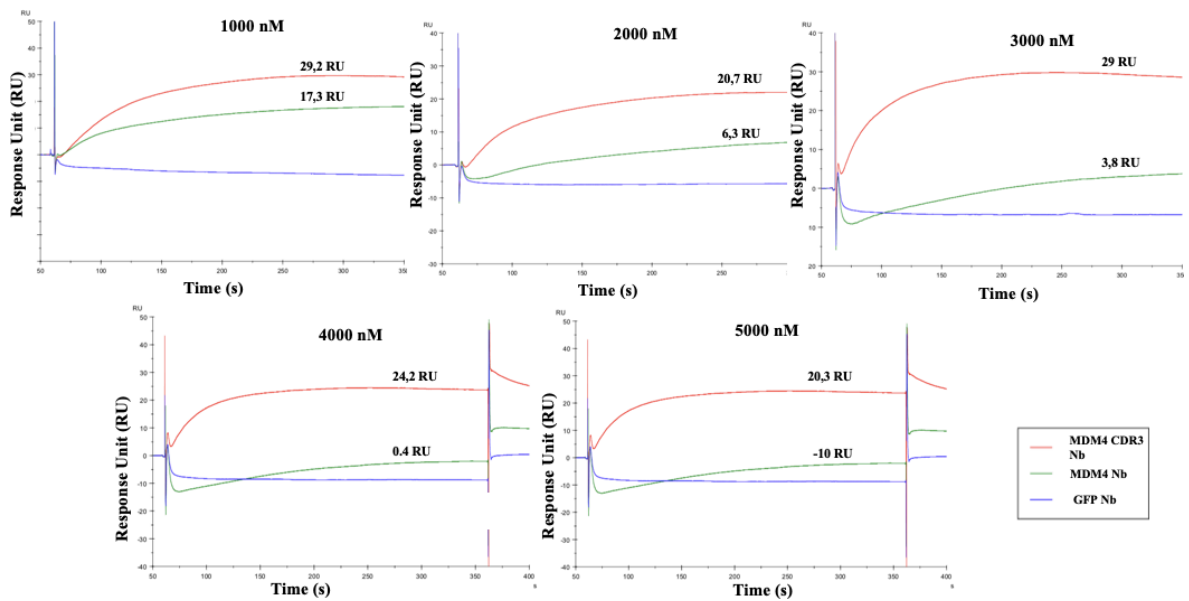


**Figure 4.21 Binding at different concentrations of the MDM4 Nb, MDM4 CDR3 Nb and GFP Nb.**

### **4.3. Fluorescent two-hybrid (F2H) assay for the interaction between nanobodies and MDM4 protein**

To attempt to measure the effects of nanobody binding on the MDM4-p53 interaction in the cellular context, we performed the F2H assay in tissue culture cells analyzed under fluorescent microscopy. The F2H is a live cell, protein-protein interaction investigating assay which uses fluorescent live-cell microscopy to detect the protein interactions as a compound or an inhibitor is given to the system. We used baby hamster kidney cells (BHK) for this assay and transfected several plasmids containing our proteins of interest linked to fluorescent proteins which are enabling visualization of the interaction (Figure 4.21). The first plasmid we expressed, p53 linked to the TagGFP protein and the second one expressed the p53 binding domain of MDM4 protein fused to the TagRFP protein. The third plasmid expressed a LacI- GFP binding protein (GBP) fusion which anchored these fluorescent proteins to lac operator sequences that were genetically inserted into an unknown locus in the genome of these BHK cells. We expressed three different nanobody sequences which were MDM4 Nb, MDM4 CDR3 Nb and GFP CDR3 Nb. All of these nanobodies were turned into chromobodies because they were expressed as fusion proteins with Tag BFP protein. We used BHK cells which were genetically modified by stable transfection to contain lac operator sites in their genome.

We seeded BHK cells onto tissue culture plates and co-transfected these four plasmids. The LacI- GBP plasmid expressed the fusion protein which was binding to LacI operators and Tag GFP protein which is part of the TagGFP- p53 fusion interacted with the GBP component of LacI-GBP. This led to the formation of green focus in the nucleus. In fact, the GBP protein is a GFP binding protein that is an anti- GFP nanobody. The p53 protein interacted with the p53 binding domain of MDM4 protein which was fused to TagRFP expressed as a fusion protein. As a result, we observed a green focus co-localized red focus. If the expressed nanobodies were interacting with the p53 binding domain of MDM4, the red focus disappeared from the nucleus and it was released into the cytoplasm which was observed as a diffuse red fluorescence in the cytoplasm and in the nucleus (Figure 4.22).

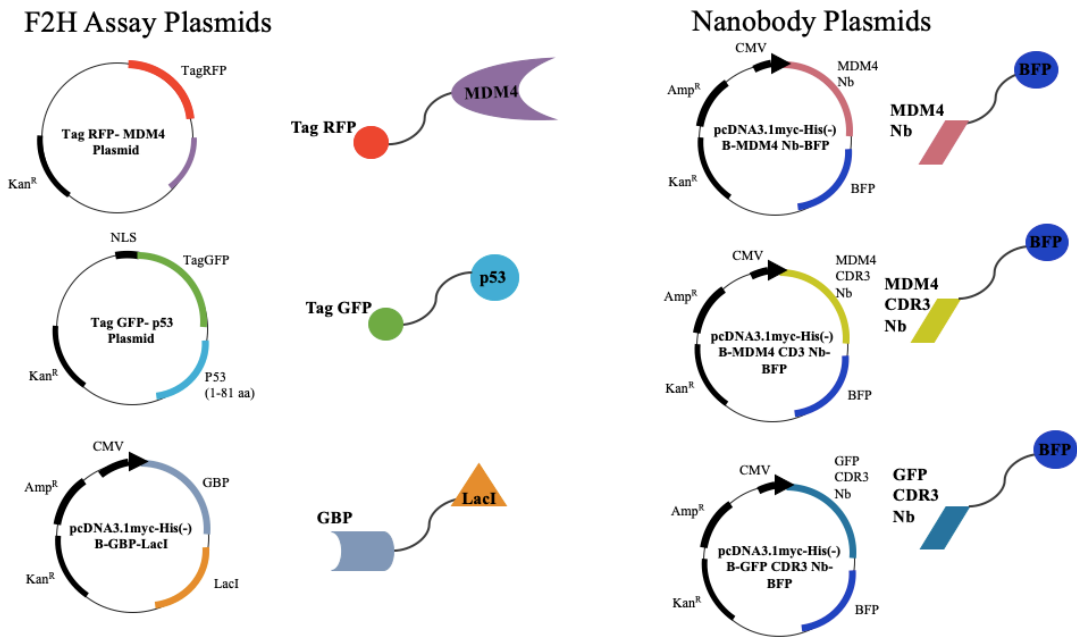


Figure 4. 22 Plasmids used in fluorescent two hybrid assay.

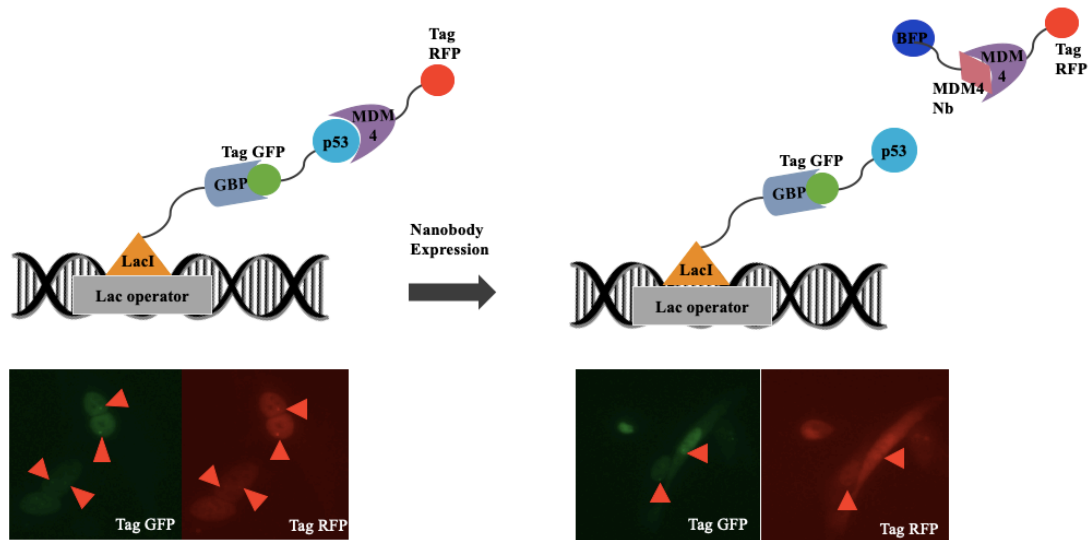
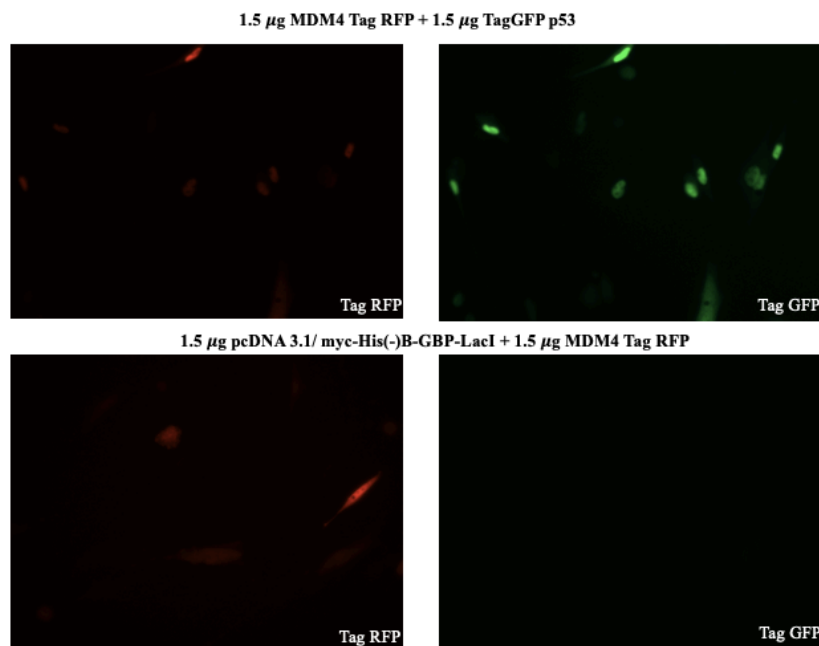


Figure 4. 23 Mechanism of the fluorescent two hybrid assay. LacI GBP fusion protein localized to lacI promoters integrated into the BHK cell genome and expressed TagGFP p53 protein binds to GBP and it is localized into a focus in the nucleus. When there is no nanobody expression, MDM4 TagRFP protein binds to p53 protein and it co-localized with p53 protein in the nucleus. However, when there is nanobody expression, if



nanobody is capable of binding to MDM4, MDM4 protein can be separated from p53 and migrate to cytoplasm and there will be no co- localization.

Before the experiments with nanobodies, to verify the system, we transfected different combinations of F2H plasmids into BHK cells. When we transfected the MDM4 Tag RFP plasmid and the Tag GFP p53 plasmid, there was no foci formation due to the lack of LacI- GBP fusion plasmid which was normally docked on the lacI operators in the genome. The second group was, LacI- GBP fusion plasmid and MDM4 Tag RFP, we observed TagRFP in the cells but there were no foci in the nucleus. The third group was, LacI- GBP fusion plasmid and TagGFP p53 plasmid and we observed green dots in the nucleus showing that for localization of p53 into the genome, LacI- GBP fusion plasmid was needed. In the last group, we transfected all plasmids together and observed both green and red dots co- localized in the nucleus (Figure 4.23).



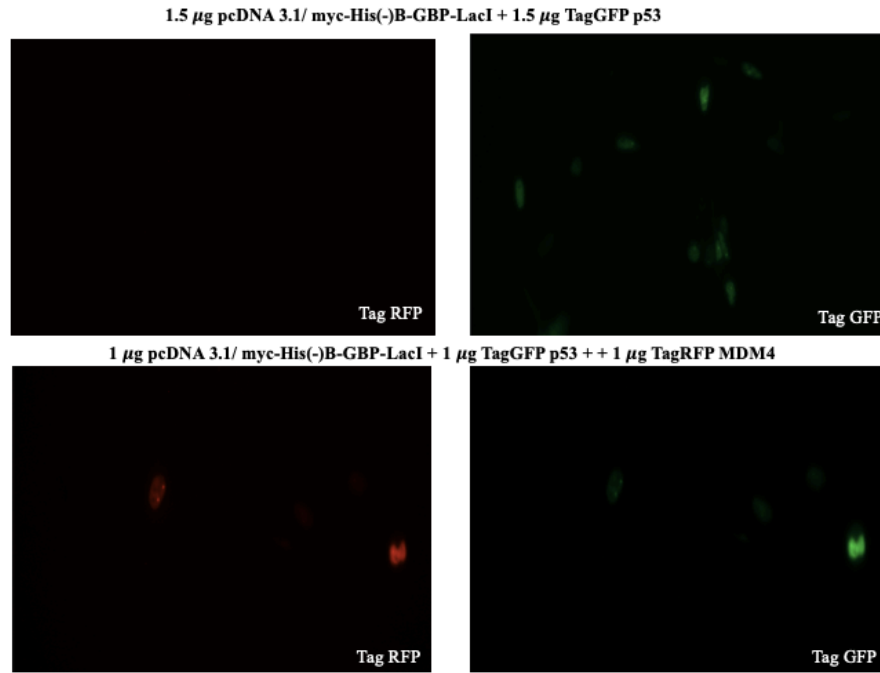


**Figure 4.24 Verification of protein- protein interaction and the disruption of interaction by nanobodies using the F2H assay.** Different combinations of three plasmids from F2H assay were transfected to BHK cells. Red and green dots co-localized when three plasmids transfected together.

In the second part, we transfected our three nanobody plasmids containing MDM4 Nb, MDM4 CDR3 and GFP CDR3 Nb along with these F2H assay plasmids. For this experiment, we used 1  $\mu$ g from each plasmid and transfected them into BHK cells using PEI reagents. After several trials, we could not observe the nanobodies fused with BFP after 24 hours, their expression was slow compared to GFP and RFP. We also checked the cells after 36 hours but GFP and RFP expression decreased after 36 hours and dots inside the nucleus could not be seen so we decided to check the cells 28 hours after the transfection. We used a fluorescent inverted Zeiss Live Cell Microscope. Tile regions were set at 20x and 25 tile regions were selected from the middle of each well.

As negative control that only expressed BFP but no nanobody fusion, we used the pRRL plasmid. BFP fusion plasmids were transfected to BHK cells together with F2H assay plasmids. Initially, we focused on green dots which were foci localized TagGFP- p53 proteins. After finding these spots manually, we counted co- localization with red dots which were localized MDM4- TagRFP proteins, in the GFP and RFP channels. For each

group, pRRL plasmid, MDM4 Nb, MDM4 CDR4 Nb and GFP CDR3, we counted cells with only green dots and co-localized green and red dots and found the percentages (Figure 4.25). pRRL plasmid containing negative control had 83% co-localization of green and red dots which we expected. On the other hand, we observed 90% only green dots in MDM4 Nb containing BHK cells. This result verified that our reference nanobody, MDM4 Nb, worked very efficiently and separated the MDM4 and p53 complex. On the other hand, in MDM4 CDR3 Nb and GFP CDR3 Nb containing BHK cells we observed 37% and %34 only GFP. This means *in silico* designed nanobodies also interacts with the p53 binding site of MDM4 but not as effectively as MDM4 Nb (Figure 4.24).

Thus, although the *in vitro* results on SPR measured MDM4 CDR3 nanobody affinity displays the highest affinity, the *in vivo* results were quite dramatic. Here the MDM4 Nb not only bound best but also displayed the highest affinity in disrupting the MDM4 and p53 interaction.

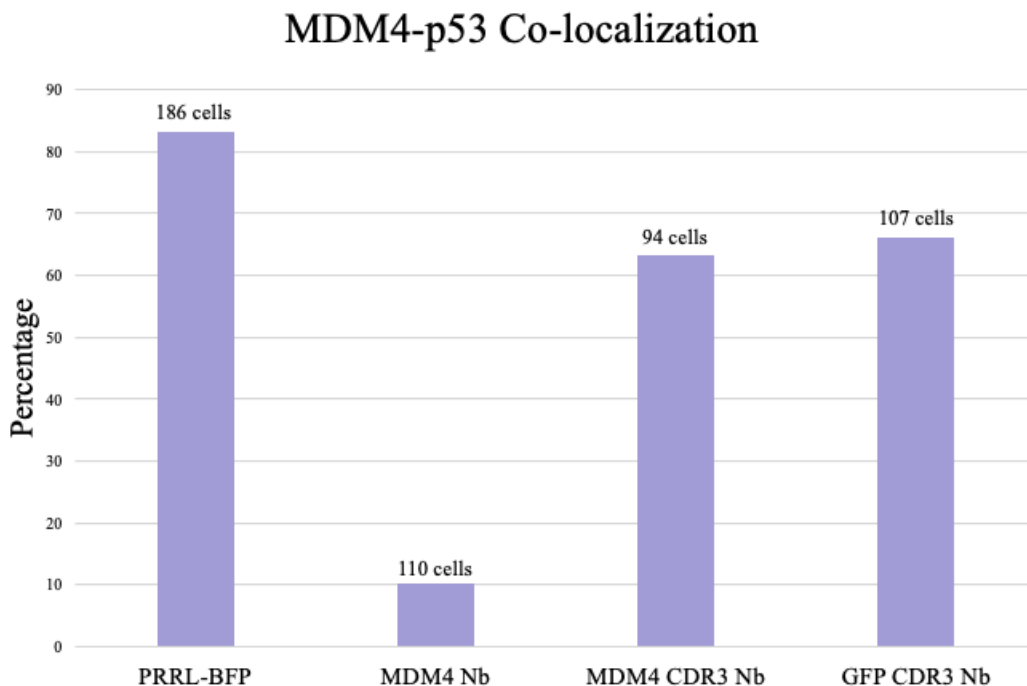
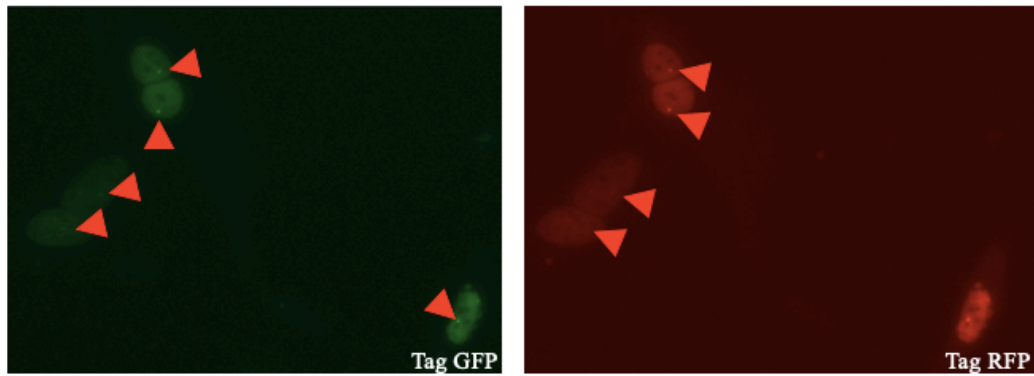
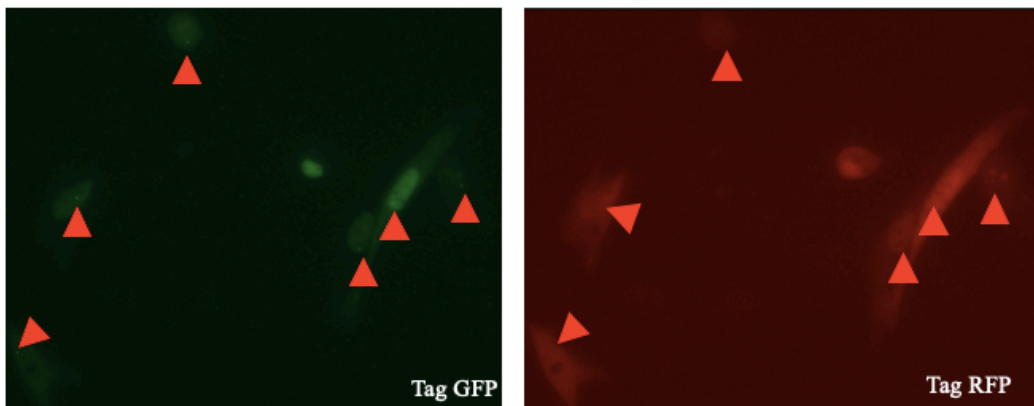


**Figure 4.25** A bar graph showing the amount of the GFP foci containing cells and the percentages of co-localization in these cells.

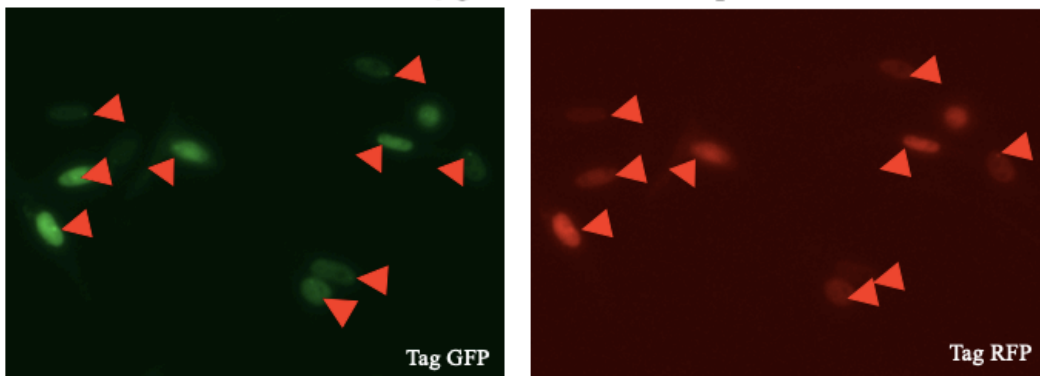
**1  $\mu$ g pRRL plasmid**



**1  $\mu$ g MDM4 Nb plasmid**



**1  $\mu$ g MDM4 CDR3 Nb plasmid**



**1  $\mu$ g GFP CDR3 Nb plasmid**

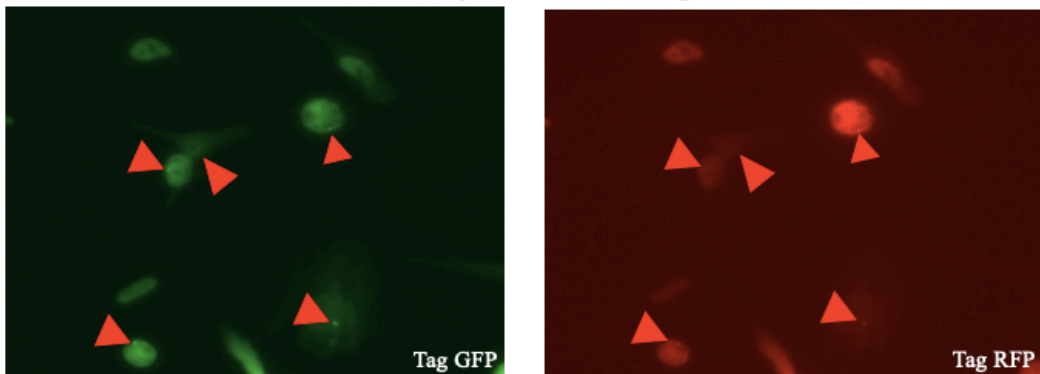


**Figure 4.26 F2H assay with nanobodies.** Nanobodies transfected together with F2H assay plasmids. In the pRRL plasmid group which was the negative control, we observed co-localization of green and red foci. In the MDM4 Nb plasmid transfected group which was the positive control, we observed only green foci but red dots mostly disappeared. In MDM4 CDR3 Nb and GFP CDR3 Nb transfected groups, there was green foci but only some of the red foci were disappeared.

## 5. DISCUSSION

Regulation of p53 protein is very important to prevent cancer development. In 50 % of cancers, p53 gene is mutated, in most of the remainder, there is an overexpression of the negative regulators of the p53 protein which results in a malfunction of this pathway (Hu et al. 2006). For human cancers, where there is an overexpression of MDM2, antagonists for MDM2 such as Nutlin-3a that activate the p53 tumor suppressor were developed (Vassilev 2004). However, for some cancer types, the use of these antagonists is not effective because of active MDM4 protein which can also inhibit the activity of the p53 protein. Moreover, in some cancers, there is an overexpression of MDM4, which makes it difficult to activate p53. With these observations, there is a need for antagonists of MDM4. In this study, we aimed to discover antagonists for MDM4 as nanobodies because they are very good candidates for tumor therapeutics because of their small size and high penetration ability to tumor cells (Van Audenhove and Gettemans 2016). However, the production of nanobodies by either injection of the antigen to llamas or phage/ yeast display and selection methods is time consuming and is expensive. We aimed to generate an alternative method which is faster and less expensive. In this method, novel nanobodies were generated from reference nanobodies by changing their complementarity determining regions (CDRs). In previous work, *in silico* methods were used to select these nanobodies that were predicted to have high stability and high binding affinity towards the p53 binding site of MDM4. The best candidates were selected by energy minimization and molecular dynamics. In this thesis I attempted to optimize the expression and purification of several of these candidate nanobodies in bacterial systems. Also, I determined the binding affinity using both *in vivo* and *in vitro* methods.

Firstly, we optimized the expression of nanobodies in bacteria. There were two reference nanobodies: MDM4 Nb from Yu *et al.* 2009 and GFP Nb from Kubala *et al.* 2010. We Other generated three ‘optimized’ nanobodies that were similar to these reference

nanobodies. Thus in total five different nanobodies were expressed. We first attempted to produce these nanobodies by periplasmic expression. Nanobody cDNA sequences were synthesized and inserted into the pET22b plasmid. This plasmid has an N- terminal pelB sequence for exporting nanobodies to the periplasmic space for disulfide formation and correct folding and a C- terminal His tag for affinity purification purposes. We chose the Rosetta 2 DE3 pLysS strain for expression because it has an extra plasmid which expressed rare codon tRNAs, that make it easier to express eukaryotic proteins.

The general problem with periplasmic expression and osmotic shock for purification was unwanted cell lysis. During the application of the protocol, sticky cells were formed and it was difficult to further process bacterial pellets. This may be due to the toxicity of the nanobodies. We encountered cell lysis especially during the culture of high volumes (eg 2 L). Bacteriophage contamination is also a possibility but was deemed unlikely because we observed this lysis in different bacterial strains and stocks. We also encountered cell lysis when we used Terrific Broth (TB), a more enriched medium compared to LB, that results in more division and larger population size. While we could express the MDM4 Nb, MDM4 CDR3 Nb and GFP Nb proteins in the periplasmic space, we could only obtain the GFP Nb in the soluble fraction with the osmotic shock protocol. We purified the other two nanobodies using the whole cell lysis protocol. We were not successful in expressing the GFP CDR3 Nb, which can be seen from colony screening experiments. This can be due to a problem in the expression plasmid itself and in order to solve it cloning into another periplasmic vector can be tried. In addition to this, we successfully expressed the MDM4 CDR1 CDR3 Nb but could not successfully purify this protein from the soluble fractions regardless of the expression (periplasmic or cytoplasmic) and purification (osmotic shock or whole cell lysis) conditions. The changes in the CDR1 region could affect the solubility of the protein possibly affecting the folding of the nanobody, sending the protein into bacterial inclusion bodies. Expression in the presence of different detergents may be a possibility to solubilize this protein.

For cytoplasmic expression, we cloned nanobody sequences into the pET28a vector and used the BL21 DE3 strain containing the Sox plasmid. While all nanobodies (except MDM4 CDR1 CDR3 Nb) were expressed as evidenced by colony screening, we could not obtain these nanobodies in soluble fractions and all of the nanobodies were stuck at the pellet. To optimize this solubilization, we attempted time dependent and IPTG

concentration dependent experiments but could not see nanobodies in the in the soluble phase. The expression of enzymes from the Sox plasmid was not determined and in their absence disulfide bond requiring nanobody proteins may have formed aggregates in the cytoplasm. Also the BL21 DE3 strain, unlike the Rosetta 2 DE3 pLysS strain does not encode rare codons tRNAs and may not be suitable for the expression of some eukaryotic proteins. Because the Rosetta 2 DE3 pLysS strain contains a plasmid encoding these tRNAs providing chloramphenicol resistance, it cannot be transformed with the Sox plasmid which also contains chloramphenicol resistance. The expression of nanobody proteins may be more suitable in mammalian cell lines such as the commonly used CHO cell line.

Secondly, we tested the affinity of purified nanobodies with surface plasmon resonance. We covalently immobilized a previously synthesized domain of MDM4 containing the p53 binding site on the CM5 chip and flowed soluble purified nanobodies over this chip. While we could detect binding of the nanobodies to the MDM4 protein, the use of a larger domain of MDM4 which folds correctly may provide a better system to detect the affinity of these nanobodies. The shape or size of the p53 binding site may not be suitable due to the defect in folding which may result in failed nanobody binding. Also, the chips with MDM4 protein were repeatedly used to test the binding of multiple nanobodies. The immobilized protein may be harmed by the regeneration cycles, decreasing the effective MDM4 protein on the surface.

Finally, we used a fluorescent two hybrid assay to assess the binding of selected nanobodies in an *in vivo* setting. We excluded GFP Nb because F2H assay contains GFP protein and GFP Nb can bind to GFP protein causing defect in F2H assay mechanism. In addition to the GFP Nb, we excluded the MDM4 CDR1 CDR3 Nb from the F2H assay because we could not purify this protein *in vitro* and we predicted that *in vivo* expression may also be problematic. As a negative control in the F2H assay, we used the pRRL plasmid which expressed the BFP protein. The nanobodies that we expressed in these BHK cell line all had BFP tags at their C terminus. Unfortunately, BFP expression was not robust as the expression of the other fluorescent proteins such as GFP and RFP. problem in BFP expression We observed maximal GFP and RFP after 24 hours but we observed BFP protein only after 36 hours.



To analyze molecular interactions *in vivo*, we initially identified green foci in the nucleus containing the p53- GFP fusion protein and counted the cells containing overlapping red foci. We assessed the activity of nanobodies in disrupting the p53- MDM4 interaction by determining the number of lost co-localization. While our positive control which is the MDM4 Nb, 90% of the analyzed cells contained only green fluorescent foci, in our negative control in 83% of the green fluorescent foci containing cells there was also red fluorescent focus co-localization. In the cells that express MDM4 CDR3 Nb and GFP CDR3 Nb, co-localization was between our positive and negative controls indicating that the original MDM4 nanobody was more effective in disrupting the MDM4-p53 interaction. Because the F2H assay can also be used to assess the interaction between MDM2 and p53, the specificity of the same nanobodies in disrupting this interaction may increase the impact of the disruption of the MDM4-p53 interaction.

In summary, both the surface plasmon resonance and F2H assay needs some optimization experiments. However, we achieved to show the effect of nanobodies *in vivo* with the F2H assay for the first time and showed that *in silico* designed nanobodies had some activity too which can be developed more with *in silico* modelling experiments and trials with more nanobody candidates. The F2H assay can be used for screening of several different nanobodies. We aim to try high number of new *in silico* designed candidates with both SPR and F2H assay. Also novel nanobodies targeting the MDM4 p53 can be selected from a yeast display nanobody library, providing larger numbers of candidate nanobodies. It is of great interest to compare the affinity and activity of *in silico* designed nanobodies with those selected from yeast display libraries.

## BIBLIOGRAPHY

- Abbady, A Q, A Al-daoude, A Al-mariri, M Zarkawi, and S Muyldermans. 2012. “Chaperonin GroEL a Brucella Immunodominant Antigen Identified Using Nanobody and MALDI-TOF-MS Technologies.” *Veterinary Immunology and Immunopathology* 146 (3–4): 254–63.  
<https://doi.org/10.1016/j.vetimm.2012.01.015>.
- Audenhove, Isabel Van, and Jan Gettemans. 2016. “Nanobodies as Versatile Tools to Understand, Diagnose, Visualize and Treat Cancer.” *EBioMedicine* 8: 40–48.  
<https://doi.org/10.1016/j.ebiom.2016.04.028>.
- Audenhove, Isabel Van, and Jan Gettemans. 2016. “Nanobodies as Versatile Tools to Understand , Diagnose , Visualize and Treat Cancer.” *EBIOM* 8: 40–48.  
<https://doi.org/10.1016/j.ebiom.2016.04.028>.
- Bannas, Peter, Julia Hambach, and Friedrich Koch-Nolte. 2017. “Nanobodies and Nanobody-Based Human Heavy Chain Antibodies as Antitumor Therapeutics.” *Frontiers in Immunology* 8 (NOV): 1–13.  
<https://doi.org/10.3389/fimmu.2017.01603>.
- Bazan, Justyna, Ireneusz Całkosiński, and Andrzej Gamian. 2012. “Phage Display — A Powerful Technique for Immunotherapy,” no. December: 1817–28.
- Beauséjour, Christian M, Ana Krtolica, Francesco Galimi, Masashi Narita, Scott W Lowe, Paul Yaswen, and Judith Campisi. 2003. “Reversal of Human Cellular Senescence: Roles of the P53 and P16 Pathways.” *The EMBO Journal* 22 (16): 4212–22. <https://doi.org/10.1093/emboj/cdg417>.
- Beghein, Els, and Jan Gettemans. 2017. “Nanobody Technology: A Versatile Toolkit for Microscopic Imaging, Protein-Protein Interaction Analysis, and Protein Function Exploration.” *Frontiers in Immunology* 8 (JUL): 1–14.  
<https://doi.org/10.3389/fimmu.2017.00771>.
- Bourdon, J. C., V. De Laurenzi, G. Melino, and D. Lane. 2003. “P53: 25 Years of Research and More Questions To Answer.” *Cell Death and Differentiation* 10 (4): 397–99. <https://doi.org/10.1038/sj.cdd.4401243>.
- Bourdon, J C, V De Laurenzi, G Melino, and D Lane. 2003. “P53: 25 Years of Research and More Questions to Answer.” *Cell Death & Differentiation* 10 (4): 397–99.

- <https://doi.org/10.1038/sj.cdd.4401243>.
- Brown, Christopher J., Sonia Lain, Chandra S. Verma, Alan R. Fersht, and David P. Lane. 2009. "Awakening Guardian Angels: Drugging the P53 Pathway." *Nature Reviews Cancer* 9 (12): 862–73. <https://doi.org/10.1038/nrc2763>.
- Bruin, C G De, Kathryn M Ferguson, Arie J Verkleij, and Guus A M S Van Dongen. 2014. "A Bi-Paratopic Anti-EGFR Nanobody Efficiently Inhibits Solid Tumour Growth" 129 (8): 2013–24. <https://doi.org/10.1002/ijc.26145.A>.
- Cahilly-Snyder, Linda, Teresa Yang-Feng, Uta Francke, and Donna L. George. 1987. "Molecular Analysis and Chromosomal Mapping of Amplified Genes Isolated from a Transformed Mouse 3T3 Cell Line." *Somatic Cell and Molecular Genetics* 13 (3): 235–44. <https://doi.org/10.1007/BF01535205>.
- Campisi, Judith. 2005. "Senescent Cells, Tumor Suppression, and Organismal Aging: Good Citizens, Bad Neighbors." *Cell* 120 (4): 513–22. <https://doi.org/10.1016/j.cell.2005.02.003>.
- Carvajal, Daisy, Frank Podlaski, Zoran Filipovic, Christian Klein, Nader Fotouhi, and Emily A Liu. 2004. "In Vivo Activation of the P53 Pathway by Small-Molecule Antagonists of MDM2." *Science* 303 (February): 844–49. <http://science.sciencemag.org/>.
- Chakravarty, Rubel, Shreya Goel, and Weibo Cai. 2014. "Nanobody : The ‘ Magic Bullet ’ for Molecular Imaging ?" 4 (4). <https://doi.org/10.7150/thno.8006>.
- Chang, J., D. H. Kim, Seung Woo Lee, Kwan Yong Choi, and Young Chul Sung. 1995. "Transactivation Ability of P53 Transcriptional Activation Domain Is Directly Related to the Binding Affinity to TATA-Binding Protein." *Journal of Biological Chemistry* 270 (42): 25014–19. <https://doi.org/10.1074/jbc.270.42.25014>.
- Chavez-Reyes, Arturo, John M. Parant, Lisa L. Amelse, Roberto Montes De Oca Luna, Stanley J. Korsmeyer, and Guillermina Lozano. 2003. "Switching Mechanisms of Cell Death in Mdm2- and Mdm4-Null Mice by Deletion of P53 Downstream Targets." *Cancer Research* 63 (24): 8664–69.
- Chen, Hui, Hudan Liu, and Guoliang Qing. 2018. "Targeting Oncogenic Myc as a Strategy for Cancer Treatment." *Signal Transduction and Targeted Therapy* 3 (1): 1–7. <https://doi.org/10.1038/s41392-018-0008-7>.
- Chen, J, V Marechal, and A J Levine. 1993. "Mapping of the P53 and Mdm-2 Interaction Domains." *Molecular and Cellular Biology* 13 (7): 4107–14. <http://www.ncbi.nlm.nih.gov/pubmed/7686617> <http://www.pubmedcentral.nih>

- .gov/articlerender.fcgi?artid=PMC359960.
- Chen, Jiandong. 2016. "The Cell-Cycle Arrest and Apoptotic and Progression." *Cold Spring Harbor Perspectives in Biology*, 1–16. <https://doi.org/doi:10.1101/cshperspect.a026104>.
- Chène, Patrick. 2004. "Inhibition of the P53-MDM2 Interaction: Targeting a Protein-Protein Interface." *Molecular Cancer Research : MCR* 2 (1): 20–28. <http://www.ncbi.nlm.nih.gov/pubmed/14757842>.
- Conrath, Katja Els, Mark Lauwereys, Lode Wyns, and Serge Muyldermans. 2001. "Camel Single-Domain Antibodies as Modular Building Units in Bispecific and Bivalent Antibody Constructs \*" 276 (10): 7346–50. <https://doi.org/10.1074/jbc.M007734200>.
- Dumoulin, Mireille, Katja Conrath, Annemie V A N Meirhaeghe, Filip Meersman, Karel Heremans, Leon G J Frenken, Serge Muyldermans, Lode Wyns, and Andre Matagne. 2002. "Single-Domain Antibody Fragments with High Conformational Stability," 500–515. <https://doi.org/10.1110/ps.34602.500>.
- Ebrahimizadeh, Walead, and Masoumeh Rajabibazl. 2014. "Bacteriophage Vehicles for Phage Display : Biology , Mechanism , and Application," 109–20. <https://doi.org/10.1007/s00284-014-0557-0>.
- El-deiry, Wafik S, Takashi Tokino, Victor E Velculescu, Daniel B Levy, Ramon Parsons, Jeffrey M Trent, David Lin, W Edward Mercer, Kenneth W Kinzler, and Bert Vogelstein. 1993. "WAF1, a Potential Mediator of P53 Tumor Suppression." *Cell* 75: 817–25.
- Emmerson, Chris D, Els J Van Der Vlist, Myrthe R Braam, Peter Vanlandschoot, Hans J W De Haard, C Theo Verrips, and Paul M P Van Bergen. 2011. "Enhancement of Polymeric Immunoglobulin Receptor Transcytosis by Biparatopic VHH" 6 (10): 1–10. <https://doi.org/10.1371/journal.pone.0026299>.
- Farasat, Alireza, Fatemeh Rahbarizadeh, Ghader Hosseinzadeh, Mehdi Kamali, and Amir Homayoun Keihan. 2016. "Affinity Enhancement of Nanobody Binding to EGFR : In Silico Site-Directed Mutagenesis and Molecular Dynamics Simulation Approaches." *Journal of Biomolecular Structure and Dynamics* 1102 (October): 1–18. <https://doi.org/10.1080/07391102.2016.1192065>.
- Fischer, M. 2017. "Census and Evaluation of P53 Target Genes." *Oncogene* 36 (28): 3943–56. <https://doi.org/10.1038/onc.2016.502>.
- Freedman, Deborah A., Charles B. Epstein, Judith C. Roth, and Arnold J. Levine. 1997.

- “A Genetic Approach to Mapping the P53 Binding Site in the MDM2 Protein.” *Molecular Medicine* 3 (4): 248–59. <https://doi.org/10.1007/bf03401678>.
- Frenken, Leon G J, Richard H J Van Der Linden, Pim W J J Hermans, J Wil Bos, Robin C Ruuls, Bernard De Geus, and C Theo Verrips. 2000. “Isolation of Antigen Specific Llama V HH Antibody Fragments and Their High Level Secretion by *Saccharomyces Cere 6 Isiae*” 78: 11–21.
- Gannon, Hugh S., and Stephen N. Jones. 2012. “Using Mouse Models to Explore MDM-P53 Signaling in Development, Cell Growth, and Tumorigenesis.” *Genes and Cancer* 3 (3–4): 209–18. <https://doi.org/10.1177/1947601912455324>.
- Garcia, Daniel, Matthew R Warr, Carla P Martins, Lamorna Brown Swigart, and Gerard I Evan. 2011. “Validation of MdmX as a Therapeutic Target for Reactivating P53 in Tumors” 53: 1746–57. <https://doi.org/10.1101/gad.16722111.et>.
- Gartel, A. L. 2006. “Is P21 an Oncogene?” *Molecular Cancer Therapeutics* 5 (6): 1385–86. <https://doi.org/10.1158/1535-7163.MCT-06-0163>.
- Gembarska, Agnieszka, Flavie Luciani, Clare Fedele, Elisabeth A. Russell, Michael Dewaele, Stéphanie Villar, Aleksandra Zwolinska, et al. 2012. “MDM4 Is a Key Therapeutic Target in Cutaneous Melanoma.” *Nature Medicine* 18 (8): 1239–47. <https://doi.org/10.1038/nm.2863>.
- Genst, Erwin De, Karen Silence, Klaas Decanniere, Katja Conrath, Remy Loris, Jörg Kinne, Serge Muyldermans, and Lode Wyns. 2006. “Molecular Basis for the Preferential Cleft Recognition by Dromedary Heavy-Chain Antibodies.” *Proceedings of the National Academy of Sciences* 103 (12): 4586–91. <https://doi.org/10.1073/pnas.0505379103>.
- Georgakilas, Alexandros G., Olga A. Martin, and William M. Bonner. 2017. “P21: A Two-Faced Genome Guardian.” *Trends in Molecular Medicine* 23 (4): 310–19. <https://doi.org/10.1016/j.molmed.2017.02.001>.
- Ghahroudi, M Arbabi, A Desmyter, L Wyns, R Hamers, and S Muyldermans. 1997. “Selection and Identification of Single Domain Antibody Fragments from Camel Heavy-Chain Antibodies.” *FEBS Letters* 414 (3): 521–26. [https://doi.org/10.1016/S0014-5793\(97\)01062-4](https://doi.org/10.1016/S0014-5793(97)01062-4).
- Gilkes, Daniele M., Lihong Chen, and Jiandong Chen. 2006. “MDMX Regulation of P53 Response to Ribosomal Stress.” *EMBO Journal* 25 (23): 5614–25. <https://doi.org/10.1038/sj.emboj.7601424>.
- Gilkes, Daniele, Yu Pan, Domenico Coppola, Timothy Yeatman, Gary W. Reuther, and

- Jiandong Chen. 2008. "Regulation of MDMX Expression by Mitogenic Signaling." *Molecular and Cellular Biology* 28 (6): 1999–2010.  
<https://doi.org/10.1128/mcb.01633-07>.
- Grasberger, Bruce L, Tianbao Lu, Carsten Schubert, Daniel J Parks, Theodore E Carver, Holly K Koblisch, Maxwell D Cummings, et al. 2005. "Discovery and Cocrystal Structure of Benzodiazepinedione HDM2 Antagonists That Activate P53 in Cells," 909–12. <https://doi.org/10.1021/jm049137g>.
- Gu, Jijie, Hidehiko Kawai, Linghu Nie, Hiroyuki Kitao, Dmitri Wiederschain, Aart G. Jochemsen, John Parant, Guillermina Lozano, and Zhi Min Yuan. 2002. "Mutual Dependence of MDM2 and MDMX in Their Functional Inactivation of P53." *Journal of Biological Chemistry* 277 (22): 19251–54.  
<https://doi.org/10.1074/jbc.C200150200>.
- Habib, Ibrahim, Dorota Smolarek, Claude Hattab, Magdalena Grodecka, Gholamreza Hassanzadeh-ghassabeh, Serge Muyltermans, Sandrine Sagan, et al. 2013. "VHH ( Nanobody ) Directed against Human Glycophorin A : A Tool for Autologous Red Cell Agglutination Assays." *Analytical Biochemistry* 438 (1): 82–89.  
<https://doi.org/10.1016/j.ab.2013.03.020>.
- Hamers-Casterman, C., T. Atarhouch, S. Muyltermans, G. Robinson, C. Hamers, E. Bajyana Songa, N. Bendahman, and R. Hamers. 1993. "Naturally Occuring Antibodies Devoid of Light Chains." *Nature* 363.  
<https://doi.org/10.1038/363446a0>.
- Hanahan, Douglas and Weinberg Robert A. 2000. "The Hallmarks of Cancer." *Cell* 100: 57–70. <https://doi.org/10.1007/BF03091804>.
- Hanahan, Douglas, and Robert A. Weinberg. 2011. "Hallmarks of Cancer: The Next Generation." *Cell* 144 (5): 646–74. <https://doi.org/10.1016/j.cell.2011.02.013>.
- Harmsen, Michiel M, and Helmi P D Fijten. 2012. "IMPROVED FUNCTIONAL IMMOBILIZATION OF LLAMA SINGLE-DOMAIN ANTIBODY FRAGMENTS TO POLYSTYRENE SURFACES USING SMALL PEPTIDES" 1819. <https://doi.org/10.1080/15321819.2011.634473>.
- Hart, Jonathan R., Yaoyang Zhang, Lujian Liao, Lynn Ueno, Lisa Du, Marloes Jonkers, John R. Yates, and Peter K. Vogt. 2015. "The Butterfly Effect in Cancer: A Single Base Mutation Can Remodel the Cell." *Proceedings of the National Academy of Sciences* 112 (4): 1131–36. <https://doi.org/10.1073/pnas.1424012112>.
- Hicke, Linda, and Rebecca Dunn. 2003. "Regulation of Membrane Protein Transport by

- Ubiquitin and Ubiquitin-Binding Proteins.” *Annual Review of Cell and Developmental Biology* 19 (1): 141–72.  
<https://doi.org/10.1146/annurev.cellbio.19.110701.154617>.
- Hmila, Issam, Dirk Saerens, Rahma Ben Abderrazek, Naima Abidi, Zakaria Benlasfar, Jochen Govaert, Mohamed El Ayeb, Balkiss Bouhaouala-zahar, Serge Muyldermans, and Service Unite. 2010. “A Bispecific Nanobody to Provide Full Protection against Lethal Scorpion Envenoming.” *FASEB Journal* 24: 3479–89.  
<https://doi.org/10.1096/fj.09-148213>.
- Honda, Reiko, Hirofumi Tanaka, and Hideyo Yasuda. 1997. “Oncoprotein MDM2 Is a Ubiquitin Ligase E3 for Tumor Suppressor P53.” *FEBS Letters* 420 (1): 25–27.  
[https://doi.org/10.1016/S0014-5793\(97\)01480-4](https://doi.org/10.1016/S0014-5793(97)01480-4).
- Hu, Baoli, Daniele M. Gilkes, Bilal Farooqi, Said M. Sebti, and Jiandong Chen. 2006. “MDMX Overexpression Prevents P53 Activation by the MDM2 Inhibitor Nutlin.” *Journal of Biological Chemistry* 281 (44): 33030–35.  
<https://doi.org/10.1074/jbc.C600147200>.
- Huet, Heather A, Joseph D Growney, Jennifer A Johnson, Jing Li, Sanela Bilic, Lance Ostrom, Mohammad Zafari, et al. 2014. “Multivalent Nanobodies Targeting Death Receptor 5 Elicit Superior Tumor Cell Killing through Efficient Caspase Induction” 6 (6): 1560–70.
- Ismaili, Ahmad, Mokhtar Jalali-javaran, Mohammad J Rasaei, Fatemeh Rahbarizadeh, Mehdi Forouzandeh-moghadam, and Hamid Rajabi Memari. 2007. “Production and Characterization of Anti- ( Mucin MUC1 ) Single-Domain Antibody in Tobacco ( Nicotiana Tabacum Cultivar Xanthi )” 19: 11–19.  
<https://doi.org/10.1042/BA20060071>.
- Itoh, Yuji, Agato Murata, Satoshi Takahashi, and Kiyoto Kamagata. 2018. “Intrinsically Disordered Domain of Tumor Suppressor P53 Facilitates Target Search by Ultrafast Transfer between Different DNA Strands.” *Nucleic Acids Research* 46 (14): 7261–69. <https://doi.org/10.1093/nar/gky586>.
- Jackson, Mark W., Mikael S. Lindström, and Steven J. Berberich. 2001. “MdmX Binding to ARF Affects Mdm2 Protein Stability and P53 Transactivation.” *Journal of Biological Chemistry* 276 (27): 25336–41.  
<https://doi.org/10.1074/jbc.M010685200>.
- Jeffrey, Philip D, Svetlana Gorina, and Nikola P Pavletich. 2016. “Crystal Structure of the Tetramerization Domain of the P53 Tumor Suppressor at 1.7 Ångströms

- Author ( s ): Philip D . Jeffrey , Svetlana Gorina and Nikola P . Pavletich  
Published by : American Association for the Advancement of Science Stable  
URL : Http” 267 (5203): 1498–1502.
- Joerger, Andreas C., and Alan R. Fersht. 2008. “Structural Biology of the Tumor Suppressor P53.” *Annual Review of Biochemistry* 77 (1): 557–82.  
<https://doi.org/10.1146/annurev.biochem.77.060806.091238>.
- Joerger, Andreas C, and Alan R Fersht. 2016. “The P53 Pathway: Origins, Inactivation in Cancer, and Emerging Therapeutic Approaches.” *Annual Review of Biochemistry* 85 (1): 375–404. <https://doi.org/10.1146/annurev-biochem-060815-014710>.
- Joseph, Thomas Leonard, Arumugam Madhumalar, Christopher John Brown, David P. Lane, and Chandra Verma. 2010. “Differential Binding of P53 and Nutlin to MDM2 and MDMX: Computational Studies.” *Cell Cycle* 9 (6): 1167–81.  
<https://doi.org/10.4161/cc.9.6.11067>.
- Karim. 2017. “On the Interaction Mechanisms of a P53 Peptide and Nutlin with the MDM2 and MDMX Proteins: A Brownian Dynamics Study” 12 (3): 394–404.  
<https://doi.org/10.4161/cc.23511>.
- Kawai, H., D. Wiederschain, and Z.-M. Yuan. 2003. “Critical Contribution of the MDM2 Acidic Domain to P53 Ubiquitination.” *Molecular and Cellular Biology* 23 (14): 4939–47. <https://doi.org/10.1128/mcb.23.14.4939-4947.2003>.
- Kazemi-lomedasht, Fatemeh, Mahdi Behdani, and Kamran Pooshang. 2015. “Inhibition of Angiogenesis in Human Endothelial Cell Using VEGF Specific Nanobody.” *Molecular Immunology* 65 (1): 58–67.  
<https://doi.org/10.1016/j.molimm.2015.01.010>.
- Koide, Shohei. 2009. “Engineering of Recombinant Crystallization Chaperones Shohei” 19 (4): 449–57. <https://doi.org/10.1016/j.sbi.2009.04.008.Engineering>.
- Kubala, Marta H., Oleksiy Kovtun, Kirill Alexandrov, and Brett M. Collins. 2010. “Structural and Thermodynamic Analysis of the GFP:GFP-Nanobody Complex.” *Protein Science* 19 (12): 2389–2401. <https://doi.org/10.1002/pro.519>.
- Lai, Zhihong, Katherine V. Ferry, Melody A. Diamond, Kevin E. Wee, Young B. Kim, Jianhong Ma, Tao Yang, Pamela A. Benfield, Robert A. Copeland, and Kurt R. Auger. 2001. “Human Mdm2 Mediates Multiple Mono-Ubiquitination of P53 by a Mechanism Requiring Enzyme Isomerization.” *Journal of Biological Chemistry* 276 (33): 31357–67. <https://doi.org/10.1074/jbc.M011517200>.



- Lambert, Paul F., Fatah Kashanchi, Michael F. Radonovich, Ramin Shiekhattar, and John N. Brady. 1998. "Phosphorylation of P53 Serine 15 Increases Interaction with CBP." *Journal of Biological Chemistry* 273 (49): 33048–53. <https://doi.org/10.1074/jbc.273.49.33048>.
- Lee, Eva Y H P, and William J Muller. 2010. "Gout Breast Cancer: Oncogenes and Tumor Suppressor Genes." *Cold Spring Harbor Perspectives in Biology* 2 (10): a003236. <https://doi.org/10.1101/cshperspect.a003236>.
- Linden, R H J Van Der, L G J Frenken, B De Geus, and M M Harmsen. 1999. "Comparison of Physical Chemical Properties of Llama V HH Antibody Fragments and Mouse Monoclonal Antibodies" 1431: 37–46.
- Lipman, Neil S, Lynn R Jackson, Laura J Trudel, and Frances Weis-garcia. 2005. "Monoclonal Versus Polyclonal Antibodies: Distinguishing Characteristics, Applications, and Information Resources." *ILAR Journal* 46 (3).
- Luo, Yan, Jerard Hurwitz, and Joan Massagué. 1995. "Cell-Cycle Inhibition by Independent CDK and PCNA Binding Domains in P21Cip1." *Nature* 375 (6527). <https://doi.org/10.1038/2F375159a0>.
- Marine, J-c, and G Lozano. 2009. "Mdm2-Mediated Ubiquitylation : P53 and Beyond." *Cell Death and Differentiation* 17 (1): 93–102. <https://doi.org/10.1038/cdd.2009.68>.
- Martín-Caballero, Juan, Juana M Flores, Pilar García-Palencia, and Manuel Serrano. 2001. "Tumor Susceptibility of P21 Waf1/Cip1-Deficient Mice 1." *Cancer Research* 61: 6234–38. <http://cancerres.aacrjournals.org/content/61/16/6234.full-text.pdf>.
- Maus, Marcela V, Stephan A Grupp, David L Porter, and Carl H June. 2019. "Antibody-Modified T Cells : CARs Take the Front Seat for Hematologic Malignancies" 123 (17): 2625–36. <https://doi.org/10.1182/blood-2013-11-492231.organs>.
- Maya, Ruth, Moshe Balass, Seong Tae Kim, Dganit Shkedy, Juan Fernando Martinez Leal, Ohad Shifman, Miri Moas, et al. 2001. "ATM-Dependent Phosphorylation of Mdm2 on Serine 395: Role in P53 Activation by DNA Damage." *Genes and Development* 15 (9): 1067–77. <https://doi.org/10.1101/gad.886901>.
- Mayo, Lindsey D, John J Turchi, and Steven J Berberich. 1997. "Advances in Brief Mdm-2 Phosphorylation by DNA-Dependent Protein Kinase Prevents Interaction Formation by Hphosphorylation of Mdm-2." *Cell Cycle*, 5013–16.

- McMahon, Conor, Alexander S. Baier, Roberta Pascolutti, Marcin Wegrecki, Sanduo Zheng, Janice X. Ong, Sarah C. Erlandson, et al. 2018. “Yeast Surface Display Platform for Rapid Discovery of Conformationally Selective Nanobodies.” *Nature Structural and Molecular Biology* 25 (3): 289–96. <https://doi.org/10.1038/s41594-018-0028-6>.
- Meyer, Thomas De, Serge Muyldermans, and Ann Depicker. 2014. “Nanobody-Based Products as Research and Diagnostic Tools.” *Trends in Biotechnology* 32 (5): 263–70. <https://doi.org/10.1016/j.tibtech.2014.03.001>.
- Migliorini, Domenico, Davide Danovi, Emanuela Colombo, Roberta Carbone, Pier Giuseppe Pelicci, and Jean Christophe Marine. 2002. “Hdmx Recruitment into the Nucleus by Hdm2 Is Essential for Its Ability to Regulate P53 Stability and Transactivation.” *Journal of Biological Chemistry* 277 (9): 7318–23. <https://doi.org/10.1074/jbc.M108795200>.
- Migliorini, Domenico, Eros Lazzerini Denchi, Davide Danovi, Aart Jochemsen, Manuela Capillo, Alberto Gobbi, Kristian Helin, Pier Guisepe Pelicci, and Jean Christophe Marine. 2002. “Mdm4 (Mdmx) Regulates P53-Induced Growth Arrest and Neuronal Cell Death during Early Embryonic Mouse Development.” *Molecular and Cellular Biology* 22 (15): 5527–38. <https://doi.org/10.1128/MCB.22.15.5527-5538.2002>.
- Mikolajczyk, Stephen D, William J Catalona, Cindy L Evans, Harry J Linton, Lisa S Millar, Kathy M Marker, Diksha Katir, Anna Amirkhan, and Harry G Rittenhouse. 2004. “Proenzyme Forms of Prostate-Specific Antigen in Serum Improve the Detection of Prostate Cancer” 1025: 1017–25. <https://doi.org/10.1373/clinchem.2003.026823>.
- Milholland, Brandon, Xiao Dong, Lei Zhang, Xiaoxiao Hao, Yousin Suh, and Jan Vijg. 2017. “Differences between Germline and Somatic Mutation Rates in Humans and Mice.” *Nature Communications* 8 (May): 1–8. <https://doi.org/10.1038/ncomms15183>.
- Momand, Jamil, Gerard P. Zambetti, David C. Olson, Donna George, and Arnold J. Levine. 1992. “The Mdm-2 Oncogene Product Forms a Complex with the P53 Protein and Inhibits P53-Mediated Transactivation.” *Cell* 69 (7): 1237–45. [https://doi.org/10.1016/0092-8674\(92\)90644-R](https://doi.org/10.1016/0092-8674(92)90644-R).
- Mullard, Asher. 2015. “2014 FDA Drug Approvals.” *Nature Publishing Group* 14 (2): 77–81. <https://doi.org/10.1038/nrd4545>.

- Muyldermans, S, T.N. Baral, V Cortez Retamozzo, P. De Baetselier, E. De Genst, J. Kinne, H. Leonhardt, et al. 2009. "Camelid Immunoglobulins and Nanobody Technology." *Veterinary Immunology and Immunopathology* 128 (1–3): 178–83. <https://doi.org/10.1016/j.vetimm.2008.10.299>.
- Muyldermans, Serge. 2013. "Nanobodies: Natural Single-Domain Antibodies." *Annual Review of Biochemistry* 82 (1): 775–97. <https://doi.org/10.1146/annurev-biochem-063011-092449>.
- Newnham, Laura E, Michael J Wright, Gill Holdsworth, Kostas Kostarelos, Martyn K Robinson, Terence H Rabbitts, and Alastair D Lawson. 2015. "Functional Inhibition of  $\beta$ -Catenin-Mediated Wnt Signaling by Intracellular VHH Antibodies" 7 (1): 180–91.
- Nguyen-Duc, Trong, Eveline Peeters, Serge Muyldermans, Daniel Charlier, and Gholamreza Hassanzadeh-Ghassabeh. 2013. "Nanobody®-Based Chromatin Immunoprecipitation/Micro-Array Analysis for Genome-Wide Identification of Transcription Factor DNA Binding Sites." *Nucleic Acids Research* 41 (5): e59–e59. <https://doi.org/10.1093/nar/gks1342>.
- Nguyen, Van, Feras Hatahet, Kirsi E.H. Salo, Eveliina Enlund, Chi Zhang, and Lloyd W. Ruddock. 2011. "Pre-Expression of a Sulfhydryl Oxidase Significantly Increases the Yields of Eukaryotic Disulfide Bond Containing Proteins Expressed in the Cytoplasm of E.Coli." *Microbial Cell Factories* 10 (1): 1. <https://doi.org/10.1186/1475-2859-10-1>.
- Onel, K, and Carlos Cordon-Cardo. 2004. "MDM2 and Prognosis." *Mol Cancer Res* 2 (1): 1–8.
- Osborne, Cynthia, Paschal Wilson, and Debu Tripathy. 2004. "Oncogenes and Tumor Suppressor Genes in Breast Cancer: Potential Diagnostic and Therapeutic Applications." *The Oncologist* 9 (4): 361–77. <https://doi.org/10.1634/theoncologist.9-4-361>.
- Pereg, Y., D. Shkedy, P. de Graaf, E. Meulmeester, M. Edelson-Averbukh, M. Salek, S. Biton, et al. 2005. "Phosphorylation of Hdmx Mediates Its Hdm2- and ATM-Dependent Degradation in Response to DNA Damage." *Proceedings of the National Academy of Sciences* 102 (14): 5056–61. <https://doi.org/10.1073/pnas.0408595102>.
- Popowicz, Grzegorz M., Anna Czarna, Siglinde Wolf, Kan Wang, Wei Wang, Alexander Dömling, and Tad A. Holak. 2010. "Structures of Low Molecular

- Weight Inhibitors Bound to MDMX and MDM2 Reveal New Approaches for P53-MDMX/MDM2 Antagonist Drug Discovery.” *Cell Cycle* 9 (6): 1104–11.  
<https://doi.org/10.4161/cc.9.6.10956>.
- Quan, Shu, Annie Hiniker, Jean-François Collet, and James CA Bardwell. 2013. “Isolation of Bacteria Envelope Proteins.” *Bacterial Cell Surfaces: Methods and Protocols* 966: 359–66. [https://doi.org/DOI 10.1007/978-1-62703-245-2\\_22](https://doi.org/DOI%2010.1007/978-1-62703-245-2_22).
- Rahimi, Fatemeh, Fatemeh Rahbarizadeh, Mohammad A Shokrgozar, Davoud Ahmadvand, Fereidoun Mahboudi, and Zahra Sharifzadeh. 2012. “Targeting High Affinity and Epitope-Distinct Oligoclonal Nanobodies to HER2 over-Expressing Tumor Cells.” *Experimental Cell Research* 318 (10): 1112–24.  
<https://doi.org/10.1016/j.yexcr.2012.03.004>.
- Reed, Damon, Ying Shen, Anang A Shelat, Leggy A Arnold, Antonio M Ferreira, Fangyi Zhu, Nicholas Mills, et al. 2010. “Identification and Characterization of the First Small Molecule Inhibitor of MDMX” 285 (14): 10786–96.  
<https://doi.org/10.1074/jbc.M109.056747>.
- Renisio, Jean G, Jeanine J Prompers, Chris J Van Platerink, Christian Cambillau, and Leon G J Frenken. 2001. “Thermal Unfolding of a Llama Antibody Fragment : A Two-State Reversible,” 74–83. <https://doi.org/10.1021/bi0009082>.
- Revets, Hilde, Patrick De Baetselier, and Serge Muyldermans. 2005. “Nanobodies as Novel Agents for Cancer Therapy.” *Expert Opinion on Biological Therapy* 5 (1): 111–24. <https://doi.org/10.1517/14712598.5.1.111>.
- Rew, Yosup, Daqing Sun, Xuelei Yan, Hilary P Beck, Jude Canon, Ada Chen, Jason Duquette, et al. 2014. “Discovery of AM-7209, a Potent and Selective 4 - Amidobenzoic Acid Inhibitor of the MDM2 – P53 Interaction” 7209.  
<https://doi.org/10.1021/jm501550p>.
- Rice, Peter, Ian Longden, and Alan Bleasby. 2000. “EMBOSS: The European Molecular Biology Open Software Suite.” *Trends in Genetics* 16 (6): 276–77.  
[https://doi.org/10.1016/S0168-9525\(00\)02024-2](https://doi.org/10.1016/S0168-9525(00)02024-2).
- Roth, Judith, Matthias Dobbstein, Deborah A. Freedman, Thomas Shenk, and Arnold J. Levine. 1998. “Nucleo-Cytoplasmic Shuttling of the Hdm2 Oncoprotein Regulates the Levels of the P53 Protein via a Pathway Used by the Human Immunodeficiency Virus Rev Protein.” *EMBO Journal* 17 (2): 554–64.  
<https://doi.org/10.1093/emboj/17.2.554>.
- Rothbauer, Ulrich, Kouros Zolghadr, Sergei Tillib, Danny Nowak, Lothar

- Schermelleh, Anja Gahl, Natalija Backmann, et al. 2006. "Targeting and Tracing Antigens in Live Cells with Fluorescent Nanobodies." *Nature Methods* 3 (11): 887–89. <https://doi.org/10.1038/nmeth953>.
- Saerens, Dirk, Gholamreza Hassanzadeh Ghassabeh, and Serge Muyldermans. 2008. "Single-Domain Antibodies as Building Blocks for Novel Therapeutics," 600–608. <https://doi.org/10.1016/j.coph.2008.07.006>.
- Saerens, Dirk, Lieven Huang, Kristien Bonroy, and Serge Muyldermans. 2008. "Antibody Fragments as Probe in Biosensor Development," 4669–86. <https://doi.org/10.3390/s8084669>.
- Saerens, Dirk, Ulrich Wernery, Serge Muyldermans, and Katja Conrath. 2004. "Single Domain Antibodies Derived from Dromedary Lymph Node and Peripheral Blood Lymphocytes Sensing Conformational Variants of Prostate-Specific Antigen \*\*" 279 (50): 51965–72. <https://doi.org/10.1074/jbc.M409292200>.
- Sakaguchi, Kazuyasu, Hiroshi Sakamoto, Marc S. Lewis, Carl W. Anderson, John W. Erickson, Ettore Appella, and Dong Xie. 1997. "Phosphorylation of Serine 392 Stabilizes the Tetramer Formation of Tumor Suppressor Protein P53." *Biochemistry* 36 (33): 10117–24. <https://doi.org/10.1021/bi970759w>.
- Salema, Valencio, and Luis Ángel Fernández. 2013. "High Yield Purification of Nanobodies from the Periplasm of E . Coli as Fusions with the Maltose Binding Protein." *Protein Expression and Purification* 91 (1): 42–48. <https://doi.org/10.1016/j.pep.2013.07.001>.
- Sapra, P, and T M Allen. 2003. "Ligand-Targeted Liposomal Anticancer Drugs" 42: 439–62. [https://doi.org/10.1016/S0163-7827\(03\)00032-8](https://doi.org/10.1016/S0163-7827(03)00032-8).
- Schon, Oliver, Assaf Friedler, Mark Bycroft, Stefan M.V. Freund, and Alan R. Fersht. 2002. "Molecular Mechanism of the Interaction between MDM2 and P53." *Journal of Molecular Biology* 323 (3): 491–501. [https://doi.org/10.1016/S0022-2836\(02\)00852-5](https://doi.org/10.1016/S0022-2836(02)00852-5).
- Shadfan, Miriam, Vanessa Lopez-Pajares, and Zhi-Min Yuan. 2013. "MDM2 and MDMX: Alone and Together in Regulation of P53" 1 (2): 88–89. <https://doi.org/10.1038/mp.2011.182.doi>.
- Shangary, Sanjeev, and Shaomeng Wang. 2009. "Small-Molecule Inhibitors of the MDM2-P53 Protein- Protein Interaction to Reactivate P53 Function : A Novel Approach for Cancer Therapy," 223–43. <https://doi.org/10.1146/annurev.pharmtox.48.113006.094723>.

- Sheng, Yi, Vivian Saridakis, Feroz Sarkari, Shili Duan, Tianne Wu, Cheryl H. Arrowsmith, and Lori Frappier. 2006. "Molecular Recognition of P53 and MDM2 by USP7/HAUSP." *Nature Structural and Molecular Biology* 13 (3): 285–91. <https://doi.org/10.1038/nsmb1067>.
- Shieh, Sheau-Yann, Masako Ikeda, Yoichi Taya, and Carol Prives. 1997. "DNA Damage-Induced Phosphorylation of P53 Alleviates Inhibition by MDM2 Phosphorylated at Sites within Its N-Terminal and C-Terminal Regions, and Several Protein Kinases Have Been Shown to Phosphorylate P53 in Vitro. One Such Kinase." *Cell* 91: 325–34.
- Shvarts, A, W T Steegenga, N Riteco, T van Laar, P Dekker, M Bazuine, R C van Ham, et al. 1996. "MDMX: A Novel P53-Binding Protein with Some Functional Properties of MDM2." *The EMBO Journal* 15 (19): 5349–57. <http://www.ncbi.nlm.nih.gov/pubmed/8895579> <http://www.pubmedcentral.nih.gov/articlerender.fcgi?artid=PMC452278>.
- Steinman, Heather A., Hayla K. Sluss, Arthur T. Sands, German Pihan, and Stephen N. Jones. 2004. "Absence of P21 Partially Rescues Mdm4 Loss and Uncovers an Antiproliferative Effect of Mdm4 on Cell Growth." *Oncogene* 23 (1): 303–6. <https://doi.org/10.1038/sj.onc.1206925>.
- Stewart, Eric J, Fredrik Åslund, and Jon Beckwith. 1998. "Disulfide Bond Formation in the Escherichia Coli Cytoplasm : An in Vivo Role Reversal for the Thioredoxins" 17 (19): 5543–50.
- Thoden, James B., Louise A. Ryan, Richard J. Reece, and Hazel M. Holden. 2008. "The Interaction between an Acidic Transcriptional Activator and Its Inhibitor: The Molecular Basis of Gal4p Recognition by Gal80p." *Journal of Biological Chemistry* 283 (44): 30266–72. <https://doi.org/10.1074/jbc.M805200200>.
- Thompson, Sarah L., and Duane A. Compton. 2011. "Chromosomes and Cancer Cells." *Chromosome Research* 19 (3): 433–44. <https://doi.org/10.1007/s10577-010-9179-y>.
- Toledo, Franck, and Geoffrey M. Wahl. 2007. "MDM2 and MDM4: P53 Regulators as Targets in Anticancer Therapy." *International Journal of Biochemistry and Cell Biology* 39 (7–8): 1476–82. <https://doi.org/10.1016/j.biocel.2007.03.022>.
- Toledo, Franck, and Geoffrey M Wahl. 2006. "Regulating the P53 Pathway: In Vitro Hypotheses, in Vivo Veritas." *Nature Reviews Cancer* 6 (12): 909–23. <https://doi.org/10.1038/nrc2012>.

- Vaneycken, Ilse, Nick Devoogdt, Naomi Van Gassen, Catarina Xavier, Ulrich Wernery, Serge Muyldermans, Tony Lahoutte, and Vicky Caveliers. 2011. "Preclinical Screening of Anti-HER2 Nanobodies for Molecular Imaging of Breast Cancer." *FASEB Journal* 25: 2433–46. <https://doi.org/10.1096/fj.10-180331>.
- Vassilev, Lyubomir T. 2004. "Small-Molecule Antagonists of P53-MDM2 Binding: Research Tools and Potential Therapeutics" 4101: 2–5. <https://doi.org/10.4161/cc.3.4.801>.
- Vogelstein, Bert, and Kenneth W. Kinzler. 2004. "Cancer Genes and the Pathways They Control." *Nature Medicine* 10 (8): 789–99. <https://doi.org/10.1038/nm1087>.
- Wade, Mark, Yao Cheng Li, and Geoffrey M. Wahl. 2013. "MDM2, MDMX and P53 in Oncogenesis and Cancer Therapy." *Nature Reviews Cancer* 13 (2): 83–96. <https://doi.org/10.1038/nrc3430>.
- Wang, Hongbo, Xujun Ma, Shumei Ren, John K. Buolamwini, and Chunhong Yan. 2012. "A Small-Molecule Inhibitor of MDMX Activates P53 and Induces Apoptosis" 10 (1): 69–79. <https://doi.org/10.1158/1535-7163.MCT-10-0581.A>.
- Wang, Xinjiang, Junru Wang, and Xuejun Jiang. 2011. "MdmX Protein Is Essential for Mdm2 Protein-Mediated P53 Polyubiquitination." *Journal of Biological Chemistry* 286 (27): 23725–34. <https://doi.org/10.1074/jbc.M110.213868>.
- Yu, Grace W., Marina Vaysburd, Mark D. Allen, Giovanni Settanni, and Alan R. Fersht. 2009. "Structure of Human MDM4 N-Terminal Domain Bound to a Single-Domain Antibody." *Journal of Molecular Biology* 385 (5): 1578–89. <https://doi.org/10.1016/j.jmb.2008.11.043>.
- Zhu, J W, D DeRyckere, F X Li, Y Y Wan, and J DeGregori. 1999. "A Role for E2F1 in the Induction of ARF, P53, and Apoptosis during Thymic Negative Selection." *Cell Growth & Differentiation : The Molecular Biology Journal of the American Association for Cancer Research* 10 (12): 829–38. <http://cgd.aacrjournals.org/cgi/content/full/10/12/829>.

## APPENDIX A- Chemicals

<b>Chemicals and Media Components</b>	<b>Supplier Company</b>
2-Mercaptoethanol	Sigma, Germany
Acetic acid (glacial)	Merck Millipore, USA
Acrylamide/Bis-acrylamide (30%)	Sigma, Germany
Agarose	Sigma, Germany
Ammonium Persulfate	Sigma, Germany
Ampicilin Sodium Salt	Sigma, Germany
Boric Acid	Molekula, France
Chloramphenicol	Deva, Turkey
Coumaric Acid	Sigma, Germany
Coomassie Blue Brilliant Blue R	Sigma, Germany
Distilled Water	Merck Millipore, USA
DMEM	Thermo Fischer Scientific, USA
DMSO	Sigma, Germany
DNA Gel Loading Dye, 6X	NEB, USA
DTT	Fermentas, USA
EDTA	Sigma, Germany
Ethanol	Sigma, Germany
Ethidium Bromide	Sigma, Germany
Fetal Bovine Serum	Thermo Fischer Scientific, USA
Glutathione Sepharose 4 Fast Flow	GE Healthcare Life Sciences, USA
Glycerol	Sigma, Germany
Glycine	Sigma, Germany
HBSS	Thermo Fischer Scientific, USA
HEPES	Sigma, Germany
HisPure Cobalt Superflow Agarose	Thermo Fischer Scientific, USA
Hydrochloric Acid	Sigma, Germany
Hydrogen peroxide	Sigma, Germany



Imidazole	Sigma, Germany
IPTG	Fermentas, USA
Isopropanol	Sigma, Germany
Kanamycin Sulfate	Thermo Fischer Scientific, USA
LB Agar	Sigma, Germany
LB Broth	Invitrogen, USA
L-Glutathione reduced	Sigma, Germany
Luminol	Sigma, Germany
Methanol	Sigma, Germany
PBS	Thermo Fischer Scientific, USA
Penicillin/Streptomycin	Thermo Fischer Scientific, USA
PIPES	Sigma, Germany
Potassium Acetate	Merck Millipore, USA
Protease Tablets (EDTA-free)	Roche, Germany
RNase A	Roche, Germany
SDS	Sigma, Germany
Sodium Azide	Amresco, USA
Sodium Chloride	Amresco, USA
Sodium Hydroxide	Sigma, Germany
TEMED	AppliChem, Germany
TCEP	Sigma, Germany
Terrific Broth	Sigma, Germany
Tris Base	Sigma, Germany
Tris Hydrochloride	Amresco, USA
Trypan Blue Solution	Thermo Fischer Scientific, USA
Tween20	Sigma, Germany

## APPENDIX B- Equipment

<b>Equipment</b>	<b>Supplier Company</b>
Autoclave	HiClave HV-110, Hirayama, Japan
Balance	Isolab, Germany
Biomolecular Imager	ImageQuant LAS 4000 mini, GE Healthcare Life Sciences, USA
Centrifuge	5418R Eppendorf, Germany 5702 Eppendorf, Germany 5415R Eppendorf, Germany Allegra X-15R, Beckman Coulter, USA Sorvall Lynx 6000, Thermo Scientific, USA
CO <sub>2</sub> Incubator	Binder, Germany
Column	HiLoad 16/60 Superdex p75, GE Healthcare Life Sciences, USA
Countless II Automated Cell Counter	Thermo Fischer Scientific, USA
Deepfreeze	-80°C, Forma 88000 Series, Thermo Fischer Scientific, USA -20°C, Bosch, Germany
Electrophoresis Apparatus	VWR, USA BIORAD, USA
Filters (0.22µm and 0.45µm)	Merk Millipore, USA
Freezing Container	Mr. Frosty, Thermo Fischer Scientific, USA
Gel Documentation	Gel Doc EZ, Biorad, USA
Heater	Thermomixer Comfort Eppendorf, Germany
Hemocytometer	Neubauer Improved, Isolab, Germany
Ice Machine	AF20, Scotsman Inc., USA
Incubator Shaker	Innova 44, New Brunswick Scientific USA
Laminar Flow	HeraSafe HS15, Heraeus, Germany HeraSafe HS12, Heraeus, Germany
Liquid Nitrogen Tank	Taylor-Wharton, 300RS, USA
Magnetic Stirrer	SB162, Stuart, UK

Microliter Pipettes	Thermo Fischer Scientific, USA
Microscope	Primovert, Zeiss, Germany CK40, Olympus, Japan In Cell Analyzer 2500HS, GE Healthcare Life Sciences, USA
Microwave Oven	Bosch, Germany
pH Meter	SevenCompact, Mettler Toledo, USA
Refrigerator	Bosch, Germany Arcelik, Turkey Panasonic, Japan Thermo Fischer Scientific, USA
Reusable Filter Holder with Receiver	Nalgene, USA
RTCA system	ACEA Biosciences, USA
Sonicator	Qsonica Q500, USA
Spectrophotometer	NanoDrop 2000, Thermo Fischer Scientific, USA Ultrospec 2100 pro, Amersham Biosciences, UK
Surface Plasmon Resonance System	BIACORE T200, GE Healthcare Life Sciences, USA
Thermal Cycler	C1000 Touch, Biorad, USA PTC-200, MJ Reseach Inc., Canada
Vortex	VWR, USA
Water Bath	Innova 3100, New Brunswick Scientific, USA

### **APPENDIX C- Molecular Biology Kits**

GenElute Agarose Spin Columns	Sigma-Aldrich, USA
InstAclone PCR Cloning	Thermo Fischer Scientific, USA

NucleoSpin Gel and PCR Clean-up	Macherey-Nagel, USA
PureLink Genomic DNA Mini Kit	Invitrogen, USA
Purelink HiPure Plasmid Midiprep Kit	Invitrogen, USA
PureLink Quick Gel Extraction Kit	Invitrogen, USA
Zero Blunt TOPO PCR Cloning Kit for Sequencing	Thermo Fischer Scientific, USA
ZymoPure Plasmid Maxiprep Kit	Zymo Research, USA

#### APPENDIX D- DNA and Protein Molecular Weight Marker

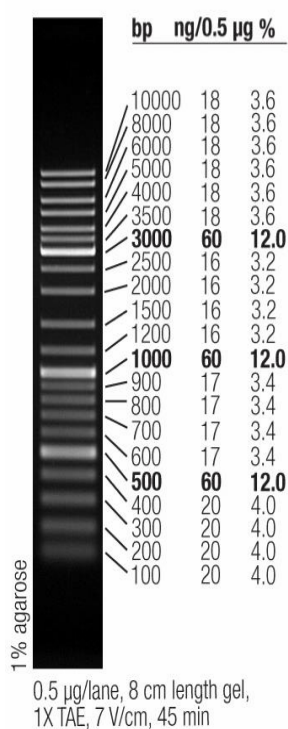


**Figure D1. GeneRuler DNA Ladder Mix (SM0331), Thermo Fischer Scientific, USA**

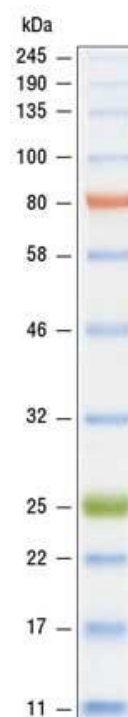


**Figure D2. Color Prestained Protein Standard, Broad Range (11-25 kDa) (P7712S), New England Biolabs**

## APPENDIX F- Plasmid Maps

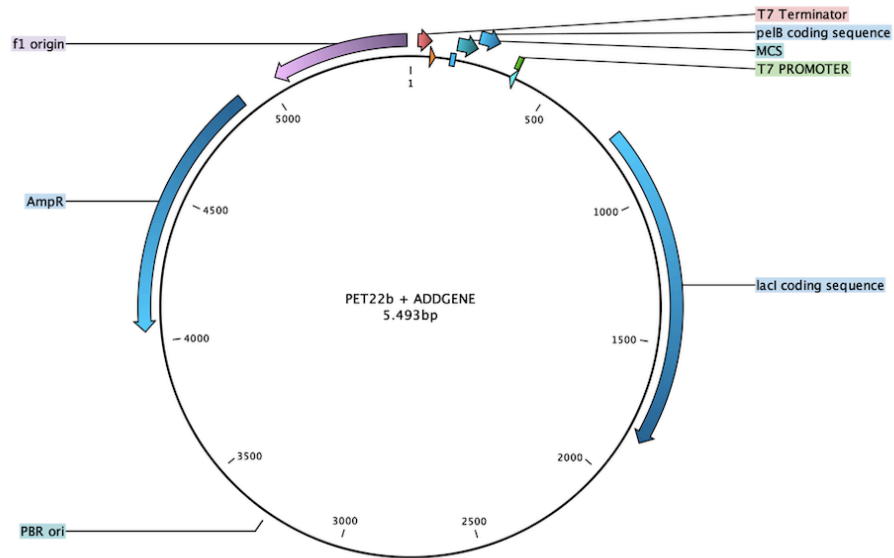


Figure F1. The plasmid map of pET22b

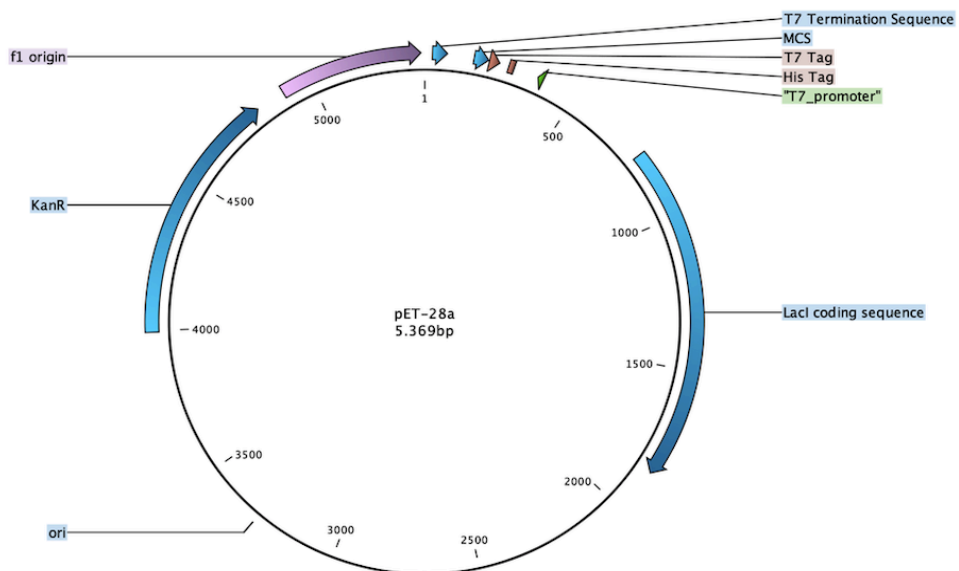
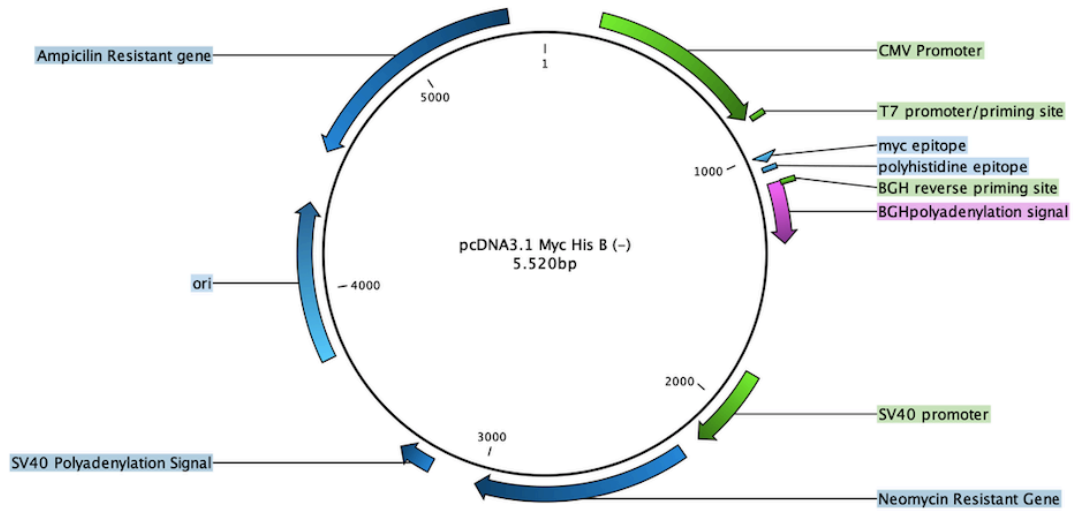
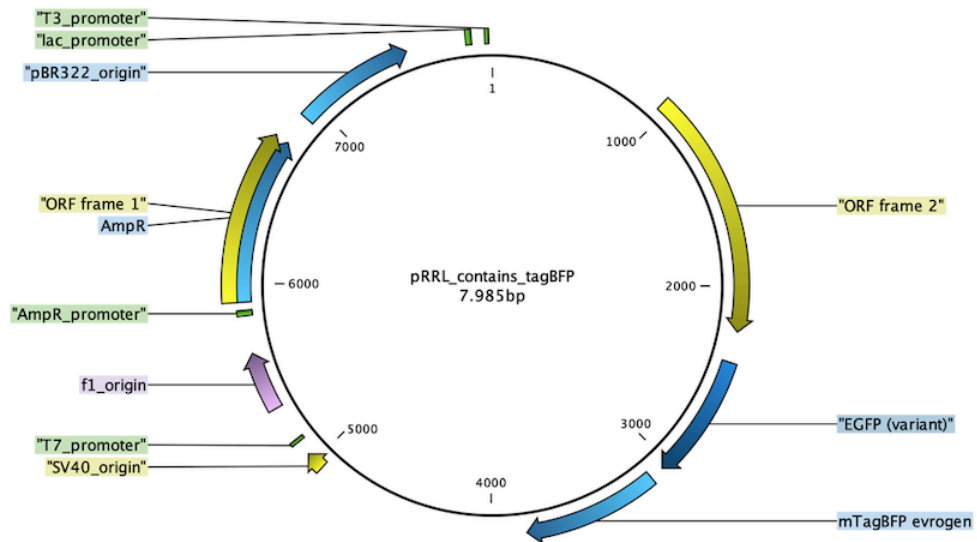


Figure F2. The plasmid map of pET28a



**Figure F3. The plasmid map of pcDNA3.1 Myc His B (-)**



**Figure F4. The plasmid map of pRRL Tag BFP Plasmid**